ฤทธิ์ต้านเบาหวานและกลไกการออกฤทธิ์ของ *p*-METHOXYCINNAMIC ACID

นาย สิริชัย อดิศักดิ์วัฒนา

วิทยานิพนธ์นี้เป็นส่วนหนึ่งของการศึกษาตามหลักสูตรปริญญาดุษฎีบัณฑิต
สาขาวิชาเภสัชวิทยา (สหสาขาวิชา)
บัณฑิตวิทยาลัย จุฬาลงกรณ์มหาวิทยาลัย
ปีการศึกษา 2548

ISBN 974-53-2540-6

ANTIDIABETIC EFFECTS AND MECHANISMS OF ACTION OF *p*-METHOXYCINNAMIC ACID

Mr. Sirichai Adisakwattana

A Dissertation Submitted in Partial Fulfillment of the Requirements
for the Degree of Doctor of Philosophy Program in Pharmacology
Inter-Department
Graduate School
Chulalongkorn University
Academic Year 2005

ISBN 974-53-2540-6

Thesis Title	Antidiabetic effects and mechanisms of action of *p*-methoxycinnamic acid
By	Mr. Sirichai Adisakwattana
Field of study	Pharmacology
Thesis Advisor	Professor Sophon Roengsumran, Ph.D.
Thesis Co-advisor	Associate Professor Sirintorn Yibchok-anun, D.V.M., Ph.D.

Accepted by the Graduate School, Chulalongkorn University in Partial Fulfillment of the Requirements for the Doctor's Degree

..... Dean of the Graduate School
(Assistant Professor M.R. Kalaya Tingsabadh, Ph.D.)

THESIS COMMITTEE

..... Chairman
(Associate Professor Supatra Srichairat, Ph.D.)

..... Thesis Advisor
(Professor Sophon Roengsumran, Ph.D.)

..... Thesis Co-advisor
(Associate Professor Sirintorn Yibchok-anun, D.V.M., Ph.D.)

..... Member
(Professor Chaivat Toskulkao, D.V.M., Ph.D.)

..... Member
(Professor Walter H. Hsu, D.V.M., Ph.D.)

..... Member
(Associate Professor Sumana Chompootaweep, M.D., M.P.H.)

..... Member
(Assistant Professor Suree Jianmongkol, Ph.D.)

สิริชัย อดิศักดิ์วัฒนา :ฤทธิ์ต้านเบาหวานและกลไกการออกฤทธิ์ของ *p*-METHOXYCINNAMIC ACID
ANTIDIABETIC EFFECTS AND MECHANISMS OF ACTION OF *p*-METHOXYCINNAMIC ACID
อ. ที่ปรึกษา:ศ.ดร.โสภณ เธียรสำราญ, อ.ที่ปรึกษาร่วม: รศ.สพ.ญ.ดร.ศิรินทร หยิบโชคอนันต์ หน้า 119.ISBN 974-53-2540-6.

พีเอ็มซีเอสามารถลดระดับน้ำตาลในกระแสเลือดและเพิ่มระดับอินสุลินทั้งในหนูปกติและถูกเหนี่ยวนำให้เป็นเบาหวานและสามารถลดภาวะกลูโคสอินโทเลอรานซ์ในหนูเบาหวาน พีเอ็มซีเอสามารถระดับน้ำตาลในกระแสเลือดในหนูเบาหวานตลอดระยะเวลาการศึกษา 4 สัปดาห์ โดยพีเอ็มซีเอลดการทำงานของเอนไซม์กลูโคสซิกซ์ฟอสฟาเทตเพิ่มการทำงานของเอนไซม์เฮกโซไคเนส กลูโคไคเนส ฟอสโฟฟรุกโตไคเนส และเพิ่มการสะสมไกลโคเจนในตับ

พีเอ็มซีกระตุ้นการหลั่งอินสุลินจากการผ่านสารดังกล่าวเข้าสู่ตับอ่อนรวมทั้งกระตุ้นการหลั่งอินสุลินในเซลไอเอ็นเอสวันตามความเข้มข้นที่เพิ่มขึ้น นอกจากนี้พีเอ็มซีเอเพิ่มระดับความเข้มข้นของแคลเซียมภายในเซลไอเอ็นวัน การกระตุ้นการหลั่งอินสุลินและการเพิ่มระดับแคลเซียมภายในเซลของพีเอ็มซีเอนั้นถูกยับยั้งในภาวะการขาดแคลเซียมภายนอกเซลและภาวะที่มีไนโมดิพีนซึ่งเป็นแอลไทฟ์แคลเซียมชาแนลแอนตาโกนิส จากผลการทดลองดังกล่าวกลไกของพีเอ็มซีเอในการกระตุ้นการหลั่งอินสุลิน เกี่ยวข้องกับการเหนี่ยวนำแคลเซียมเข้าสู่เซลโดยผ่านทางแอลไทฟ์แคลเซียมชาแนล ไดอะซอกไซด์ไม่สามารถยับยั้งกลไกของพีเอ็มซีเอดังกล่าวในการกระตุ้นการหลั่งอินสุลินและเพิ่มระดับแคลเซียมภายในเซล นอกจากนี้พีเอ็มซีเอเพิ่มฤทธิ์ของกลูโคสและไกลบูไรด์และเสริมฤทธิ์ของเคซีแอลและแอลไทฟ์แคลเซียมชาแนลในการหลั่งอินสุลินและเพิ่มระดับแคลเซียมภายในเซล พีเอ็มซีเอสามารถเพิ่มระดับไวคลิกเอเอ็มพีภายในเซลรวมทั้งเสริมฤทธิ์ของฟอร์สโคลินซึ่งเป็นอะดินาลิลไซเคสแอกติเวเตอร์ แต่อย่างไรก็ตามพีเอ็มซีเอไม่สามารถเพิ่มไซคลิกเอเอ็มพีในกรณีที่กระตุ้นด้วยสามไอโซบิวทิลวันเมทิลแซนทีน พีเอ็มซีเอสามารถยับยั้งการทำงานของเอนไซม์อัลฟากลูโคซิเดสจากยีสต์ด้วยกลไกแบบแข่งขันได้แต่ไม่สามารถยับยั้งเอนไซม์ดังกล่าวจากสัตว์เลี้ยงลูกด้วยนมและเอนไซม์อัลฟาอะไมเลส

สาขาวิชา.... เภสัชวิทยา (สหสาขาวิชา).... ลายมือชื่อนิสิต.....
ปีการศึกษา.....2548..... ลายมือชื่ออาจารย์ที่ปรึกษา.....
ลายมือชื่ออาจารย์ที่ปรึกษาร่วม .....

4489109020 : MAJOR PHARMACOLOGY

KEY WORD: ANTIDIABETIC / *p*-METHOXYCINNAMIC ACID / MECHANISMS

SIRICHAI ADISAKWATTANA : ANTIDIABETIC EFFECTS AND MECHANISMS OF ACTION OF *p*-METHOXYCINNAMIC ACID THESIS ADVISOR: PROF. SOPHON ROENGSUMRAN, Ph.D. THESIS COADVISOR ASSOC.PROF. SIRINTORN YIBCHOK-ANUN, D.V.M., Ph.D., pp.119 ISBN 974-53-2540-6.

p-MCA decreased fasting plasma glucose and increased insulin concentrations in both normal and diabetic rats. In addition, it improved also glucose intolerance in diabetic rats. During 4 weeks of the study, *p*-MCA reduced plasma glucose concentration in diabetic rats but not in normal rats. *p*-MCA reduced the excessive activities of hepatic glucose-6-phosphatase, and increased hepatic hexokinase, glucokinase, phosphofructokinase, hepatic glycogen in diabetic rats.

p-MCA increased insulin secretion from the perfused rat pancreas and INS-1 cells in a concentration-dependent manner. In addition, *p*-MCA increased intracellular Ca^{2+} concentration ($[Ca^{2+}]_i$) in INS-1 cells. The *p*-MCA-induced insulin secretion and rise in $[Ca^{2+}]_i$ were markedly inhibited in the absence of extracellular Ca^{2+} or in the presence of an L-type Ca^{2+} channel blocker nimodipine. Diazoxide, an ATP-sensitive K^+ channel opener, did not alter *p*-MCA-induced insulin secretion, nor $[Ca^{2+}]_i$ response. These results suggested that *p*-MCA increased Ca^{2+} influx via the L-type Ca^{2+} channels, but not through the closure of ATP-sensitive K^+ channels In addition, *p*-MCA enhanced glucose- and glyburide-induced insulin secretion and it also the increase in insulin secretion and a rise of $[Ca^{2+}]_i$ induced by KCl- and Bay K 8644, an L-type Ca^{2+} channel. Furthermore, *p*-MCA increased cyclic AMP content of INS-1 cells and enhanced the increase of cyclic AMP content induced by forskolin; however, *p*-MCA failed to enhance the effect of a phosphodiesterase inhibitor 3-isobutyl-1-methylxanthine. *p*-MCA was a potent competitive inhibitor against yeast α-glucosidase However, it had no inhibitory activities on mammalian α-glucosidases and α-amylase.

Field of study....Pharmacology(Inter-department) Student's signature..S. Adisakwattana

Academic year.....2005..... Advisor's signature.....

Co-advisor's signature....S. Yibchokanun.

ACKNOWLEDGEMENTS

I am deeply indebted to Professor Dr. Sophon Roengsumran, Associate Professor Dr. Sirintorn Yibchok-anun and Professor Dr. Walter H. Hsu for their helping, stimulating suggestions and encouragement at all time of research and writing of this dissertation.

I would like to thank the members of my dissertation committee, Professor Dr.Chaivat Toskulkao, Associate Professor Dr.Suman Chompootaweep, Associate Professor Dr.Supatra Srichairat and Assistant Professor Dr.Suree Jianmongkol for their valuable discussion and advice.

I wish to extend my warmest thanks to all those who have helped me with my work in the Research Centre for Bioorganic Chemistry, Department of Chemistry, Faculty of Science, Department of Pharmacology, Faculty of Veterinary Science, Chulalongkorn University and Department of Biomedical Sciences, College of Veterinary Medicine, Iowa state University, USA.

I would also like to express my appreciation to my family and Assistant Professor Wilaiwon Tiravanit for their great support and encouragement throughout the course of my education and I am grateful thank to all friends for their friendship and help during my graduate studies.

Moreover, thanks are extended to the Thailand Research Fund (RGJ) and National Science and Technology Development Agent (NSTDA) for The Royal Golden Jubilee Ph.D scholarship and Local Graduate scholarship.

Many more persons participated in various ways to ensure my dissertation succeeded than those and I am thankful for them all.

CONTENTS

LIST OF FIGURES

LIST OF TABLES

ABBREVIATIONS

AMPK	=	adenosine monophosphate-activated protein kinase
AUC	=	Area under the curve
BSA	=	Bovine serum albumin
DAG	=	diacylglycerol
DHP	=	dihydropyridine
EDTA	=	ethylenediaminetetraacetic acid
EGTA	=	ethylene glycol bis(2-aminoethyl ether)-N,N,N'N'-tetraacetic acid
ER	=	endoplasmic recticulum
FBP	=	fasting plasma glucose
GLP-1	=	glucagon-like-peptide-1
GLUT	=	glucose transporter
G6P	=	glucose-6-phosphate
G6Pase	=	glucose-6-phosphatase
G6PDH	=	glucose-6-phosphate dehydrogenase
IDDM	=	Insulin-Dependent Diabetes Mellitus
IP_3	=	inositol 1,4,5-triphosphate
K_{ATP} channel	=	ATP-sensitive K^+ channels
KRB	=	Krebs-Ringer bicarbonate buffer
NADH	=	nicotinamide adenine dinucleotide
NADPH	=	nicotinamide adenine dinucleotide phosphate
NB-DNJ	=	N-butyldeoxynojirimycin
NIDDM	=	Noninsulin-Dependent Diabetes mellitus
NMDA	=	N-methyl-D-aspartate
MAPK-1	=	mitogen-activated protein kinase 1
PDEs	=	cyclic nucleotide phosphodiesterases
PDK-1	=	3-phosphoinositide-dependent protein kinase 1
PEPCK	=	phosphoenolpyruvate carboxykinase
PI3K	=	phosphatidylinositol 3-kinase
PLC	=	phospholipase C

PPARγ	=	peroxisome proliferator-activated receptor gamma
PPG	=	postprandial plasma glucose
p-MCA	=	*p*-methoxycinnamic acid
SREBP-1	=	sterol-regulatory-element-binding-protein-1
SUR	=	sulfonylurea receptor
STZ	=	streptozotocin
TNF-α	=	tumor necrosis factor- α
VDCC	=	Voltage-dependent calcium channels

CHAPTER I

INTRODUCTION

Diabetes Mellitus (DM) is a group of metabolic diseases characterized by hyperglycemia, dyslipidemia, and abnormal protein metabolism that results from defects in both insulin secretion and/or insulin action. This disease is a major health problem associated with reduced quality of life and increased risk factors for mortality and morbidity. It is estimated that the global total number of persons with diabetes will rise from 151 million in the year 2000, to 221 million by the year 2010 and to 300 million by 2025 (King et al., 1998). This rise is predicted with the greatest increases expected in developing countries from every nation in the world (Zimmet et al., 2001). There are mainly two types of diabetes, namely type 1 and type 2. Type 1 diabetes, the insulin-dependent diabetes mellitus (IDDM), the disease in which the body does not any insulin, most often occurs in children and young adults. Patients with type 1 diabetes must take daily insulin injections to control the condition. Type 1 diabetes accounts for 5–10% of DM. Type 2, noninsulin-dependent diabetes mellitus (NIDDM), the disease in which the body does not secrete sufficient, or properly use, insulin, is the most common form of the disease. It accounts for 90–95% of diabetes. Type 2 diabetes is nearing epidemic proportions, due to an increased number of elderly people, and a greater prevalence of obesity and sedentary lifestyles

The long-term hyperglycemia is an important factor in the development and progression of micro- and macrovascular complications, which include neuropathy, nephropathy, cardiovascular and cerebrovascular diseases (Altan et al., 2003; Strojek et al., 2003). The underlying goal of all diabetes treatment and management is to maintain an appropriate blood glucose concentration. Four major classes of oral hypoglycemic agents have been used extensively in treatment of type 2 DM: insulin secretagogues, biguanides, thiazolidinediones and α-glucosidase inhibitors (Charpentier, 2002). Each drug class works on different mechanism of actions, including stimulation of insulin secretion, reduction of hepatic gluconeogenesis, increase in insulin receptor sensitivity

and delay of digestion and absorption of carbohydrate. Unfortunately, these agents could produce severe hypoglycemia, weight gain and gastrointestinal disturbances.

Cinnamon is one of the natural products that has been explored for antidiabetic activity. It increases glucose uptake and glycogen synthesis (Jarvill-Taylor et al., 2001; Qin et al., 2003), and improves glucose and lipid profiles of type 2 diabetic patients (Khan et al., 2003). The main constituent of cinnamon bark is cinnamon oil that contains mainly cinnamic acid, cinnamaldehyde, and cinnamic alcohol (Morozumi, 1978). Interestingly, cinnamic acid and it derivatives have been reported to possess a variety of pharmacological properties, including hepatoprotective (Perez-Alvarez et al., 2001), anti-malarial (Wiesner et al., 2001), antioxidant (Natella et al., 1999), and antihyperglycemic activities (Liu et al., 1999).

p-Methoxycinnamic acid (*p*-MCA) has been isolated from the roots of *Scrophularia buergeriana* (Kim et al., 2000). The interest in biological activities of this compound has been accelerated in recent years. For examples, *p*-MCA has shown the hepatoprotective activity in CCl_4-induced toxicity in rat hepatocytes (Lee et al., 2002). It also exerts protective effect against glutamate-induced neurodegeneration in cortical neurons (Kim et al., 2002). However, the antidiabetic effect of *p*-MCA has not been reported in any literatures. The purpose of this study was to investigate the antihyperglycemic effects of *p*-MCA in normal and streptozotocin (STZ)-induced diabetic rats. Furthermore, the effects of *p*-MCA on the activities of hepatic enzymes in normal and diabetic rats were also investigated in an effort to reveal possible mechanisms underlying its antihyperglycemic effect. Moreover, the effect of *p*-MCA-stimulated insulin secretion and its signaling pathways were examined. Finally, *p*-MCA was investigated for α-glucosidases and α-amylase inhibition.

1.1 Objectives of the study

1. To investigate the antihyperglycemic effects of *p*-MCA in normal and streptozotocin (STZ)-induced diabetic rats

2. To determine the effects of *p*-MCA on the activities of hepatic enzymes in normal and diabetic rats

3. To investigate the stimulatory effects and mechanism of action of *p*-MCA on insulin secretion

4. To investigate the inhibitory effects of *p*-MCA on α-glucosidase, pancreatic lipase and α -amylase

1.2 Research hypothesis

p-MCA shows the hypoglycemic effect by stimulating insulin secretion from pancreas. The compound displays the extrapancreatic effect such as increase of hepatic glycolytic and decrease of hepatic gluconeogenic enzymes, and inhibition of alpha glucosidase, and alpha amylase enzymes.

CHAPTER II

LITERATURE REVIEW

2.1 Diabetes Mellitus

Classifications, causes and complications of diabetes

In 1979, The National Diabetes Data group formally classified diabetes mellitus and other categories of glucose intolerance as follows:

Type 1 diabetes, previously known as Insulin-dependent Diabetes Mellitus or IDDM, is characterized by the marked inability of the pancreas to secrete insulin from β-cells. The onset of type 1 diabetes is usually in childhood and early adulthood (< 35 years). The first clinical symptoms are polydipsia, polyuria, loss of weight and a tendency to keto-acidosis of the patients. The pathogenesis of type 1 diabetes involves environmental triggers that may activate autoimmune mechanisms in genetically susceptible individuals, leading to progressive loss of pancreatic islet β-cells (Von Herrath and Homann, 2003). In addition, type 1 diabetes has been postulated that environmental factors such as certain viral infections and possibly chemical or nutritional agents may worsen these genetic factors.

Type 2 diabetes, previously known as non-Insulin dependent Diabetes Mellitus or NIDDM, is characterized by impaired insulin secretion and/or peripheral insulin resistance in liver, skeletal muscle, and adipocytes (Hauner H, 2004). Type 2 diabetes occurs in approximately 90% of all diabetic patients in the world. The onset of the disease is usually between 40 and 75 years of age. The defects in insulin secretion include a markedly impaired and often absent first-phase glucose-induced insulin release, while second-phase insulin release is often impaired by more than 50%.

Other types of diabetes can be subdivided according to known (Gabir et al., 2000) or suspected etiological relationships, where diabetes may be secondary to:

1. Pancreatic disease such as pancreatitis, pancreatectomy, fibrocalculous pancreatopathy, and cystic Fibrosis

2. The administration of certain hormones, drugs and chemical agents, such as oral contraceptives, tricyclic antidepressants, diazoxide and nicotinic acid

3. Insulin receptor abnormalities, either in the number of receptors or their affinity for insulin, or even because of the presence of antibodies to receptors (with or without associated immune disorders)

4. Certain genetic syndromes, *e.g.* metabolic disorders, insulin resistance, hereditary muscle disorders and cytogenic disorders like Down's syndrome

5. Gestational diabetes mellitus (GDM), which occurs simultaneously during pregnancy, usually in the second or third trimester.

2.2 Diagnostic Criteria for Diabetes Mellitus

Diabetes mellitus is diagnosed on the basis of WHO recommendations from 1999, incorporating both fasting and 2-h after glucose load (75 g) criteria into a practicable diagnostic classification (Table 2.1).

A normal fasting plasma glucose level is less than 110 mg per dL (6.1 mmol/l) and normal 2h postprandial plasma glucose (PPG) concentration are less than 140 mg/dl (7.75 mmol/l). Blood glucose concentration above the normal level but below the criterion established for diabetes mellitus indicate impaired glucose homeostasis. Persons with fasting plasma glucose levels ranging from 110 to 126 mg/dl (6.1 to 7.0 mmol/l) are classified to have impaired fasting glucose, while those with a 2hrPPG level between 140 mg per dL (7.75 mmol/l) and 200 mg/ dl (11.1 mmol/l) are classified to have impaired glucose tolerance. Both impaired fasting glucose and impaired glucose tolerance are associated with an increased risk of developing type 2 diabetes mellitus.

Person with fasting plasma glucose levels over 126 mg/dl (> 7.0 mmol/l) and normal 2hPPG levels are higher 200 mg/dL (11.1 mmol/l) are classified to be diabetes mellitus.

Table 2.1 Criteria for the Diagnosis of Diabetes Mellitus and Impaired Glucose Homeostasis

---

Diabetes mellitus--positive findings from any two of the following tests on different days:

DM with plasma glucose concentration ≥ 200 mg/dl (11.1 mmol/l) or

FPG ≥126 mg/dl (7.0 mmol/l) or

2hPPG ≥200 mg/dl (11.1 mmol/l) after a 75-g glucose load

Impaired glucose homeostasis

Impaired fasting glucose: **FPG** from 110 to <126 mg/dl (6.1 to 7.0 mmol/l)

Impaired glucose tolerance: **2hPPG** from 140 to <200 mg/dl (7.75 to <11.1 mmol/l)

Normal

FPG <110 mg/dl (6.1 mmol/l)

2hrPPG <140 mg/dl (7.75 mmol/l)

Adapted from Report of the Expert Committee on the Diagnosis and Classification of Diabetes Mellitus. Diabetes Care 1997; 20:1183-97.

2.3 Pathogenesis of type 2 diabetes

Type 2 diabetes is a metabolic disorder that results from complex interactions of multiple factors. It is characterized by 2 major defects: 1) decreased secretion of insulin by the pancreas and 2) resistance to the action of insulin in various tissues (muscle, liver and adipose), which results in impaired glucose uptake. The precise molecular mechanism of insulin resistance is not clearly understood. However, the deficits in the postinsulin receptor intracellular signaling pathways are believed to

play a major/essential role (Virkamaki et al.,1999; Saltiel and Kahn, 2001). Insulin resistance, which is usually present before the onset of diabetes, is determined by a number of factors, including genetics, age, obesity and, later in the disease, hyperglycemia itself. Excess visceral adiposity, dyslipidemia and hypertension often accompany insulin resistance. Other findings may include impaired fibrinolysis, increased platelet aggregation, vascular inflammation, endothelial dysfunction and premature atherosclerosis (Fonseca, 2003). The inability to suppress hepatic glucose production is a major contributor to the fasting hyperglycemia seen in diabetes (Firth et al.,1987).

The increase in lipolysis by adipocytes that are resistant to insulin and the subsequent increased levels of circulating free fatty acids also contribute to the pathogenesis of type 2 diabetes by impairing β-cell function, decreasing glucose uptake in skeletal muscles and promoting glucose release from the liver (Yaney and Corkey, 2003). In addition to its role as a source of excess circulating free fatty acids, adipose tissue has emerged in the last decade as an endocrine organ. Adipose tissue is a source of a number of hormones (adipo-cytokines or "adipokines") that appear to regulate insulin sensitivity (e.g., adiponectin, resistin), as well as appetite regulation (e.g., leptin), inflammation (e.g., tumour necrosis factor-α, interleukin-6 and coagulability (e.g., plasminogen activator inhibitor-1). The initial response of the pancreatic β-cell to insulin resistance is to increase insulin secretion. As the disease progresses, pancreatic insulin production and secretion decrease, which lead to progressive hyperglycemia. Postprandial hyperglycemia can precede fasting hyperglycemia. Hyperglycemia itself exacerbates insulin resistance and impairs insulin secretion, which is called "glucotoxicity." The cause of progressive pancreatic β-cell failure is not completely understood, but it appears to result from a number of factors, including genetic determinants, chronic inflammation, glucotoxicity and the deleterious effects of elevated levels of free fatty acids on β-cell function, which is called "lipotoxicity" (Buchanan, 2003; Kashyap et al., 2003)

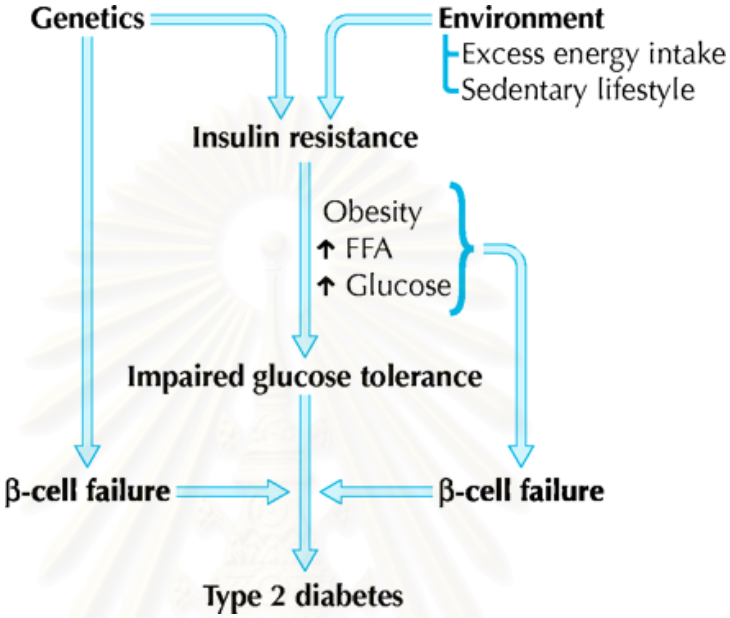

Figure 2.1 Overview of the pathogenesis of type 2 diabetes mellitus. FFA = free fatty acids (Figure :Cheng and Fantus, 2005).

These interacting defects in multiple organs such as muscle, liver, adipose tissue and pancreas, which generate the pathogenic milieu that results in diabetes. Various classes of oral antihyperglycemic agents are now available that target the different pathophysiologic factors contributing to diabetes. For examples, α-glucosidase inhibitors to delay intestinal carbohydrate absorption, biguanides to target hepatic insulin resistance, insulin secretagogues to increase pancreatic insulin secretion, insulin sensitizers or thiazolidinediones to target adipocyte and muscle insulin resistance, and intestinal lipase inhibitor or orlistat to inhibit fat absorption and promote weight loss in obese patients.

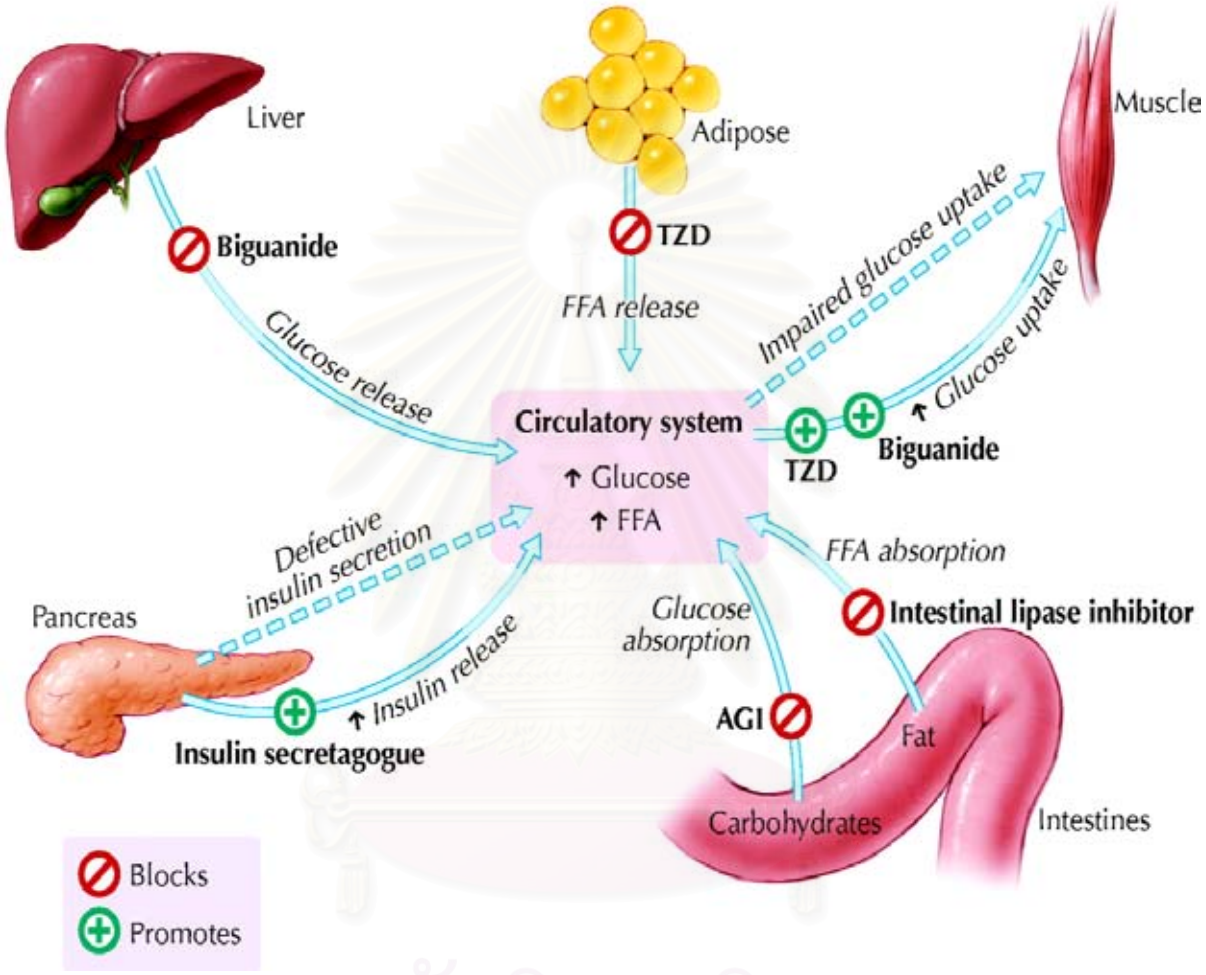

Figure 2.2 Major target organs and actions of orally administered antihyperglycemic agents in type 2 diabetes mellitus. TZD = thiazolidinedione; FFA = free fatty acid; AGI = α-glucosidase inhibitor (Figure :Cheng and Fantus, 2005).

2.4 Oral antidiabetic drugs

Insulin secretagogues

Insulin secretagogues can be divided into 2 subclasses: sulfonylureas and non-sulfonylureas. Sulfonylureas are commonly used in type 2 diabetic patients, including gliclazide, glimepiride, and glyburide. The new class of non-sulfonylureas are currently represented by nateglinide and repaglinide.

Mechanism of sulfonylureas activates insulin secretion *via* binding to the sulfonylurea receptor on the surface of pancreatic β-cells. The sulfonylurea receptor is intimately involved with subunits of an adenosine triphosphate-sensitive potassium channel (kir6.2). The binding of a sulfonylurea to the sulfonylurea receptor–kir6.2 complex results in closure of the potassium channels and inhibition of the efflux of potassium ions from the β-cell (Fig 2.3). This results in depolarization of the cell membrane and, in turn, opens voltage-dependent calcium channels. The influx of calcium ion causes microtubules to contract and the exocytosis of insulin from vesicles. The mechanism of action of non-sulfonylureas is similar to that of the sulfonylureas

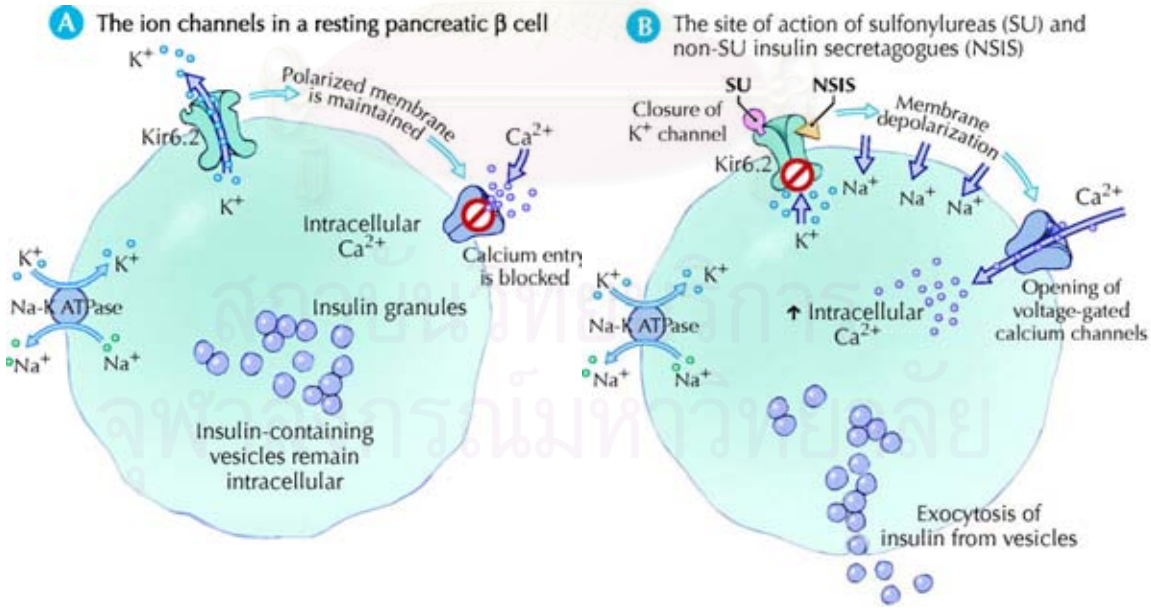

Figure 2.3 Insulin secretagogues mimic glucose to close adenosine triphosphate-sensitive potassium channels (kir6.2) and stimulate insulin secretion. (A) shows the K_{ATP} channel in a resting pancreatic β-cell. (B) shows the action of insulin secretagogues on the cell (Figure :Cheng and Fantus, 2005).

(closure of the K_{ATP} channel, leading to calcium-dependent insulin secretion). However, they bind to the sulfonylurea receptor at a different site and with different kinetics than the sulfonylureas (Proks et al., 2002). The main side effects of sulfonylureas are hypoglycemia and weight gain. The risk of hypoglycemia of non-sulfonylureas is lower than that with sulfonylureas (Phillips and Dunning, 2003).

Biguanides

Over 30 years ago, various biguanides (e.g., metformin, phenformin, buformin) were used in different countries for the treatment of diabetes. Phenformin was removed from the international market because of the associated high risk of lactic acidosis (Bailey and Turner, 1996). Only metformin is clinical used for treatment of DM at this time.

The mechanisms by which metformin exerts its antihyperglycemic effects are still not entirely clear. Its major action is to decrease hepatic glucose output, primarily by decreasing gluconeogenesis, but it may also, as a lesser effect, increase glucose uptake by skeletal muscles (Kirpichnikov et al., 2002). Metformin also activates hepatic and muscle adenosine monophosphate-activated protein kinase (AMPK), an enzyme normally activated by adenosine monophosphate (Fig. 2.4), the breakdown product of adenosine triphosphate and a cellular signal for increased energy requirements (Zhou et al., 2001). Activation of hepatic AMPK results in the phosphorylation and inhibition of acetyl-coenzyme A carboxylase, which catalyzes the rate-limiting step of lipogenesis. This block in fatty acid synthesis promotes fatty acid oxidation. In addition, activation of hepatic AMPK decreases expression of sterol-regulatory-element-binding-protein-1 (SREBP-1), a transcription factor implicated in the pathogenesis of insulin resistance, dyslipidemia and diabetes. Decreased SREBP-1 expression results in decreased gene expression of lipogenic enzymes, which further contributes to decreased triglyceride synthesis and hepatic steatosis. AMPK activation appears to be a critical step in the metformin-mediated reduction of hepatic glucose production and increase in skeletal muscle glucose uptake. Thus, AMPK is a major regulator of lipid and glucose metabolism and may be the key mediator of all the

beneficial effects of metformin. Results of earlier studies, particularly those using other biguanide compounds (e.g., phenformin, buformin), suggest that another mechanism of action may be disruption of coupled oxidative phosphorylation in mitochondria (Kirpichnikov et al., 2002). Whether this underlies the increase in AMPK activity because of a subtle increase in the ratio between adenosine monophosphate and adenosine triphosphate remains unclear. Other effects, such as increased expression of muscle hexokinase and the insulin-sensitive glucose transporter, may be secondary phenomena (Holmes et al., 1999).

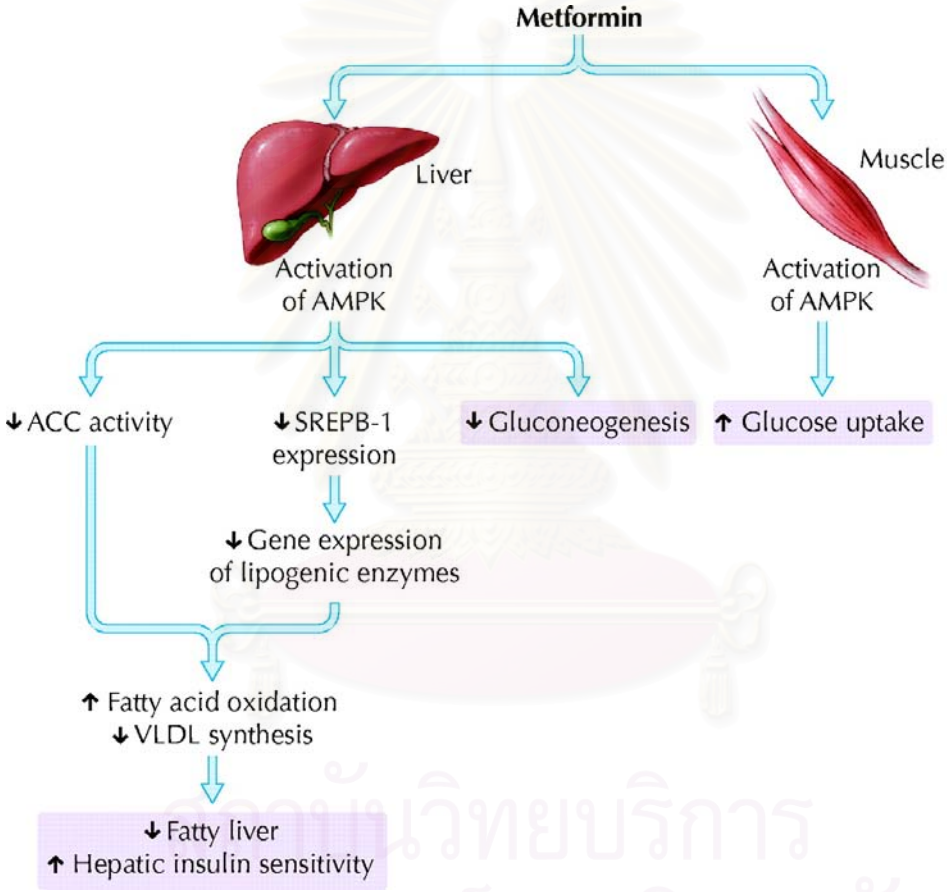

Figure 2.4 Metformin activates AMPK in liver and muscle to improve glucose and lipid MetabolismAMPK = adenosine monophosphate-activated protein kinase; ACC = acetyl-CoA carboxylase; SREPB-1 = sterol-regulatory-element-binding-protein-1; VLDL = very low density lipoprotein
(Figure :Cheng and Fantus, 2005).

Thiazolidinediones

The 2 thiazolidinediones currently available are rosiglitazone and pioglitazone. Troglitazone, an earlier thiazolidinedione introduced in 1997 in the United States, was removed from the world market because of an unacceptable risk of fulminant hepatic failure.

Thiazolidinediones function as ligands for the peroxisome proliferator-activated receptor gamma (PPARγ), which is most highly expressed in adipocytes (Fig. 2.5). These nuclear receptors, which are ligand-activated transcription factors, play an integral part in the regulation of the expression of a variety of genes involved in carbohydrate and lipid metabolism (Lohray and Bhushan, 2004). Thiazolidinediones improve insulin sensitivity, particularly in the peripheral tissues. Although unproven, this appears to be mainly mediated through an effect on adipocytes, since there are fewer PPARγ receptors in muscle tissue. In the adipocyte, differentiation is enhanced, lipolysis is reduced, and levels of circulating adipo-cytokines or "adipokines" are altered, namely a decrease in tumor necrosis factor-α and leptin and an increase in adiponectin. The recruitment of a greater number of smaller adipocytes, which is associated with improved lipogenesis and storage, results in a reduction in circulating free fatty acids. Decreased tumor necrosis factor-α and free fatty acid levels and increased adiponectin levels are expected to enhance insulin sensitivity (Aldhahi and Hamdy, 2003).

α-glucosidase inhibitor

α-glucosidase inhibitors currently available are acarbose, voglibose, and miglitol. These drugs do not target a specific pathophysiologic aspect of diabetes. α-glucosidase inhibitor competitively inhibits enzymes in the small intestinal brush border (Fig 2.6) that are responsible for the breakdown of oligosaccharides and disaccharides into monosaccharides suitable for absorption (Lebovitz, 1997). It works primarily on α-glucosidase, which is found predominantly in the proximal half of the small intestine. The intestinal absorption of carbohydrates is therefore delayed and shifted to more distal parts of the small intestine and colon. This decreases glucose entry into the systemic

circulation and lowers postprandial glucose levels. α-Glucosidase inhibitors act locally at the intestinal brush border and are not absorbed. They are excreted into feces.

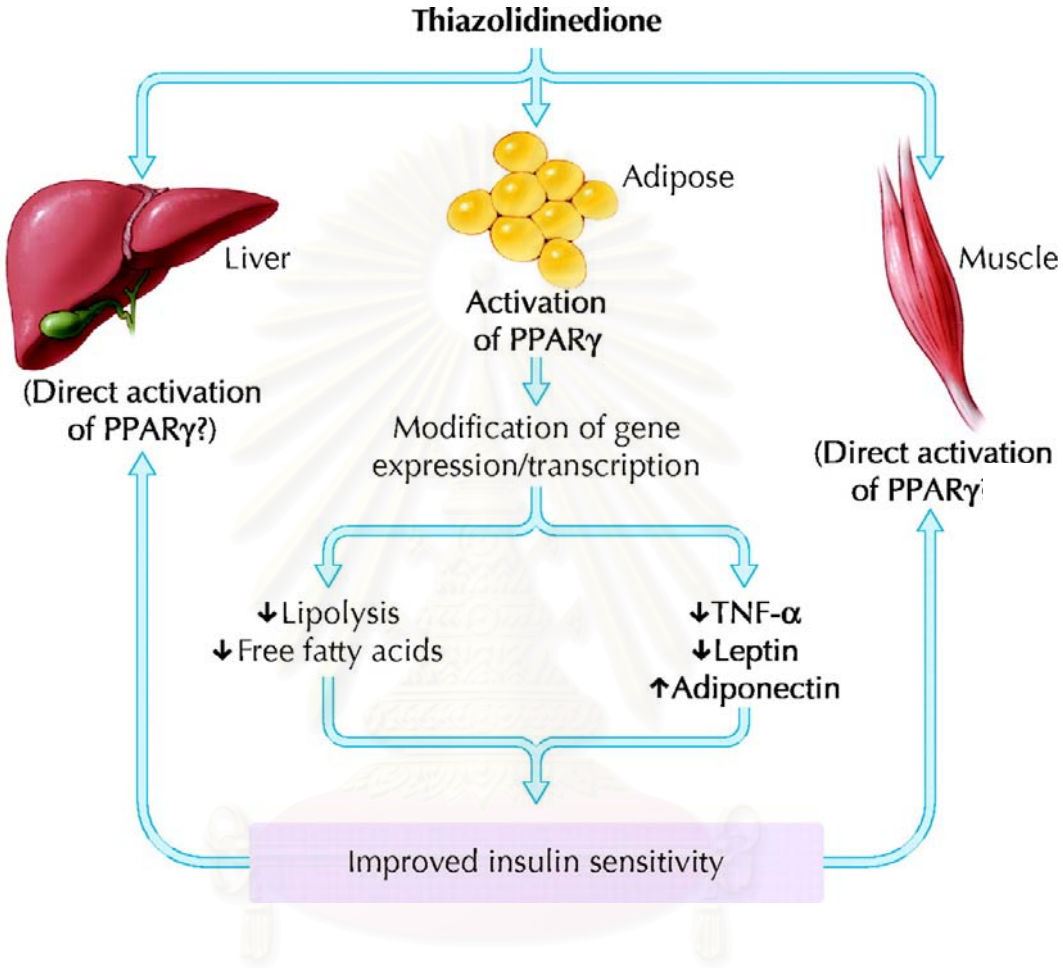

Figure 2.5 Mechanism of action of thiazolidinediones. PPARγ = peroxisome proliferator-activated receptor-gamma; TNF-α = tumor necrosis factor- α. (Figure :Cheng and Fantus, 2005).

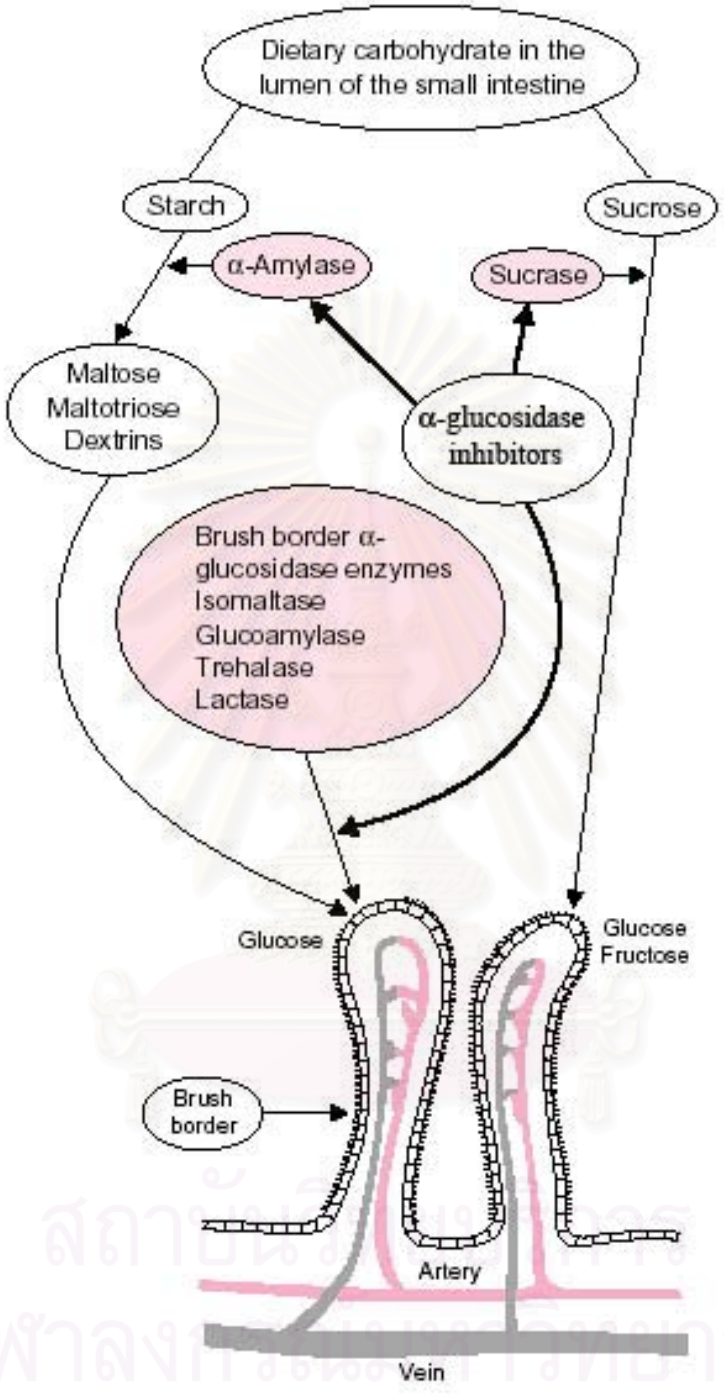

Figure 2.6 The schematic representation of enzymatic degradation of carbohydrates by glucosidases. The bold arrows indicate the points at which α-glucosidase inhibitors delay carbohydrate degradation, consequently, inhibit the uptake of glucose in the small intestine and reduce the increase in postprandial plasma glucose levels (Adapted from Scott and Spencer, 2000).

2.5 The synthesis, distribution, and degradation of insulin

Insulin is a pluripotent hormone in that has a wide sphere of influence. It directly or indirectly affects virtually every organ and tissue in the body. The main function of insulin is to stimulate anabolic reactions for carbohydrates, proteins and fats. All of which will have the metabolic consequence of producing a lowered blood glucose level. Molecular weight of insulin is 5,700-6,100 daltons.

Insulin is synthesized from a single-chain precursor of 110 amino acids termed preproinsulin at the β-cells of pancreatic islets (Beckers and Balch, 1989). After translocation through the membrane of the rough endoplasmic reticulum, the 24-amino acid N-terminal signal peptide of preproinsulin is rapidly cleaved off to form proinsulin. After cleavage of proinsulin by proprotein convertases and carboxypeptidase H, insulin is stored in secretory granules as osmotically inactive zinc-insulin crystals. Insulin is composed of two separate peptide chains, designated as the A chain and the B chain. These two chains are joined together by two disulfide bridges. The A chain consists of 21 amino acid residues and the B chain of 30 amino acid residues. The primary amino acid of human insulin is shown in figure 2.7

Insulin circulates in the blood as the free monomer, and its volume of distribution approximates the volume of extracellular fluid. Under fasting conditions, the pancreas secretes about 40 micrograms of insulin per hour into the portal vein, to achieve a concentration of insulin in portal blood of 2 to 4 ng/ml, and in the peripheral circulation of 0.5 ng/ml or about 0.1 nM. The half life of insulin in plasma is about 5 to 6 minutes in normal subjects and patients with uncomplicated diabetes. Degradation of insulin occurs primarily in the liver (60%, mainly as first passage), and the kidney (30%). The renal handling of insulin involves filtration, reabsorption in the proximal tubules, followed by degradation. The rest of insulin degradation mainly occurs in muscle. Adipose tissue is less capable of internalizing and degradating insulin (Sodoyez et al., 1983).

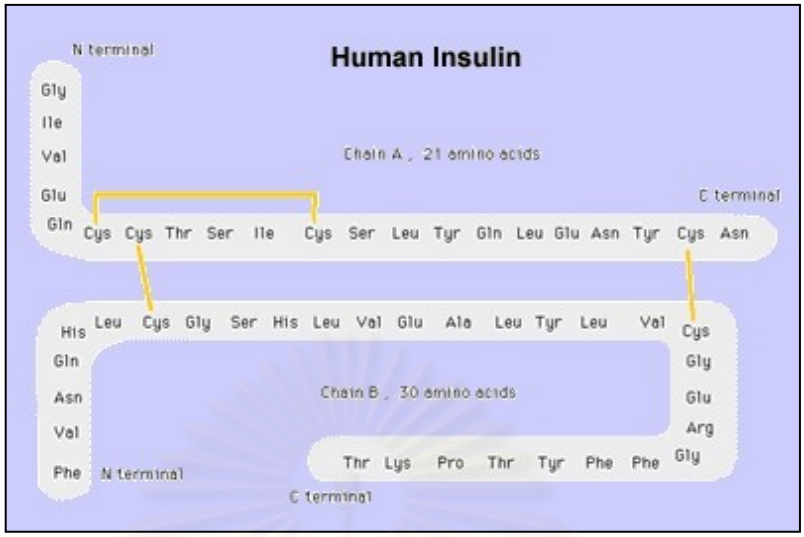

Figure 2.7 The primary sequence of human insulin

(Figure : Gerritsen, http://www.expasy.org/spotlight/back_issues/sptlt009.shtml)

2.6 The molecular mechanisms of insulin secretion

Blood glucose levels are very tightly controlled by rapid pulsatile release of insulin from β-cells (Fig 2.8). Glucose equilibrates through the glucose transposrter (GLUT2) across the plasma membrane of the β-cells. It is rapidly phosphorylated to glucose-6-phosphate by glucokinase, which thereafter determines the rate of glycolysis. This enzyme acts as the glucose sensor and pyruvate generation for entry into the tricarboxylic acid (TCA) cycle in the mitochondria. Subsequent oxidative metabolism provides the link between the products of glucose metabolism and insulin secretion. The resultant increase in the ATP/ADP ratio in the cytosol causes depolarization of plasma membrane by closure of the ATP-sensitive K^+ channels (K_{ATP} channel). This permits opening of voltage-dependent Ca^{2+} channels and an increase in cytosolic Ca^{2+}, which then triggers fusion of insulin-containing secretory vesicles to the plasma membrane, and exocytosis of insulin flows rapidly (Eliasson et al.,1997).

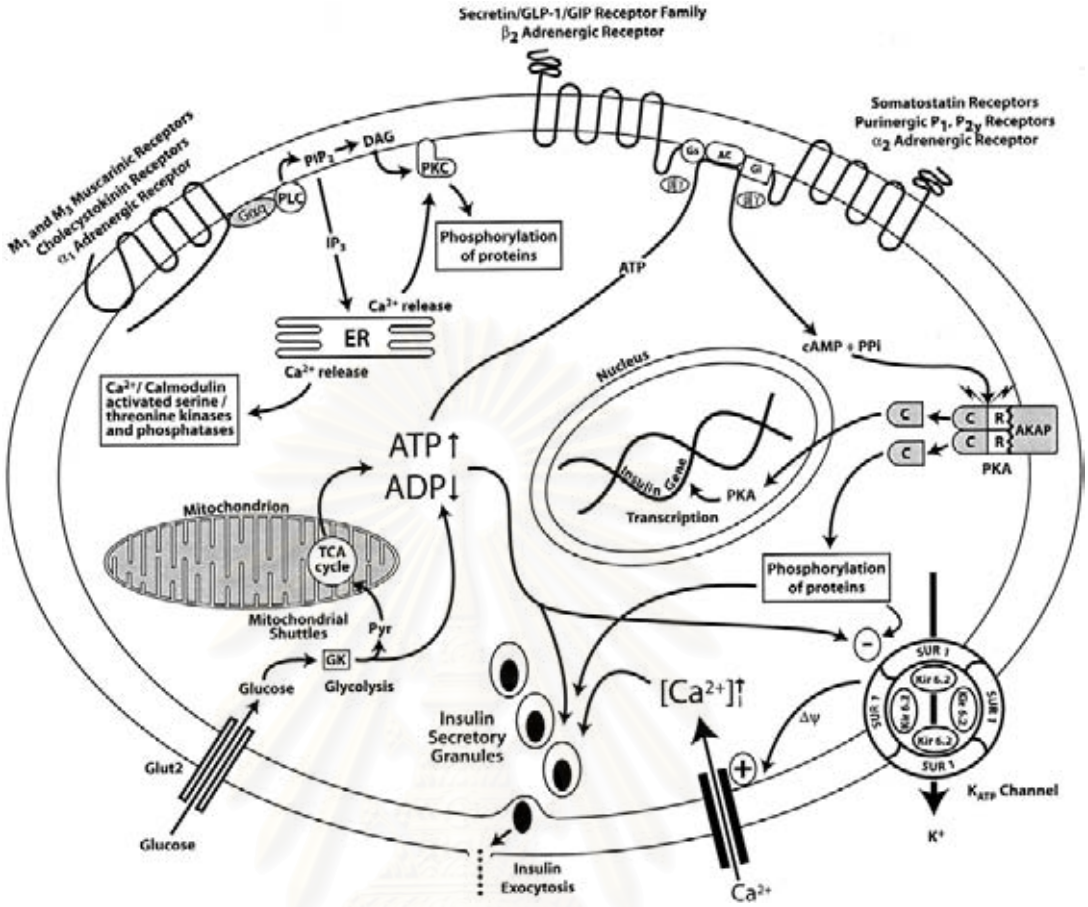

Figure 2.8 Schematic showing of the main molecular mechanisms of insulin secretion in pancreatic β-cells (Figure: Doyle and Egan, 2003).

The G-protein-coupled receptors present on the plasma membrane of the β-cells belong to G-protein-coupled receptors. Includes in this family are glucagon-like-peptide-1 (GLP-1), glucagon, secretin, pituitary adenylyl cyclase activating peptide, calcitonin, parathyroid hormone and calcitonin gene-related peptide receptors. These proteins are ligands for hormone-specific seven-transmembrane receptors that are coupled to the Gs protein and stimulate adenylyl cyclase. Activation of adenylyl cyclase leads to an increase cAMP in production and results in a significant up regulation of the activity of the cAMP-dependent protien kinase A (PKA) family, comprising ubiquitous serine/threonine phosphorylating enzymes. This leads to cascade in which phosphorylation of vesticular plasma membrane protein, voltage-dependent calcium

channels (VDCC), and potentially other ion channels. This effect results in augmentation of glucose-induced exocytosis of insulin, as well as phosphorylation of transcription factors, which increases insulin gene promoter activity (Liang and Matschinsky, 1994).

Cyclic nucleotide Phosphodiesterases (PDEs) is enzyme, which hydrolyzes cyclic AMP and cyclic GMP to their biologically inactive 5' derivatives. At least 11 families of PDEs have been identified. PDEs, present in β-cells, have been determined as total PDE activities from crude islet preparations and the presence of PDEs 1, 3, 4, and calcium-sensitive PDEs (Conti, 2000). Cyclic nucleotide is generally known as an important amplifier of glucose induced insulin release (Holz and Habener, 1992), particularly when its cellular concentrations are increased by various gut hormones implicated as incretins. In addition, cyclic AMP augments glucose-induced insulin secretion through a number of mechanisms including increased opening of VDCC (et al., 1998), Ca^{2+}-induced Ca^{2+}-release (Kang et al.,2001), activation of ryanodine receptors in the ER (Islam et al., 1998) and direct effects on exocytosis (Harndahl et al., 2001). 3-isobutyl-1-methylxanthine (IBMX) is a nonspecific inhibitor of phosphodiesterases which augments glucose-induced insulin secretion and has been used widely as a tool to investigate the role of cAMP in β-cell.

Activation of the muscarinic receptors on the β-cells of the pancreas mediates insulin secretion. Acetylcholine (ACh), the major parasympathetic neurotransmitter, is released by intrapancreatic vagus nerve endings during the preabsorptive and absorptive phases of feeding. In β-cells, ACh binds to muscarinic M_3 receptors and are coupled to Gq, which activates PLC, subsequently, generates diacylglycerol (DAG). ACh also activates PLA_2, then produces arachidonic acid and lysophosphatidylcholine. These phospholipid-derived messengers, particularly diacylglycerol, activate PKC, thereby increasing the efficiency of free cytosolic Ca^{2+} concentration $[Ca^{2+}]_i$ on exocytosis of insulin granules. Inositol 1,4,5-triphosphate (IP_3) also produced by PLC that causes a rapid elevation of free cytosolic Ca^{2+} concentration by mobilizing Ca^{2+} from the ER. The resulting fall in Ca^{2+} in the organelle produces a small capacitative Ca^{2+} entry (Gilon and Henquin, 2001).

There is physiologic and pharmacologic evidence for the presence of inhibitory and stimulatory adrenoreceptors on the β-cell. The inhibitory α-adrenoreceptor has been characterized as being of the α_2-subtype (Cherksey et al., 1983) and the stimulatory β-adrenoreceptor as the β_2-subtype (Fyles et al., 1986). The α_2-subtype is coupled to G_i/G_o, and the β_2 is coupled to the Gs protein. Stimulation of the α_2-adrenoreceptors in the β-cell directly activate a G_i/G_o-gated K^+ channel, thereby inhibiting exocytosis (Rorsman et al., 1991). Epinephrine, which activates both types of adrenoreceptors, inhibits glucose-induced insulin secretion (Cawthorn and Chan, 1991) indicating that α_2 is the predominant adrenergic receptor in β-cells.

2.7 The molecular mechanisms of insulin action

The insulin receptor is structurally related to receptor tyrosine kinases (such as the epidermal growth factor receptor) and the cytokine receptor superfamily (tyrosine kinase-associated receptors). The insulin receptor is dimerized by disulfide bond formed between two α subunits in the absence of the ligand. The β subunits contain the transmembrane domain and the tyrosine kinase catalytic activity (Fig 2.9). The two α subunits bind a single ligand, which alters the conformation of the entire receptor leading to autophosphorylation of the β subunits (Jiang and Zhang, 2005). After autophosphorylation, receptor tyrosine kinases typically generate docking sites for second messenger proteins containing Src homology 2 (SH2) domain. Instead, they phosphorylate NPXY (Asn-Pro-X-Tyr) motifs, which bind proteins containing pleckstrin homology (PH) or the closely related phosphotyrosine binding (PTB) domains. The insulin receptor substrate (IRS) proteins (IRS-1 through IRS-4) contain a PH and a PTB domain in the tendem near their N-teminus. During a transient binding *via* the PH and PTB domians, the activated insulin receptor phosphorylates the IRS proteins at multiple tyrosine residues, thereby generating docking sites for proteins with SH2 domians. A single activated IRS docking protein may bind multiple second mesengers *via* SH2 domains, such as the SH2/SH3 adapter proteins, *Grb-2*, *nck*, *crk*, the tyrosine kinase *fyn*, the protein kinase C zeta (PKCζ) and, the most importantly, phosphatidylinositol 3-kinase (PI3-K).

A major pathway activated by IRS molecules involve PI3-K (Di Guglielmo GM et al., 1998), a dimer composed of a 110-kDa catalytic subunit, which is associated with one of five different SH2 domain protein regulatory subunits ($p555^{PIK}$, $p55^{\alpha}$, $p50^{\alpha}$, $p85^{\alpha}$, $p85^{\beta}$). The regulatory subnits vary with the target cell of insulin. PI3-K phosphorylates membrane lipids to yield phosphatidylinositol-3,4,5-triphosphate [PtdIns(3,4,5)P_3]. PI3-K activates protein kinase B (PKB) by a complex mechanism. PtdIns(3,4,5)P_3 locate in the inner leaflet of the membrane binds the PH domain of PKB. The results in a conformational change the expose a threonine residue of PKB to constitutively active PDK1 (3-phosphoinositide-dependent protein kinase 1). PtdIns(3,4,5)P_3 at the membrane activates PDK2, which phosphorylates a serine residue of PKB. After being phosphorylated at both sites, PKB detaches from the plasma membrane and phosphorylates its targets. PKB is also known as AKT or RAC, which serves as a focal point of several PI3-K mediated metabolic and growth factor-like effects of insulin. The metabolic actions of PKB include:

1. Translocation of GLUT4 from vesicular compartment to the cell surface plasma membrane in skeletal muscle.

2. Activation of cyclic nucleotide phosphodiesterase (cyclic PDE). Because stimulation of glucagon and β–adrenergic receptors achieve intracellular signaling by increasing cyclic AMP, insulin may directly antagonize these hormones *via* increasing the degradation of cyclic AMP. This mechanism may be important in the insulin-induced inhibition of hormone-sensitive lipase in adipose tissue, and the inhibition of glycogenolysis in liver and muscle.

3. Inactivation of glycogen synthase kinase-3 results in decreased phosphorylation state of glycogen synthase. This action equals to increased activity of glycogen synthase.

4. PKB directly activates acetyl-CoA carboxylase, thereby stimulating fatty acid synthesis. The action is complemented by an activation of PDH phosphatase, which activates PDH. The activation of PDH is an IRS-mediated action that does not involve the PI3-K-PKB pathway.

5. PKB induces nitric oxide synthase (NOS) in endothelial cells. The NO generated by the endothelium activates the soluble guanylyl cyclase in the adjacent vascular smooth muscle cells.

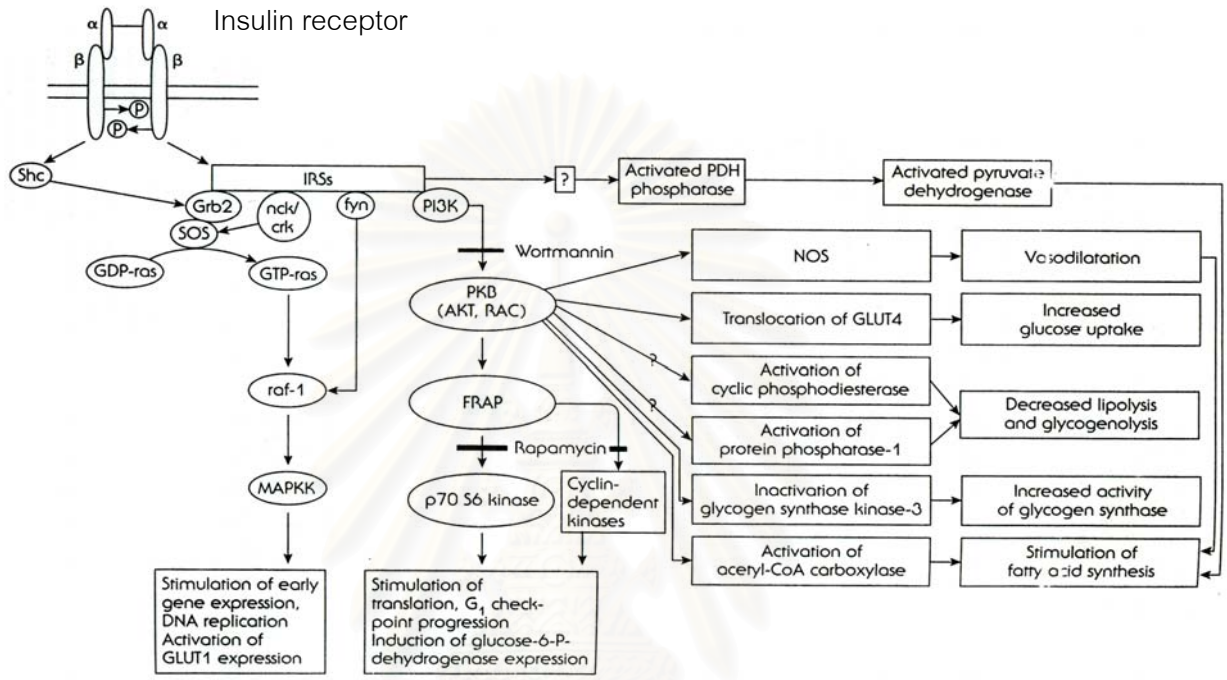

Figure 2.9 A model for the signaling cascade of insulin.

The activated insulin receptor participate in the mitogen-associated protein kinase pathway *via* the SH2/SH3 domain adapter proteins Grb-2, crk, and Nck or the tyrosine kinase fyn. The activation of the pathway results in early gene expression and stimulation of DNA replication. The activated insulin receptor recruits the MAP kinase pathway via a small SH2/SH3 domain adapter protein known as Grb-2. Depending on the cell type, Grb-2 may engage a number of insulin receptor-activated proteins such as IRS-1, IRS-2, or shc. The activated Grb-2 forms a complex with the guanine nucleotide exchange of GDP for GTP in $p21^{ras}$. The activated $p21^{ras}$ then recruits the MAP kinase pathway. Activation of the MAP-kinase pathway increases the expression of GLUt1 and stimulates glucose uptake. IRS molecules also serve as Grb-2 independent docking sites for other SH2/SH3 adapter proteins such as crk and nck, which may also activate the MAP-kinase pathway *via* SOS. Fyn, a tyrosine kinase, also may bind to IRS and activate the MAP-kinase pathway *via* activating raf (Shepherd PR, et al.,1998).

2.8 Glucose metabolism

Hepatocytes take up glucose independently of insulin by the low-affinity, high-capacity glucose transporter, GLUT-2, which facilitates the entry of glucose in the presence of high concentrations of sinusoidal glucose. There, glucose is rapidly phosphorylated by the hepatic hexokinase isoform, glucokinase, to glucose-6-phosphate. From glucose-6-phosphate, the glucose flux is directed into glycogen via uridine diphosphate (UDP)-glucose (direct pathway of glycogen synthesis), the pentose phosphate shunt or into glycolysis, yielding carbon-3 compounds such as pyruvate and lactate (Fig. 2.10).

Carbon-3 compounds undergo further oxidation in the tricarboxylic acid cycle or serve as substrates for de novo synthesis of glucose, glucose-6-phosphoneogenesis, and glycogen, the indirect or gluconeogenic pathway of glycogen synthesis (Landau, 2001). Several enzymes regulate substrate cycles between

gluconeogenesis exerted by phosphoenolpyruvate carboxykinase (PEPCK) and fructose-1,6-biphosphatase, and glycolysis exerted by phosphofructo-1-kinase and pyruvate kinase. These substrate cycles provide a system in which rates and direction of flux can be finely tuned by small changes in the concentration of specific effector enzymes and/or by covalent modification of involved enzymes. In addition, the control of metabolic flux can be influenced by changes in the gene expression of these enzymes (Nordlie et al.,1999).

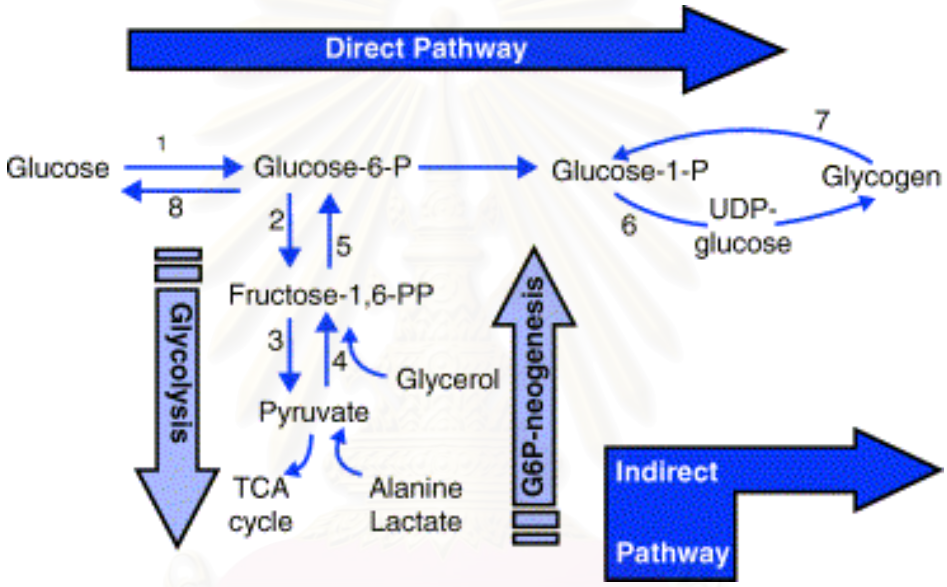

Figure 2.10 The glucose metabolism in the hepatocyte. [1]glucokinase, [2]phosphofructo-1-kinase, [3]pyruvate kinase, [4]phosphoenolpyruvate carboxykinase (PEPCK), [5]fructose-1,6-biphosphatase, [6]glycogen synthase, [7]glycogen phosphorylase, [8]glucose-6-phosphatase.

The activities of glycogen synthase and branching enzymes are responsible for the spherical shape of glycogen particles, which aggregate to larger complexes. Degradation of glycogen, glycogenolysis, requires the concerted action of glycogen phosphorylase and the bifunctional debranching enzyme to release glucose-1-phosphate, which is in equilibrium with glucose-6-phosphate. Glucose-6-phosphatase

catalyses the dephosphorylation of glucose-6-phosphate and represents the ultimate step prior to the release of free glucose into hepatic veins. It is derived from glycogenolysis or gluconeogenesis. As only the liver and the kidneys express glucose-6-phosphatase, glucose-6-phosphoneogenesis can result in the release of glucose by these tissues but only in the release of lactate from skeletal muscle, from where it can shuttle back to the liver (Bollen et al., 1998; Villar-Palasi and Guinovart, 1997).

2.9 Streptozotocin (STZ)

Streptozotocin (Fig 2.11) is nitrosurea derivative isolated from *streptomyces achromogens* with broad-spectrum antibiotic and anti-neoplastic activity. It also has been synthesized by three different procedures (Szkudelski et al., 2001): (1) from tetra-*O*-acetyl glucosamine hydrochloride, (2) from D-glucosamine + *N*-nitrosomethyl carbamyl-azide, and (3) from D-glucosamine *N*-methylurea. Its molecular structure is shown in 2.11, and corresponds to a 2-deoxy-D-glucose molecule substituted at C_2 with a N-methyl-*N*-nitrosourea group. In general, STZ is taken up by pancreatic β-cells via glucose transporter (GLUT2). STZ action in β-cells is accompanied by characteristic alterations in blood insulin and glucose concentrations. Two hours after injection, the hyperglycemia is observed with concomitant drop in plasma insulin. About six hours later, hypoglycemia occurs with high levels of plasma insulin concentration. Finally, hyperglycemia develops and plasma insulin concentration decrease. STZ causes in changes of DNA in pancreatic β-cells comprising its fragmentation (Bolzan and Bianchi, 2003). STZ induces β-cells death by alkylation of DNA that related to nitrosourea moiety of STZ, especially at position 6 of guanine. STZ is also a nitric oxide (NO) donor and NO was found to destroy of pancreatic islet cells. When β-cells expose to STZ manifested changes characteristic for NO action by increasing activity of guanylyl cyclase, and enhancing formation of cGMP. However, STZ is not a spontaneous nitric oxide donor. The molecule is liberated when STZ is metabolized inside cells without activity of NO synthase.

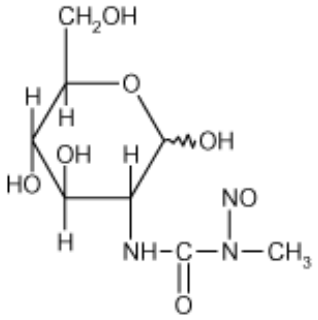

Figure 2.11 Chemical structure of streptozotocin

Interestingly, STZ is able to generate others reactive oxygen species, which also contribute to DNA fragmentation and evoke other deleterious change in the cells. STZ inhibits the Krebs cycle, and substantially decreases oxygen consumption by mitochondrial ATP generation. It is partially mediated by NO (Szkudelski , 2001). Augmented ATP dephosphorylation increases the supply of substrate for xanthine oxidase, and enhances the production of uric acid. Xanthine oxidase catalyses the formation of the superoxide anion that it is consequently formed hydrogen peroxide, and hydroxyl radicals. STZ-induced DNA damage activates poly ADP-ribosylation. This process leads to depletion of cellular NAD^+, further reduction of the ATP content, and subsequent inhibition of insulin synthesis and secretion (Fig 2.12).

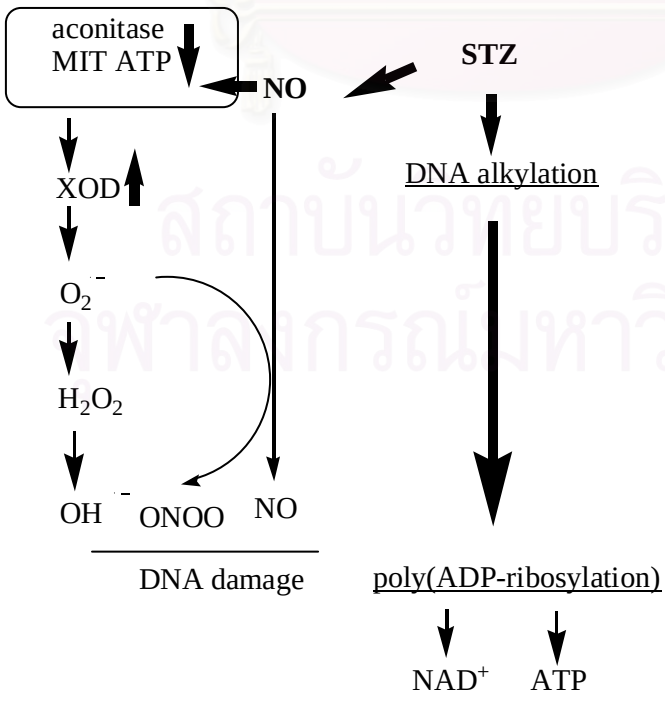

Figure 2.12 The mechanism of STZ-induced toxic events in β-cells of rat pancreas. MIT = mitochondria; XOD= xanthine oxidase (Figure : Szkudelski et al., 2001)

2.10 *p*-methoxycinnamic acid and its pharmacological activities

p-Methoxycinnamic acid (*p*-MCA) is a cinnamic acid derivative, which is isolated from the roots of *Scrophularia buergeriana* Miquel (Scrophulariaceae), leaves with stems of *A. vulgaris* L. Molecular weight of *p*-MCA is 178 and melting point is 172-174^{o}C. There are various literatures reported to pharmacological activities of *p*-MCA. For examples, *p*-MCA exerted significant hepatoprotective effects on carbon tetrachloride (CCl_4)-induced hepatotoxicity in primary cultures of rat hepatocytes. The hepatoprotective activity is likely to be attributed to the maintenance of the glutathione (GSH) redox system in CCl_4-injured rat hepatocytes and thereby reduce lipid peroxidation and cellular damage (Lee et al., 2002). *p*-MCA appeared to play the neuroprotective activity against glutamate-induced neurotoxicity in primary cultures of cortical neurons by an action of partial glutamatergic antagonism (Kim et al., 2002).It also improved impairments of spatial learning and memory induced by scopolamine, in experimental mice (Kim et al., 2002). Moreover, p-MCA was a potent non-competitive inhibitor on mushroom tyrosinase. The inhibition of tyrosinase is becoming important constituents of cosmetic products that relate to hyperpigmentation.

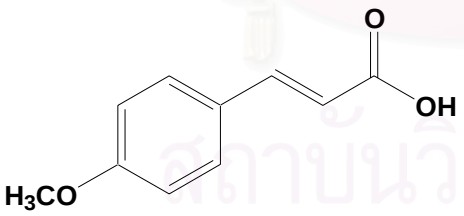

Figure 2.13 Chemical structure of *p*-MCA

CHAPTER III

MATERIALS AND METHODS

3.1 Animals

Animal facilities and protocol were approved by the Laboratory Animal Care and Use Committee at Faculty of Veterinary Science, Chulalongkorn University, Bangkok, Thailand. Male Wistar rats were purchased from the National Laboratory Animal Center, Mahidol University, Salaya, Thailand. Rats weighing 380-480 g were used in pancreatic perfusion. They were housed in individual stainless steel cages and fed with ad libitum commercial pellet diet and free access to water in a room maintained at 24 ± 1 °C on approximately 12:12-hour light-dark cycle.

3.2 Drugs

p-MCA was purchased from ACROS (Pittsburgh, PA, USA). Streptozotocin, glucose oxidase commercial kit, and all others enzymes were purchased from Sigma Chemical Co. (St. Louis, MO, USA). Radioimmunoassay (RIA) insulin kits were purchased from Diagnostic Products Corporation (Los Angeles, CA, USA). All other chemical reagents used in this study were of analytical grade.

3.3 Induction of diabetes

The rats weighing 180-220 g were used in this experiment. The mild diabetes was induced with 45 mg/kg of streptozotocin (STZ), administered Intraperitoneally. The STZ was freshly dissolved in citrate buffer (0.01 M, pH 4.5) and kept on ice prior to use. One week after STZ administration, rats with fasting blood glucose concentrations of 180-250 mg/dl were considered to be mild diabetes and were used in the experiment.

3.4 Acute effect of *p*-MCA on plasma glucose and insulin concentrations in fasting normal and diabetic rats

Normal and diabetic rats were fasted overnight and divided into 4 groups, each groups contained 6 animals. Group 1 orally received only 1 ml of distilled water. Group 2,3 and 4 received three different doses of *p*-MCA (10, 40 and 100 mg/kg), in 1 ml of water suspension, respectively. Blood samples (0.25 ml) were collected in chilled tubes containing heparin from tail vein at 0, 0.5, 1, 2, 3 hours. Plasma was removed and stored at –20°C. The plasma glucose concentrations were determined by glucose oxidase method and measured the absorbance with spectrophotometer at the wavelength 450 nm. Plasma insulin concentrations were determined by using radioimmunoassay (RIA) kits.

3.5 Acute effect of *p*-MCA on plasma glucose and insulin concentrations in fasting normal and diabetic rats by the oral glucose tolerance test (OGTT)

After an overnight of food withholding, normal and diabetic rats were divided into 4 groups. Group 1 received only distilled water (1ml). Group 2, 3 and 4 received *p*-MCA at doses of 10, 40, and 100 mg/kg, PO, as suspension (1 ml). 10 min later, glucose (2 g/kg/ml) was administered PO to each rat with a feeding tube. Blood samples (0.25 ml) were collected in chilled tubes containing heparin from tail vein before and after 30, 60 and 120 min glucose loading and rapidly centrifuged at 2,000 x g. Plasma was removed and stored at –20°C. The plasma glucose and insulin concentrations were determined according to the above method.

3.6 The long-term administration of *p*-MCA in normal and diabetic rats

Normal and mild diabetic rats were divided into two groups: untreated and treated groups. The untreated and treated groups received distilled water and *p*-MCA (40 mg/kg, orally), respectively. The fasting plasma glucose and insulin concentrations were measured on day 0. The treatments were then administered once a

day at 9.00 a.m. for 4 weeks. Body weight and plasma glucose concentration were monitored each week. At the end of the experiment, rats were fasted overnight and blood sample were collected at 9.00 a.m. for determination of fasting plasma glucose and insulin concentrations. Thereafter, animals were euthanized by cervical dislocation and the liver was removed immediately, frozen in liquid nitrogen and stored at -70°C. These tissues were used for the assay of hepatic glycogen, glucose-6-phosphate, hexokinase, glucokinase, phosphofructokinase and glucose-6-phosphatase.

3.7 Assay of hepatic glycogen

The frozen liver (0.5 g) was homogenized in ice-cold 0.6 M $HClO_4$. The mixture was immediately centrifuged at 3,000 x *g* and subjected to determination of free glucose in the tissue by the glucose oxidase method. Amyloglucosidase solution (15 U/mg protein) in 0.2 M sodium acetate buffer (pH 4.8) was then mixed and incubated in the mixture at 40°C for 2 h. After incubation, pH of the mixture was adjusted to 7 and subjected to determination of total glucose. Free glucose was subtracted from total glucose to obtain glycogen content. The glycogen was expressed as mg/g wet tissue (Keppler and Decker, 1974).

3.8 Assay of hepatic glucose-6-phosphate

The frozen liver was homogenized in ice-cold 0.6 M 0.6 M $HClO_4$ and centrifuged at 3,000 x g for 10 min. The pH of the supernatant was adjusted to 3.5 with K_2CO_3 and used for the measurement of glucose-6-phosphate content according to the method of Lang and Michal (1974). The frozen liver (1 g) was homogenized in ice-cold 0.6 M $HClO_4$. The mixture was immediately centrifuged at 3,000 x *g* and subjected to determination of glucose-6-phosphate by the coupled enzyme assay. Briefly, homogenate (1 ml) was added to reaction mixture which had a total volume of 1.04 ml containing 0.2 M Tris/HCl buffer (pH 7.6), 0.2 mM NADP, and 5 mM $MgCl_2$. After mixing, the background reaction is monitored for 1 minute. Then, the reaction was initiated with 10 μl of glucose-6-phosphate dehydrogenase (140 U/mg protein). After 5 min of reaction, the increase in absorbance of NADPH was recorded at 340 nm. One

micromole of glucose-6-phosphate corresponds to the amount of the enzyme producing 1 μmol of NADPH under assay condition at 30°C. The glucose-6-phosphate was expressed as nmol/g wet tissue.

3.9 Assay of hepatic hexokinase and glucokinase

The frozen liver (0.5 g) was minced and homogenized with 10 volumes of ice-cold 50 mM Tris/HCl buffer (pH 7.4) containing 100 mM KCl, 5 mM $MgCl_2$, 1 mM EDTA and 2.5 mM dithiothreitol. The homogenates were centrifuged at 20,000 x g for 15 min at 4°C and the supernatant was then used for the measurement of hexokinase and glucokinase activities by the coupled enzyme assay procedures as previously described (Pilkis, 1975). Briefly, 0.1 ml the supernatant was added to reaction mixture which had a total volume of 1.8 ml containing 50 mM Tris/HCl buffer (pH 7.4), 0.2 mM $NADP^+$, 5mM $MgCl_2$, 0.1U/mg protein glucose-6-phosphate dehydrogenase (G6PDH) and either 0.5 mM glucose for hexokinase activity and 100 mM glucose for total enzyme activities (hexokinase+glucokinase). After mixing, the background reaction is monitored for 1 minute. Then, the reaction was initiated with 0.1 ml of 100 mM ATP. After 5 min of reaction, the increase in absorbance of NADPH was recorded at 340 nm. The glucokinase and hexokinase were calculated in terms of mU/mg protein. One unit of the enzyme corresponds to the amount of the enzyme producing 1 μmol of NADPH under assay condition at 30°C. Hexokinase activity was subtracted from the total enzyme activities to obtain glucokinase activity. The hexokinase and glucokinase activities were expressed as U/mg protein, and mU/mg protein, respectively.

3.10 Assay of phosphofructokinase

The frozen liver (0.5g) was minced and homogenized with 10 volumes of ice-cold 50 mM Tris/HCl buffer (pH 7.4) containing 100 mM KCl, 5 mM $MgCl_2$, 1 mM EDTA and 2.5 mM dithiothreitol. The homogenates were centrifuged at 20,000 x g for 15 min at 4°C and the supernatant was then used for phosphofructokinase activity was assayed spectrophotometrically according to the method of Thomas (1973). Briefly, a

stock assay reaction mixture was prepared as follows: 2 ml of 0.5 M Tris/HCl, 2 ml of 50 mM $MgCl_2$, 2 ml of 0.5 M KCl, 70 μl of 50 mM 2-mercaptoethanol, 0.2 ml of aldolase (10 mg/mL), 0.1 ml of α-glycerolphosphate dehydrogenase/triosephosphate isomerase mixture (10 mg/ml), 0.2 ml of NADH, 0.4 mL of ATP, and 6.5 ml of distilled water. For assays, 0.1 mL of the supernatant was added to 1 mL of the reaction mixture and then recorded the background for 1 min. Then, the reaction was initiated with 40 μl of 0.125 M fructose-6-phosphate. After 5 min of reaction, the decrease of NADH was recorded at 340 nm. One unit of the enzyme corresponds to the amount of the enzyme reducing 1 μmol of NADH under assay condition at 30°C. The phosphofructokinase activity was expressed as unit/mg protein.

3.11 Assay of hepatic glucose-6-phosphatase

The frozen liver (0.5 g) was homogenized with 10 volumes of ice-cold 0.1 M citrate buffer (pH 6.5) and centrifuged at 1,800 x *g* for 10 min at 4°C. The homogenate was used for the assay. The activity of glucose-6-phosphatase was determined by measurement of inorganic phosphate released from glucose-6-phosphate (Koida and Oda, 1959). Briefly, the reaction mixture contained 0.7 ml of 0.1 M citrate buffer (pH 6.5), 0.3 ml of 0.1 M glucose-6-phosphate and 0.1 ml of the supernatant and then incubated at 37°C for 30 min. After incubation, 2.5 mL of 8% (w/v) trichloroaceic acid was added and the mixture was kept on ice for 20 min. Centrifuge at 1,000x*g* for 15 min at 4°C, then remove 1 ml of supernatant to a glass tube for determination of inorganic phosphate which was performed according to the method of Fiske and Subbarow (1925). Briefly, 1mL of supernatant was incubated with 1.15 ml of distilled water, 0.25 mL of 2.5% (w/v) ammonium molybdate in 2.5 M H_2SO_4, and Fiske-Subbarow reduction solution (1g / 6.3 ml of distilled water) at 100 °C for 10 min. The mixture was then allowed to cool to room temperature. The absorbance was recorded at 820 nm in a UV-VIS spectrophotometer. Phosphate concentrations were calculated by comparison against a standard curve generated using sodium phosphate monohydrate ($NaH_2PO_4.H_2O$). The glucose-6-phosphatase activity was expressed as unit/ mg protein.

3.12 Protein determination

Protein content was determined according to the method of Bradford (1976) using bovine serum albumin as the standard. Briefly, 100 mg of Coomassie Blue was dissolved in 50 ml of methanol. The solution was added to 100 ml of 85% H_3PO_4, and diluted to 200 ml with water. The solution was kept in a dark bottle at 4°C. Prepare six standard solutions (1 ml each) containing 0, 250, 500, 1000, 1500 and 2000 μg/mL BSA. The reaction was initiated by adding 2.0 ml of Coomassie Blue, and 0.04 ml of protein standard solution or protein extract, and then incubated at room temperature for 5 min. The mixture was recorded the absorbance at 590 nm in a UV-VIS spectrophotometer.

3.13 Histological Study

The pancreas from diabetic and normal rats were removed and immediately immersed in 10% formalin. The formalin-fixed pancreata were then dehydrated with ethanol and embedded in paraplast. After paraffin embedding, 5 μM thick sections were prepared and stained by hematoxylin and eosin. Necrosis and inflammation of islets were examined under a light microscope. The pathological changes of rat pancreas were graded: 0, normal; +1, mild degree; +2 moderate degree and +3, severe degree.

3.14 The pancreatic perfusion

Male rats were anesthetized with pentobarbital sodium (60 mg/kg ip) and were maintained at 37°C on a hot plate during the experiment. The celiac arteries were cannulated with polyvinyl tubing, and then the pancreata were immediately perfused with the Krebs-Ringer Bicarbonate buffer (KRB) supplemented with 20 mM HEPES, 5.5 mM glucose, 1% dextran, and 0.2% bovine serum albumin (BSA) as a basal medium. The KRB was continuously aerated with 95% O_2-5% CO_2 at pH 7.4. The perfusion rate was 1 ml/min, and the effluent fluid from the portal vein, which was cannulated with a vinyl tubing, was ~1 ml/min. The rats were euthanized immediately

after the placement of cannulas and the beginning of the flow. The perfused pancreas was equilibrated for 20 min before the onset of the experiment. The pancreatic perfusions were performed in three different experiments. For the first study, after the baseline period of 10 min, the perfusate containing *p*-MCA (10 μM or 100 μM) was administered for 30 min followed by a washout period with the basal medium for 10 min. The perfusate containing glucose (10 mM) was administered as a positive control for 10 min at the end of the experiments. For the second study, after the baseline period of 10 min, the perfusate containing 10 mM glucose was administered for 20 min and followed by glucose with or without 10 μM *p*-MCA for 20 min. For the third study, after the baseline period of 10 min, the perfusate containing 1 μM Bay K 8644 (L-type Ca^{2+} channel agonist) with or without 10 μM *p*-MCA was administered for 30 min. (Yibchok-anun et al., 1998).

3.15 Cell culture

INS-1 cells, an insulin-secreting cell line derived from rat pancreatic β-cells were cultured in RPMI 1640 medium containing 11 mM glucose and supplemented with 10% fetal bovine serum, 2 mM L-glutamine, 1 mM sodium pyruvate and 50 μM 2-mercaptoethanol in an atmosphere of 5% CO_2 in air at 37°C.

3.16 Insulin Secretion Studies

INS-1 Cells were plated onto 24-well plates at a density of 1×10^5 cells per well and grown for 48 h. For static secretion studies, cells were preincubated for 15 min in KRB containing 4 mM glucose and 0.1% BSA. Cells were then incubated for 30 min in KRB containing test agents.

Experiment 1. Dose dependency study: The cells were incubated with various concentrations of *p*-MCA (1 – 300 μM).

Experiment 2. The cells were incubated with 100 μM *p*-MCA in Ca^{2+} free KRB or 1 μM Nimodipine (L-type Ca^{2+} channel blocker).

Experiment 3. The cells were incubated with 100 μM *p*-MCA in presence of 400 μM diazoxide(K_{ATP} channel opener). 10 μM glyburide was used as a positive control for this study.

Experiment 4. The cells were incubated with 10 mM glucose for 15 min and then *p*-MCA (10 or 100 μM) was added to the cells for 15 min.

Experiment 5. The cells were incubated with *p*-MCA (10 or 100 μM) in presence of 15 mM KCl.

Experiment 6. The cells were incubated with *p*-MCA (10 or 100 μM) in presence of 1 μM Bay K 8644 (L-type Ca^{2+} channel agonist).

Experiment 7. The cells were incubated with *p*-MCA (10 or 100 μM) in presence of 10 μM glyburide.

Experiment 8. The cells were incubated with *p*-MCA (10 or 100 μM) in presence of 1 μM forskolin (adenylyl cyclase activator). After incubation, the cell were determined for the cAMP contents.

Experiment 9. The cells were incubated with *p*-MCA (10 or 100 μM) in presence of 100 μM IBMX (phosphodiesterase inhibitor). After incubation the cell were determined for the cAMP contents.

After incubation, the buffer was kept at 4°C and subsequently assayed for insulin. *p*-MCA was dissolved in dimethyl sulfoxide (DMSO) to obtain desired concentrations (final concentration, 0.2%).

3.17 Measurement of $[Ca^{2+}]_i$

Cells were grown in culture flasks for 5 days until 80–90% confluence had been reached. Thereafter, the cells were harvested by treatment with trypsin/EDTA and prepared for experiments. Measurement of $[Ca^{2+}]_i$ was accomplished by loading cells with 2 μM fura 2-AM(Fura-2 acetoxymethylester) for 30min at 37°C in KRB The loaded cells were centrifuged at 300x*g* for 2 min and resuspended with KRB. The 340/380nm fluorescence ratios were monitored using a spectrofluorometer (USA.). The $[Ca^{2+}]_i$ was calibrated as described previously (Cheng et al., 2005).

Experiment 1. Dose dependency study: Baseline was run for 60 second, then the various concentrations of *p*-MCA (1 – 300 μM) were added to the cells.

Experiment 2. Experiments in Ca^{2+}-free medium were done by centrifugation at 300***g*** for 60s followed by resuspension of the cells in Ca^{2+}-free KRB containing 100 μM EGTA. In presence of Ca^{2+} free KRB, baseline was run for 60 seconds, then 100 μM *p*-MCA was added to the cells. After 120 seconds, 1 μM thapsigargin was added to the cells.

Experiment 3. Baseline was run for 60 seconds, then 1 μM Nimodipine was added to the cells. After 120 seconds, 100 μM *p*-MCA was added to the cells. Finally, 1 μM Bay K 8644 was added to the cells after 120 seconds of adding *p*-MCA

Experiment 4. Baseline was run for 60 seconds, then 400 μM diazoxide was added to the cells. 100 μM *p*-MCA was added to the cells after 120 seconds adding of diazoxide.

Experiment 5. Baseline was run for 60 seconds, then 10 mM glucose was added to the cells. 10 or 100 μM *p*-MCA was added to the cells after 120 seconds adding of glucose.

Experiment 6. Baseline was run for 60 seconds, then 15 mM KCl was added to the cells. 10 or 100 μM *p*-MCA was added to the cells after 120 seconds adding of KCl.

Experiment 7. Baseline was run for 60 seconds, then 1 μM Bay K 8644 was added to the cells. 10 or 100 μM *p*-MCA was added to the cells after 120 seconds adding of Bay K 8644.

Experiment 8. Baseline was run for 60 seconds, then 10 μM glyburide was added to the cells. 10 or 100 μM *p*-MCA was added to the cells after 120 seconds adding of glyburide.

3.18 cAMP determination

Cells were incubated with *p*-MCA (10 or 100 μM) in presence of 1 μM forskolin or 100 μM IBMX for 30 min. After remove the KRB solution, the cells were homoginized with 0.1 M HCl and the cells were scraped off. The cells were incubated in the water at 70°C. After incubation, the cell were centrifuged at 2,000*g* at 4 °C for 10 min and the supernatant was neutralized with 0.1 M NaOH. The solution was added the acetylating reagent (0.5 ml of acetic anhydride and 1 ml of triethylamine) and determined the cAMP level by using radioimmunoassay as previously described (Prapong et al., 2001).

3.19 Microbial and mammalian α-glucosidase inhibition

Briefly, α-glucosidase from baker's yeast was assayed using 0.1 M phosphate buffer at pH 6.9, and 1 mM *p*-nitrophenyl-α-D-glucopyranoside (PNP-G) was used as a substrate. The concentration of the enzymes were 1 U/ml in each experiment. Forty microlitre of α-glucosidase was incubated in the absence or presence of various concentrations of *p*-MCA (10 μl) at 37°C. The preincubation time was specified at 10 min and PNP-G solution (950 μl) was added to the mixture. The reaction was carried out at 37 °C for 20 min, and then 1 ml of 1 M Na_2CO_3 was added to terminate the reaction. Enzymatic activity was quantified by measuring the absorbance at 405 nm. One unit of α-glucosidase is defined as the amount of enzyme liberating 1.0 μmol of PNP per minute under the conditions specified. 1-Deoxynorjirimycin was used as the

positive control in this study. In order to evaluate the type of inhibition using the Lineweaver-Burk plot, the enzyme reaction was performed according to the above reaction with various concentrations of *p*-MCA and PNP-G (Mutsui et al., 1996). The IC_{50} values was expressed as mean ± SE ; n=3.

α-glucosidase from intestinal mammalian was assayed according to the method of Toda (2000). Briefly, rat intestinal acetone powder (100 mg) was homogenized in 3 ml of 0.9% NaCl solution. After centrifugation at 12,000xg for 30 min, 10 μl of the supernatant was incubated with 70 μl of substrate solution (37 mM maltose, 56 mM sucrose), and 20 μl of *p*-MCA at various concentrations in 0.01 M phosphate buffer saline pH 6.9 at 37 °C for 30 min (maltase assay) and 60 min (sucrase assay). The concentrations of glucose released from the reaction mixtures were determined by using glucose oxidase method. Acarbose was used as the positive control in this study The IC_{50} values were expressed as mean ± SE; n=3.

3.20 α-amylase inhibition

Pancreatic porcine α-amylase was dissolved in 0.1 M phosphate buffer saline, pH 6.9. *p*-MCA was added to solution containing in 1g/l starch and phosphate buffer. The reaction was initiated by adding amylase (1U/ml) to the incubation medium to a final volume of 150 μl. After 10 min the reaction was stopped by adding 1 ml dinitrosalicylic (DNS) reagent (1% 3,5-dinitrosalicylic acid, 0.2% phenol, 0.05% Na_2SO_3, and 1% NaOH in aqueous solution) to the reaction mixture. The capped test tubes were heated at 100 °C for 15 min to develop the yellow-brown colour. After then 300 μl of a 40% potassium sodium tartarate (Rochelle salt) solution was added to the test tubes to stabilize the color. After cooling to room temperature in a cold water bath, absorbance was recorded at 540 nm using spectrophotometer (Kanda et al., 2005). Acarbose was used as the positive control in this study. The IC_{50} values were expressed as mean ± SE; n=3.

Calculation of the percent inhibition and IC_{50} values

$$\% \text{ Inhibitory activity} = \frac{(Ac - At)}{Ac} \times 100$$

Ac = Absorbance of control

At = Absorbance of test samples

IC_{50} values were determined from plots of concentration vs percent inhibition curves using Sigma Plot 8.0.

3.20 Data analysis

Data are expressed as means ± S.E.M. Area under the curve (AUC) values are reported as total areas and are calculated using a modification of the trapzodial rule. In animal models, statistical analysis was performed by 1) one-way analysis of variance (ANOVA) in the dose-response experiments, and 2) two-way ANOVA with a factorial design (diabetes x treatment). In the data from perfusion experiments, areas under the curve (AUCs) for the treatment period were calculated using Transforms and Regressions (SigmaPlot 8.0; SPSS, Chicago, IL) and expressed as a percentage of the area of the basal control group. The Least Significant Difference test was used for mean comparisons; $P<0.05$ was considered to be statistically significant.

CHAPTER IV

RESULTS

4.1 Effect of *p*-MCA on fasting plasma glucose and insulin concentrations

The fasting plasma glucose concentrations in normal and diabetic rats are shown in Fig 1. The normal rats treated with 40 and 100 mg/kg *p*-MCA orally resulted in the lowering of fasting plasma glucose concentrations 60 min after administration (Fig 4.1A). In diabetic rats with overnight fasting, the plasma glucose concentrations were 2 times higher than those of normal rats (Fig 4.1B) within 1 week after STZ administration (normal control rats: 105.8 ± 6.4 mg/dl; STZ-induced diabetic rats: 232.6 ± 8.9 mg/dl). A significant decrease in plasma glucose concentrations in diabetic rat treated with *p*-MCA (40 and 100 mg/kg) was observed at the first hour after single administration ($P<0.05$). At the dose of 100 mg/kg *p*-MCA, the maximum reduction of plasma glucose concentrations was 26 % after 1 h and maintained up to 3 h during fasting.

The fasting plasma insulin concentrations in normal and diabetic rats are shown in Fig 4.2. In normal rats treated with *p*-MCA (40 and 100 mg/kg), basal plasma insulin concentrations significantly increased ($P<0.05$) at 60 min after administration when compared to control groups (Fig 4.2A). One week after diabetes induction, the diabetic rats had insulin insufficiency. Our results showed that the basal plasma insulin concentrations in these diabetic rats were about 2.3-fold lower than those of normal rats (normal rats = 808.4 ± 35.7 pg/ml; diabetic rats = 363.5 ± 36.3 pg/ml). The results showed that *p*-MCA (40 and 100 mg/kg) significantly increased plasma insulin concentrations, which reached 730.9 ± 113.9 pg/ml, and 645.2 ± 89.5 pg/ml at 1 h after administration; the plasma insulin concentrations were 2.0 and 1.76 times of the concentration at time 0, respectively (Fig 4.2B). On the contrary, *p*-MCA (10 mg/kg) did not have any significant effect on the fasting plasma glucose and insulin concentrations in both diabetic and normal rats.

4.2 Effect of *p*-MCA on oral glucose tolerance test

The plasma glucose concentration of normal and diabetic rats treated with *p*-MCA at 40 and 100 mg/kg ($P<0.05$) were significantly decreased in both normal (Figure 4.3A) and diabetic rats (Figure 4.3B) after glucose loading. The AUC in diabetic rats was significantly lower than those in normal rats by 54 and 69% ($P<0.05$), respectively (AUC for normal control group = 80.9 ± 10.2 mg/dl.h, AUC for normal treated group with 40 mg/kg = 36.0 ± 4.4 mg/dl.h; 100 mg/kg = 24.9 ± 21.4 mg/dl.h). The effects of *p*-MCA on suppression of plasma glucose were also observed in diabetic rats at 30 min after glucose administration. A dose of 40 and 100 mg/kg *p*-MCA markedly reduced the AUC of diabetic rats by 37 and 45% ($P<0.05$), respectively (AUC for diabetic control group = 352.8 ± 41.7 mg/dl.h; AUC for groups treated with 40 mg/kg = 219.0± 43.3 mg/dl.h; 100 mg/kg = 160.8 ± 41.6 mg/dl.h).

The plasma insulin concentrations of normal and diabetic rats are shown in Fig 4.5. In normal rats, the plasma insulin concentrations were raised to maximum levels 30 min after loading glucose (Fig 4.5A). *p*-MCA induced the significant increase in plasma insulin concentrations 1 h after loading glucose. The AUC of groups treated with *p*-MCA (40 and 100 mg/kg) were 2395.6±82.6 and 2403.2 ± 32.8 pg/ml.h, respectively (AUC for control groups = 2037.9±74.5 pg/ml.h). At 30 min of OGTT (Fig 4.5B), the diabetic rats showed the lower responses to glucose on stimulatory insulin secretion (basal insulin = 272.2±30.7 pg/ml; 30 min = 372.1±61.4 pg/ml). In groups treated with *p*-MCA (40 and 100 mg/kg), the plasma insulin concentrations were significantly greater ($P<0.05$) than the untreated diabetic rats at 30 and 60 min of the OGTT. The AUC for those groups were 85 and 62% greater, respectively (AUC for diabetic control group = 717.4±83.3 pg/ml.h; AUC for groups treated with 40 mg/kg = 1332.7 ± 162.3 pg/ml.h; 100mg/kg = 1116.4± 88.4 pg/ml.h). There were no differences between the AUC of plasma glucose and insulin between the groups treated with *p*-MCA (10 mg/kg) and control groups.

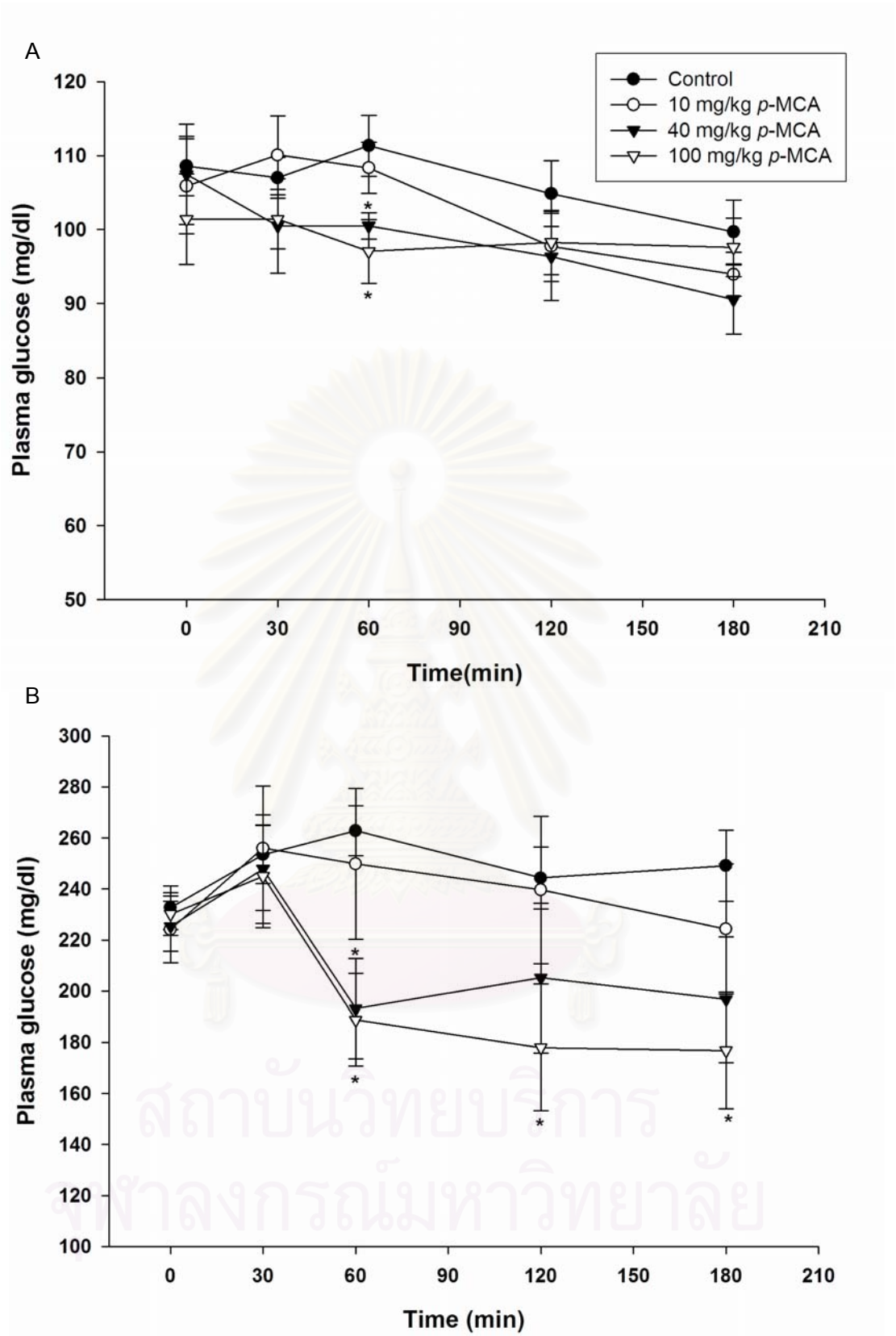

Figure 4.1 Effect of *p*-MCA on fasting plasma glucose concentrations in normal (A) and diabetic rats (B). Results are expressed as means ± S.E.M., n = 6. **P*<0.05 compared with control.

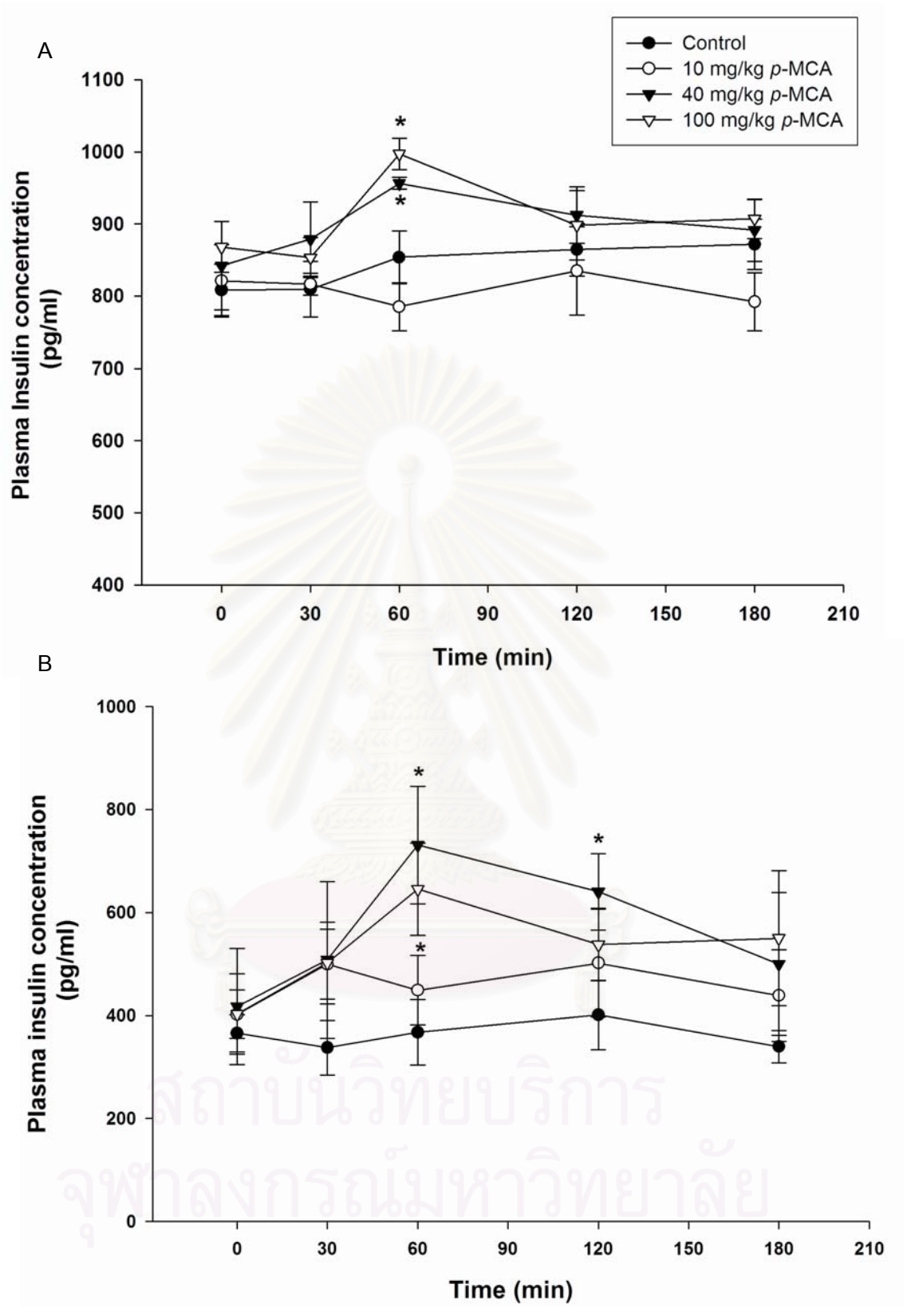

Figure 4.2 Effect of *p*-MCA on fasting plasma insulin concentrations in normal (A) and diabetic rats (B). Results are expressed as means ± S.E.M., n = 6. **P*<0.05 compared with control.

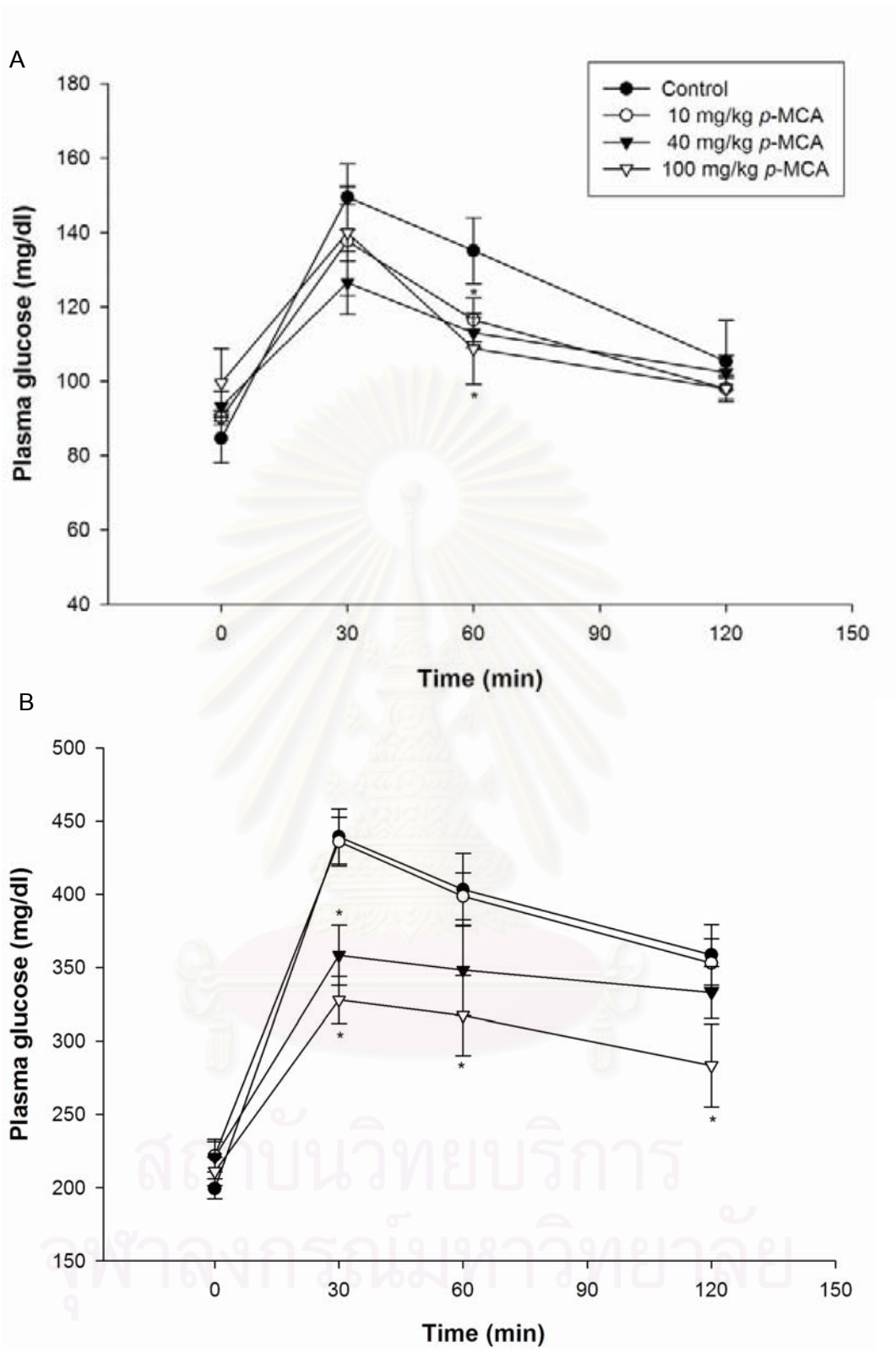

Figure 4.3 Effect of *p*-MCA on plasma glucose concentration after glucose administration in normal (A) and diabetic rats (B). Glucose (2 g/kg) was administered orally at time 0. Results are expressed as means ± S.E.M., n = 6. **P*<0.05 compared with control.

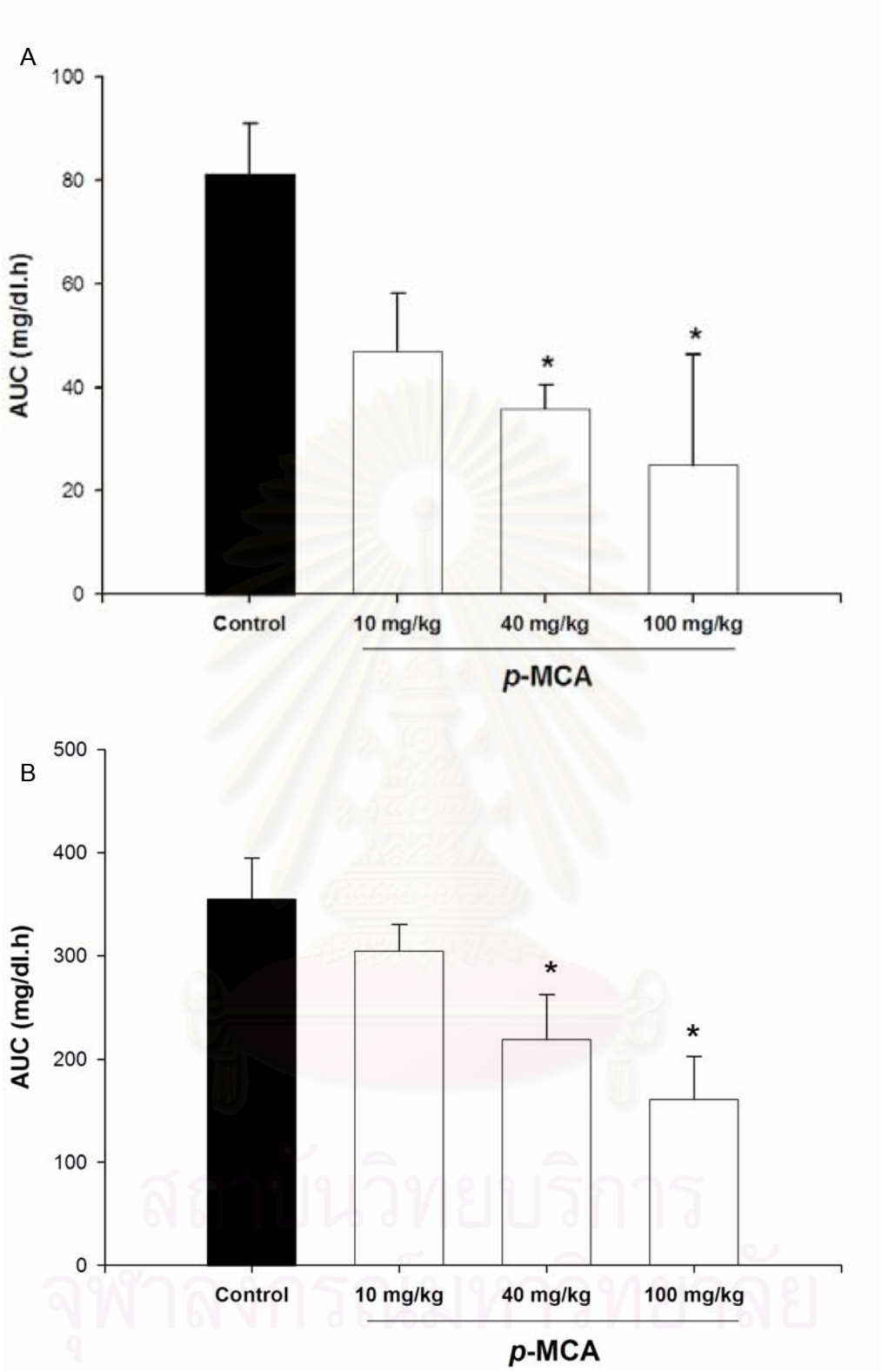

Figure 4.4 Effect of *p*-MCA on plasma glucose concentration after glucose administration in normal (A) and diabetic rats (B). Total areas under glucose response curves were calculated for each group of rats. Results are expressed as means ± S.E.M, n = 6. **P*<0.05 compared with control.

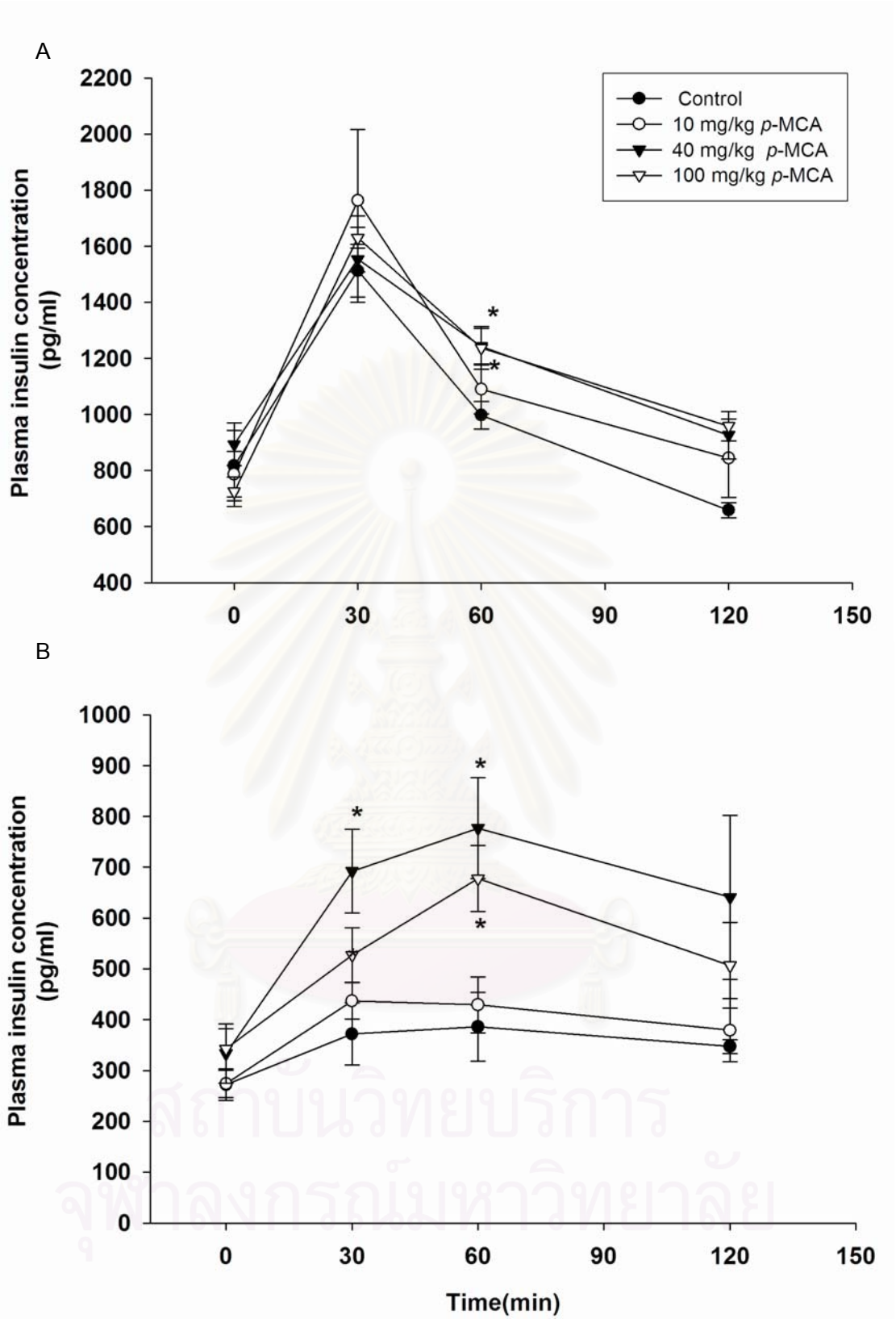

Figure 4.5 Effect of *p*-MCA on plasma insulin concentration after glucose administration in normal (A) and diabetic rats (B). Glucose (2 g/kg) was administered orally at time 0. Results are expressed as means ± S.E.M., n = 6. **P*<0.05 compared with control.

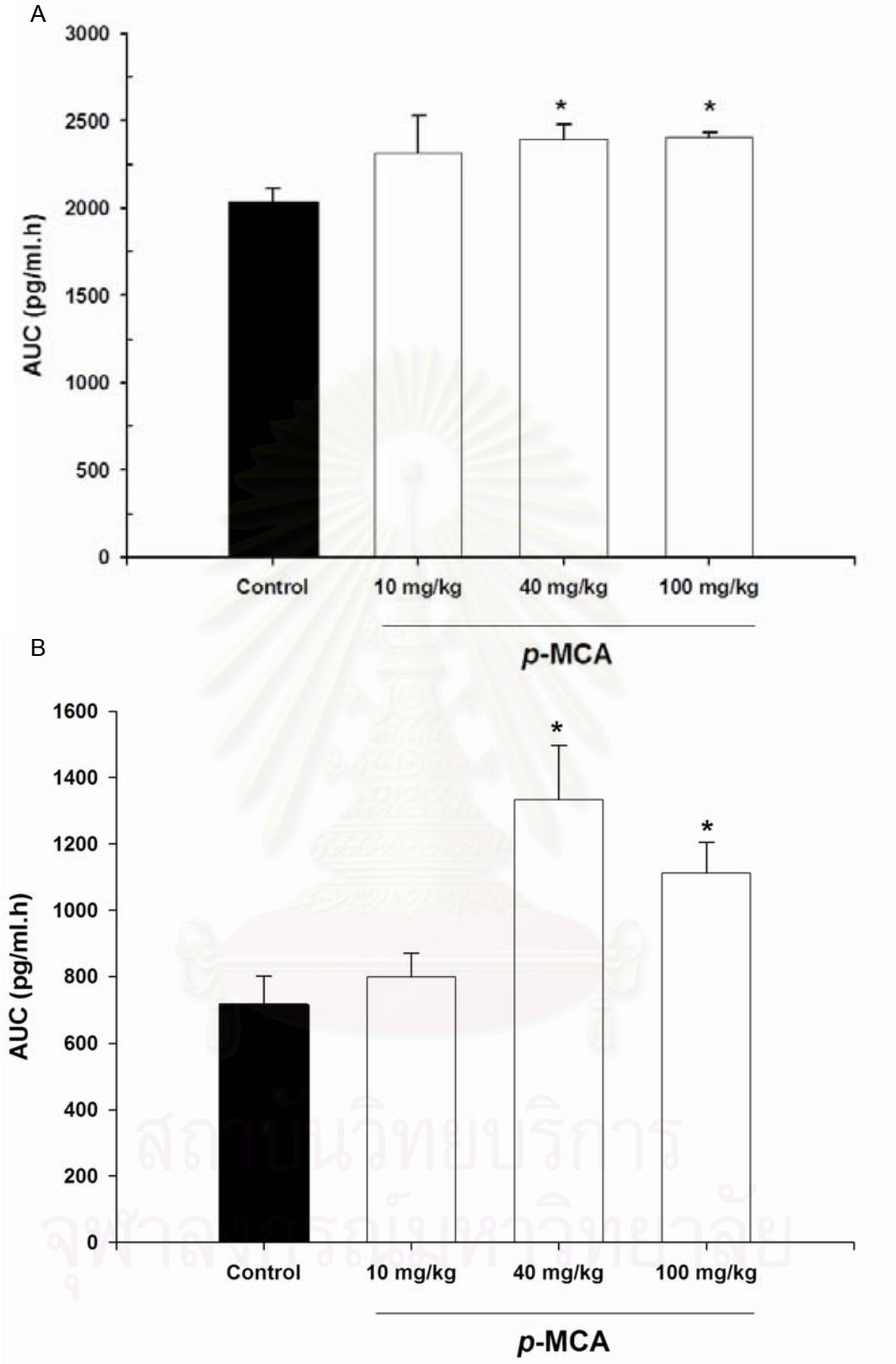

Figure 4.6 Effect of *p*-MCA on plasma insulin concentration after glucose administration in normal (A) and diabetic rats (B). Total areas under insulin response curves were calculated for each group of rats. Results are expressed as means ± S.E.M, n = 6. **P*<0.05 compared with control.

4.3 Effect of *p*-MCA on plasma glucose and insulin concentrations during 4 weeks

Changes in the body weight, the concentrations of fasting plasma glucose and insulin after administration of *p*-MCA for 4 weeks are summarized in Table 4.1. The daily administration of *p*-MCA to normal rats did not cause any changes in body weight, plasma glucose or insulin concentrations at the end of the study. In diabetic rats, 40 mg/kg of *p*-MCA significantly lowered fasting plasma glucose concentration ($P<0.05$) but it did not increase plasma insulin concentration at the end of the study. As shown in Figure 4.7, antihyperglycemic effect of *p*-MCA was observed throughout the 4-week study ($P<0.05$). The reduction plasma glucose in diabetic rats treated with *p*-MCA were seen in 1 week of administration.

4.4 Hepatic enzymes

The activities of hepatic hexokinase, glucokinase, phosphofructokinase and glucose-6-phosphatase in normal and diabetic rats are shown in Table 2. The untreated diabetic rats had low hepatic hexokinase and glucokinase activities, whereas *p*-MCA significantly increased hexokinase ($P<0.05$) and glucokinase ($P<0.05$) activities in diabetic rats. In addition, *p*-MCA-treated diabetic rats had significantly higher phosphofructokinase activity ($P<0.05$) than untreated diabetic rats. *p*-MCA also suppressed glucose-6-phosphatase activity in diabetic rats ($P<0.05$). However, *p*-MCA did not significantly change hepatic hexokinase, glucokinase, phosphofructokinase or glucose-6-phosphatase activity in normal rats.

4.5 Hepatic glycogen and glucose-6-phosphate concentrations

p-MCA-induced changes in hepatic glycogen and glucose-6-phosphate are shown in Table 2. Concentrations of hepatic glycogen and glucose-6-phosphate were lower in diabetic rats than those in normal rats. *p*-MCA induced a significant

increase in hepatic glycogen ($P<0.05$) in diabetic rats. Glucose-6-phosphate concentration was not significantly increased in *p*-MCA-treated diabetic rats. In addition, *p*-MCA did not significantly modify hepatic glycogen or glucose-6-phosphate in normal rats.

4.6 Pancreatic section

Fig. 4.8-4.11 demonstrate typical pancreatic sections of normal, normal treated with *p*-MCA, diabetic and diabetic rats treated with *p*-MCA, respectively. Diabetic rats showed a marked change of pancreatic islets, which decreased its size and contained relatively small numbers of cells (severity of pancreas injury of +2.5), whereas well-defined cells were seen in the pancreatic islets of the normal rats. No significance increase in the number of islets was observed in diabetic treated with *p*-MCA (severity of pancreas injury of +2.5) when compared to diabetic rats. In addition, there were no significant pathophysiological changes in normal rats treated with *p*-MCA when compared to normal rats (severity of pancreas injury of 0).

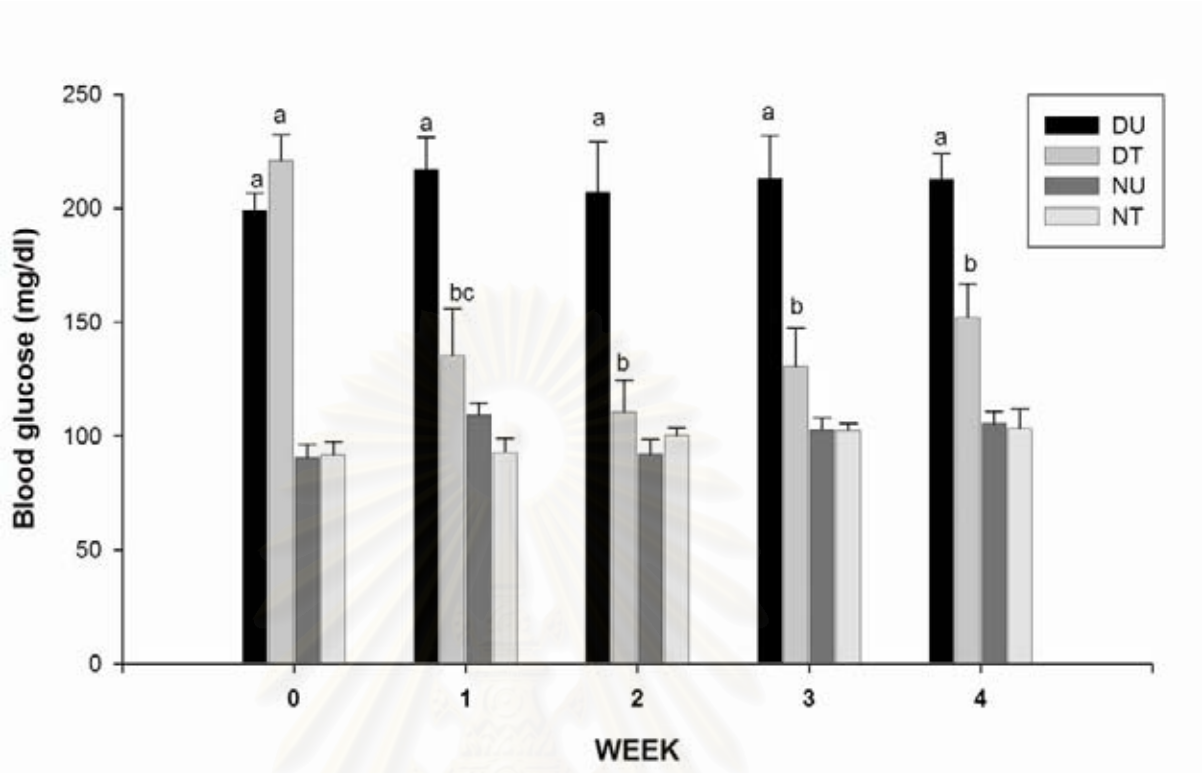

Figure 4.7 Fasting plasma glucose concentrations after a daily oral administration of *p*-MCA (40 mg/kg) for 28 days: untreated diabetic rats [DU]; treated diabetic rats [DT]; untreated normal rats [NU]; treated normal rats [NT] Data are expressed as means ± S.E.M. [*n*=7 for diabetic rat and *n*=8 for normal rats]. Differences among groups were analyzed by the two-way ANOVA for diabetes and treatment. Week 1; diabetes ($P<0.001$), treatment ($P<0.001$), and diabetes x treatment ($P<0.01$). Week 2; diabetes ($P<0.001$), treatment ($P<0.001$), and diabetes x treatment ($P<0.001$). Week 3; diabetes ($P<0.001$), treatment ($P<0.01$), and diabetes x treatment ($P<0.01$). Week 4; diabetes ($P<0.001$), treatment ($P<0.01$), and diabetes x treatment ($P<0.01$). $^{a}P< 0.05$ compared with [NU], $^{b}P< 0.05$ compared with [DU], $^{c}P< 0.05$ compared with [NT].

ต้นฉบับไม่มีหน้านี้

NO THIS PAGE IN ORIGINAL

Table 4.1 Effect of *p*-MCA on body weight, fasting plasma glucose and insulin concentrations in normal and diabetic rats

Groups	Body weight (g)		Fasting plasma glucose (mg/dl)	Plasma Insulin (μU/ml)
	Initial (0 day)	Final (28 day)	Final (28 day)	Final (28 day)
Normal rats (n=8)	175 ± 3	244 ± 6	105.52 ± 5.37	779.96±95.32
p-MCA (40mg/kg) in Normal rats (n=8)	175 ± 5	231 ± 4	103.43 ± 5.37	884.79± 68.83
Diabetic rats (n=7)	173 ± 3	188 ± 15[a]	212.52±11.43[a]	241.5± 41.19[a]
p-MCA (40mg/kg) in Diabetic rats (n=7)	169 ± 3	193 ± 23[a]	152.29 ± 14.94[a,b]	381.7± 53.41[a]

Data are expressed as means ± S.E.M. Differences among groups were analyzed by two-way ANOVA for diabetes and treatment. Body weight: diabetes ($P<0.01$), treatment ($P>0.05$), and diabetes x treatment ($P<0.05$). Fasting plasma glucose: diabetes ($P<0.001$), treatment ($P<0.01$), and diabetes x treatment ($P<0.01$). Insulin concentration: diabetes ($P<0.001$), treatment ($P<0.01$), and diabetes x treatment ($P>0.05$). Means with different letters are significantly different ($P<0.05$). [a]$P< 0.05$ compared with normal rats, [b]$P< 0.05$ compared with diabetic rats

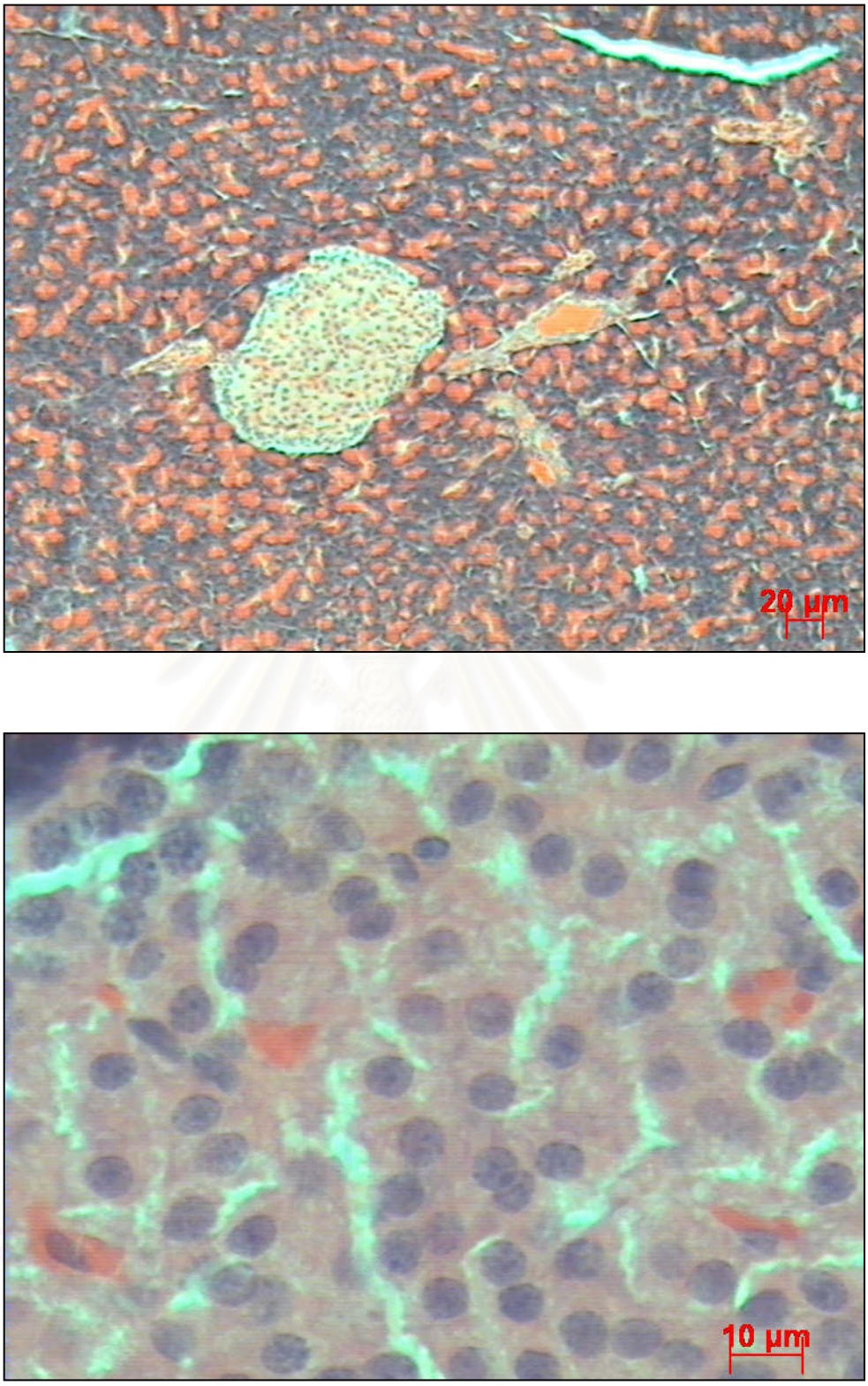

Figure 4.8 The pancreatic section of normal rats treated with distilled water for 28 days.

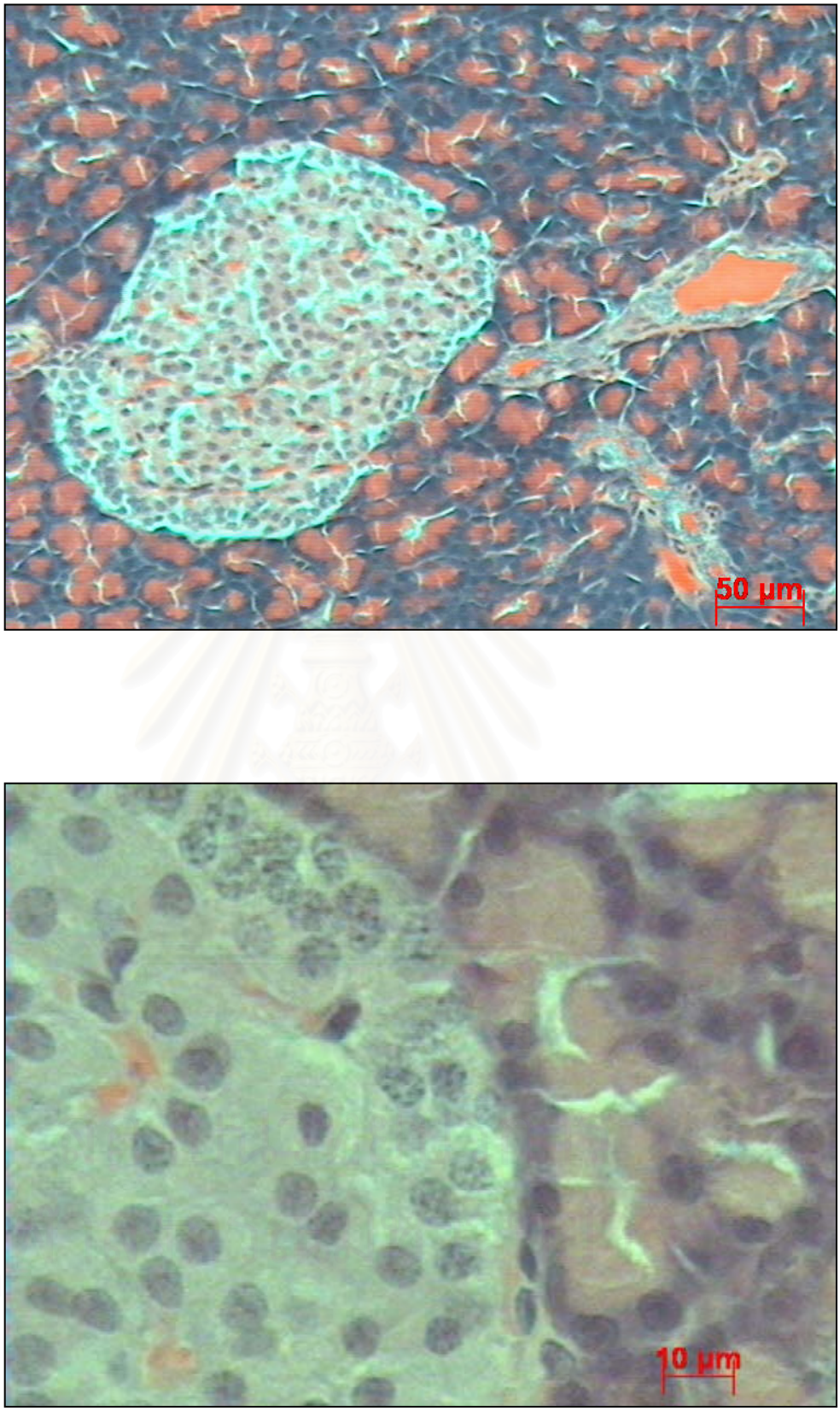

Figure 4.9 The pancreatic section of normal rats treated with 40 mg/kg *p*-MCA for 28 days

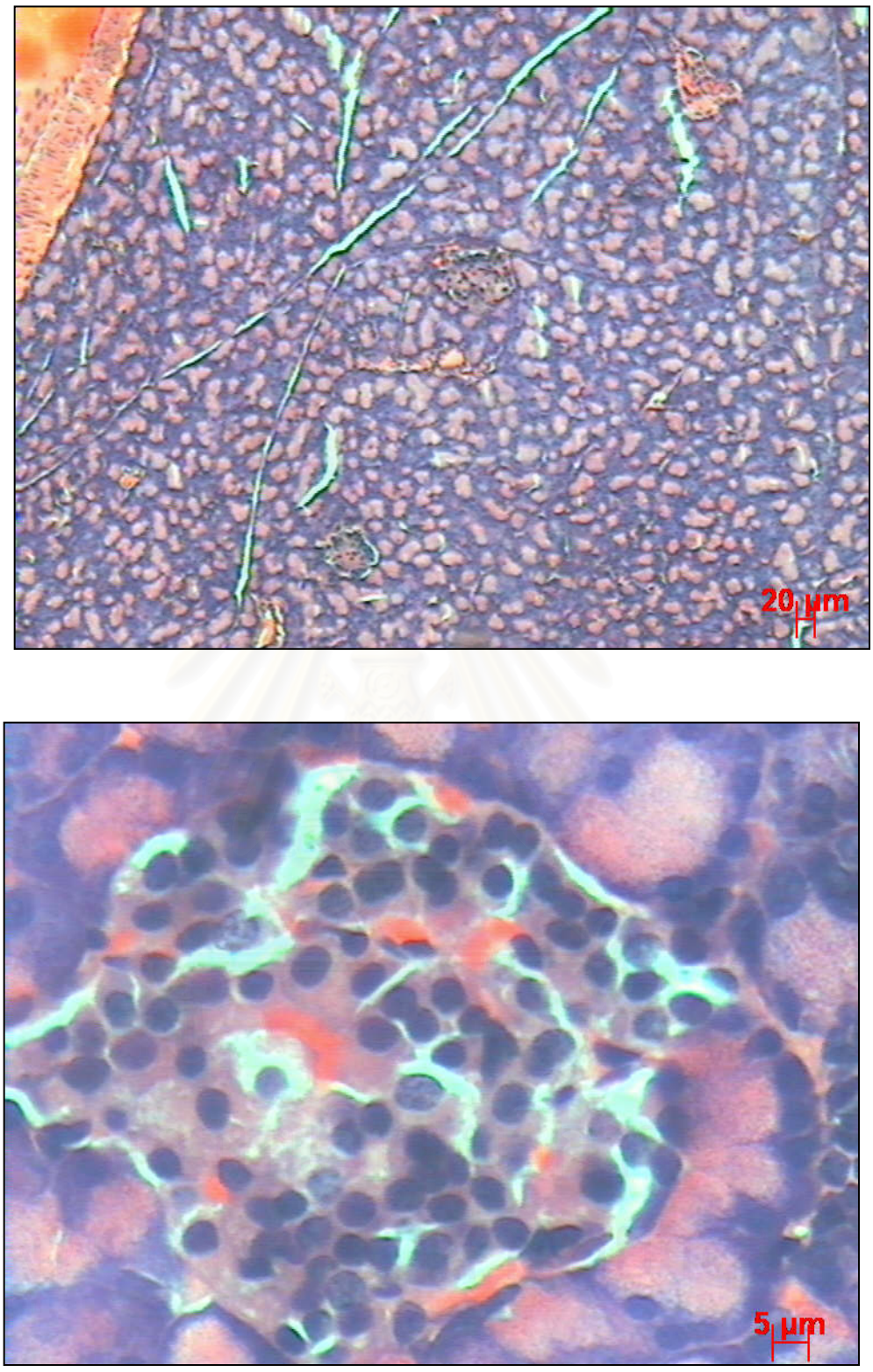

Figure 4.10 The pancreatic section of diabetic rats treated with distilled water for 28 days.

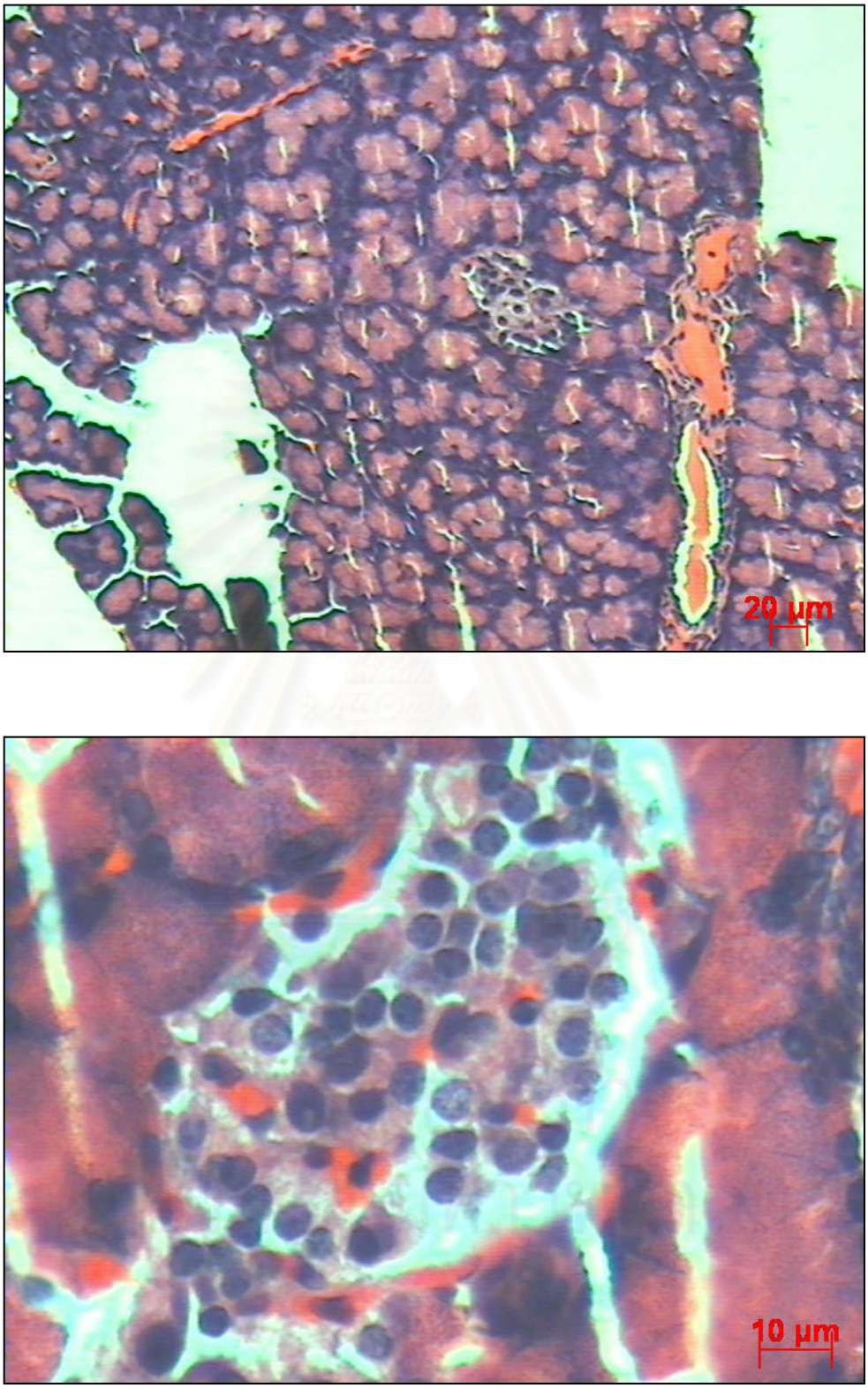

Figure 4.11 The pancreatic section of diabetic rats treated with 40 mg/kg *p*-MCA for 28 days.

ต้นฉบับไม่มีหน้านี้

NO THIS PAGE IN ORIGINAL

Table 4.2 Activities of hexokinase, glucokinase, phosphofructokinase, glucose-6-phosphatase, glycogen and glucose-6-phosphate content in liver of normal and diabetic rats.

Parameters	NU	NT	DU	DT
Hexokinase (mU/mg protein)	251.62±17.75	226.32 ± 8.74	101.27 ± 4.35[a]	143.26 ± 8.47[ab]
Glucokinase (mU/mg protein)	7.38 ± 0.88	6.67 ± 2.03	2.63 ± 0.40[a]	7.20 ±1.33[b]
Phosphofructokinase (mU/mg protein)	10.90 ± 1.39	8.90 ± 1.38	5.13 ± 0.61[a]	9.29 ± 1.53[b]
Glucose-6-phosphatase (mU/mg protein)	181.76 ± 16.71	162.77 ± 16.40	256.86 ±16.04[a]	187.34 ±19.87[b]
Glycogen (mg/g tissue)	24.79 ± 1.96	29.12 ±1.70	10.79 ± 1.77[a]	19.33 ± 2.90[bc]
Glucose-6-phosphate (nmol/g tissue)	456.13 ± 48.95	517.8 ± 68.51	199.72 ± 18.68[a]	266.33 ±23.69[a]

Data are expressed as means ± S.E.M. [n=7 for diabetic rat and n=8 for normal rats] ; untreated diabetic rats [DU]; treated diabetic rats [DT]; untreated normal rats [NU]; treated normal rats [NT]. Differences among group were analyzed by two-way ANOVA for diabetes and treatment. Hexokinase activity: diabetes (P<0.001), treatment (P>0.05), and diabetes x treatment (P<0.001). Glucokinase activity: diabetes (P>0.05), treatment (P>0.05), and diabetes x treatment (P<0.05). Phosphofructokinase activity: diabetes (P<0.05), treatment (P>0.05), and diabetes x treatment (P<0.05). Glucose-6-phosphatase activity: diabetes (P<0.01), treatment (P<0.01), and diabetes x treatment (P<0.05). Glycogen concentration: diabetes (P<0.001), treatment (P<0.01), and diabetes x treatment (P<0.01). Glucose-6-phosphate concentration; diabetes (P<0.001), treatment (P>0.05), and diabetes x treatment (P>0.05).[a]P< 0.05 compared with [NU], [b]P< 0.05 compared with [DU], [c]P< 0.05 compared with [NT].

4.7 Effects of *p*-MCA on insulin secretion

The results in Fig 1 show the profile of *p*-MCA on insulin secreted from perfused rat pancreata and INS-1 cells. *p*-MCA (10 and 100 μM) increased insulin secretion from the perfused rat pancreata to 1.4 and 3.1 times of the basal control group, respectively (Fig 4.12). The effluent insulin concentrations returned to the baseline during the washout period, and increased to 6 times of the baseline value upon administration of 10 mM glucose. By calculating the percentage of AUC of the control group, *p*-MCA significantly increased insulin secretion when compared with the corresponding the control group (control = 100%; 10 μM *p*-MCA = 142.4 ± 22.1%; 100 μM *p*-MCA = 314.6 ± 15.6%). *p*-MCA (30 – 300 μM) also increased insulin secretion from INS-1 cells in a concentration-dependent manner (Fig 4.13). From cytotoxicity testing by MTT assay demonstrated that *p*-MCA (100 μM*)* did not affect cell viability of INS-1 cells, suggesting that *p*-MCA is not acutely toxic to this β-cell line.

4.8 Effects of *p*-MCA on $[Ca^{2+}]_i$ of INS-1 Cells

Since Ca^{2+} is an important intracellular signal, and it mediates the effect of many insulin secretagogues, the experiments were next performed to determine the effect of *p*-MCA on $[Ca^{2+}]_i$ in INS-1 cells, and the results of these experiments are shown in Fig 4.14. *p*-MCA (10-100 μM) increased $[Ca^{2+}]_i$ in a concentration-dependent manner. *p*-MCA-induced $[Ca^{2+}]_i$ increase reached maximum within 60 s of administration, which was followed by a small sustained phase. At 10 and 30 μM *p*-MCA, the $\Delta[Ca^{2+}]_i$ increases were 23 ± 1 nM and 40 ± 2 nM above the basal level, respectively. Exposure of cells to 100 μM *p*-MCA induced a larger increase in $\Delta[Ca^{2+}]_i$ of 63 ± 3 nM over the basal level. The results suggested that *p*-MCA-stimulated insulin secretion was associated with a rise in $[Ca^{2+}]_i$

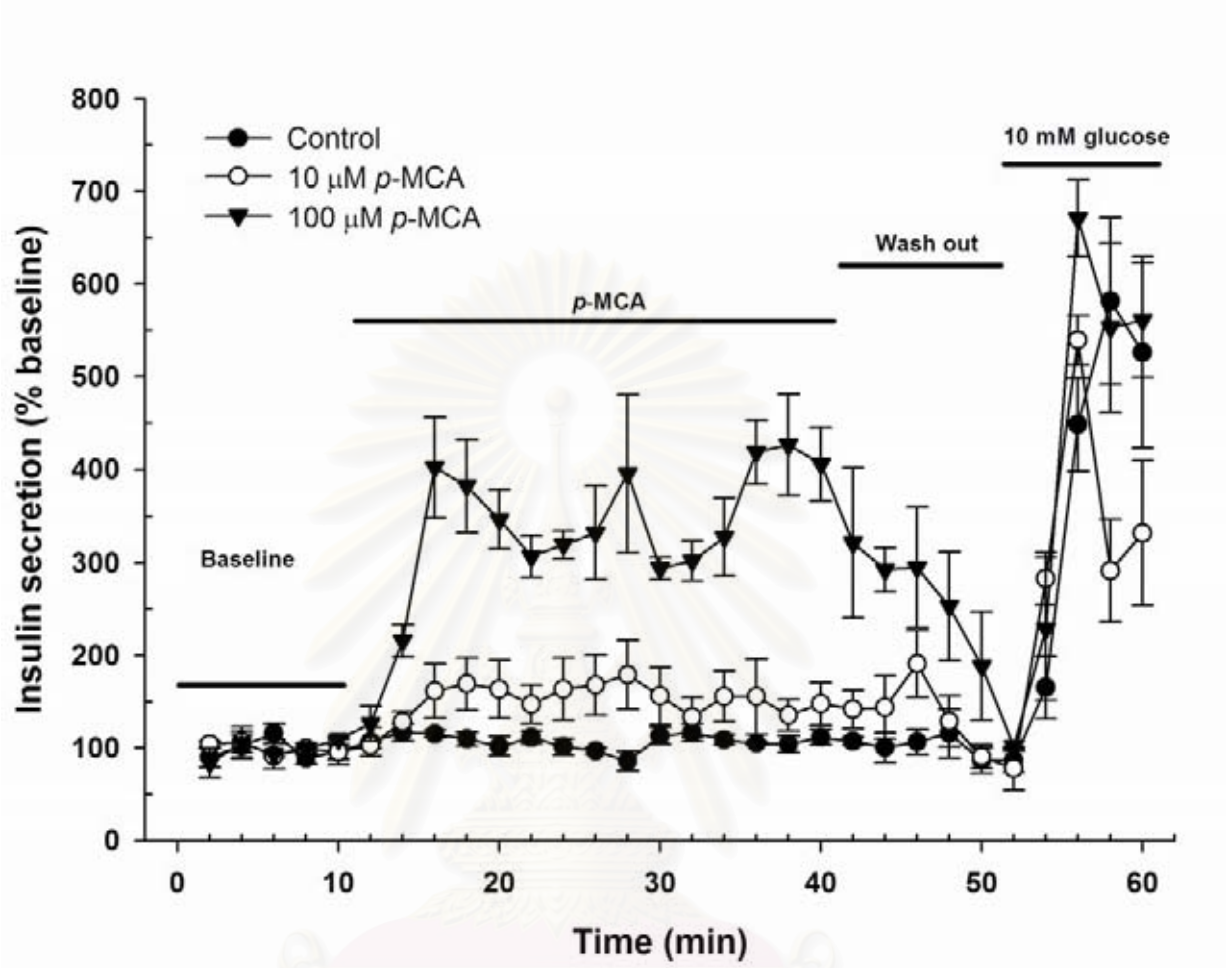

Figure 4.12 Effect of *p*-MCA (10 and 100 μM) on insulin secretion from perfused rat pancreas. In these experiments, a 20-min equilibration period preceded *time 0*. *p*-MCA was administered for 30 min. Values are means ± S.E.M.; *n* = 3, pancreata. Range of baseline insulin concentrations of effluents was 1.7 – 3.6 ng/ml.

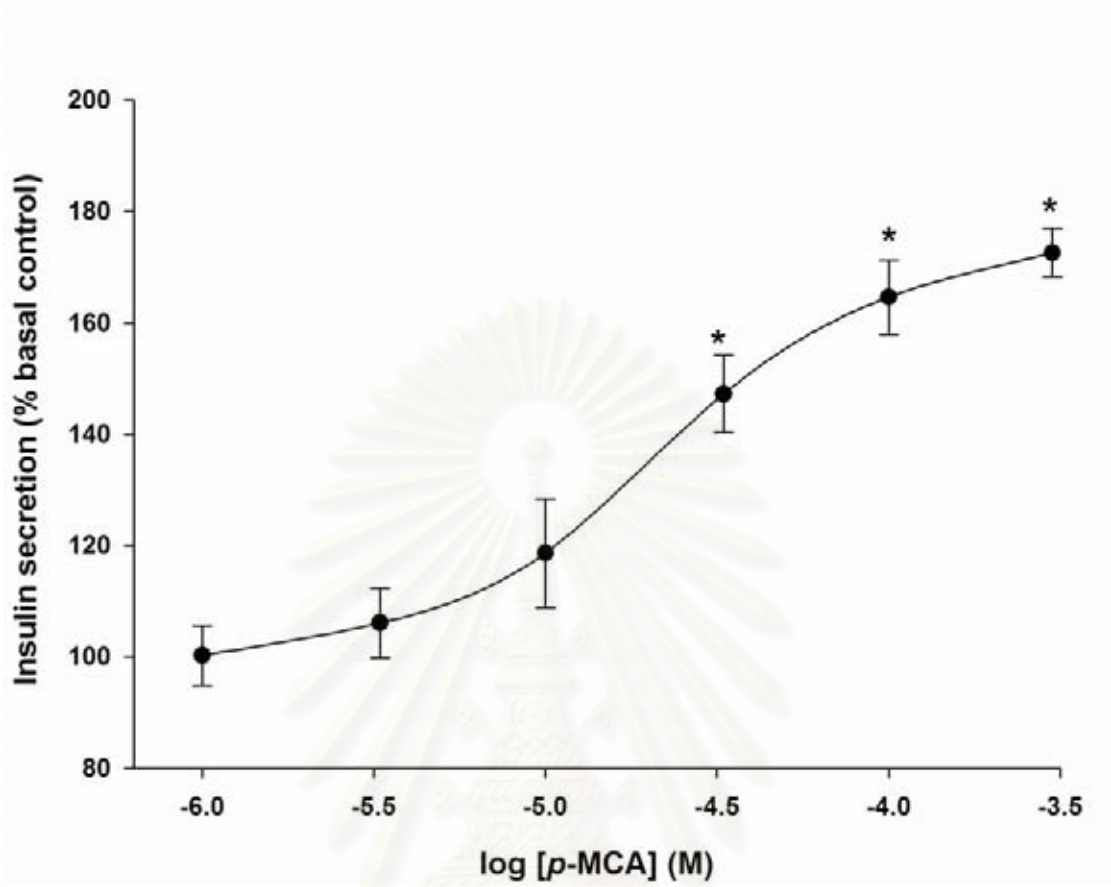

Figure 4.13 Effect of *p*-MCA on insulin secretion in INS-1 cells. The cells were preincubated for 15 min in KRB containing 4 mM glucose and 0.1% BSA. Cells were then incubated for 30 min in various concentrations of *p*-MCA. The control group had 3.54 ± 1.19 ng/well/ 30 min. Data are expressed as means ± S.E.M.; n= 3 independent experiments with quadruplicates in each experiment. * $P < 0.05$ vs. control group.

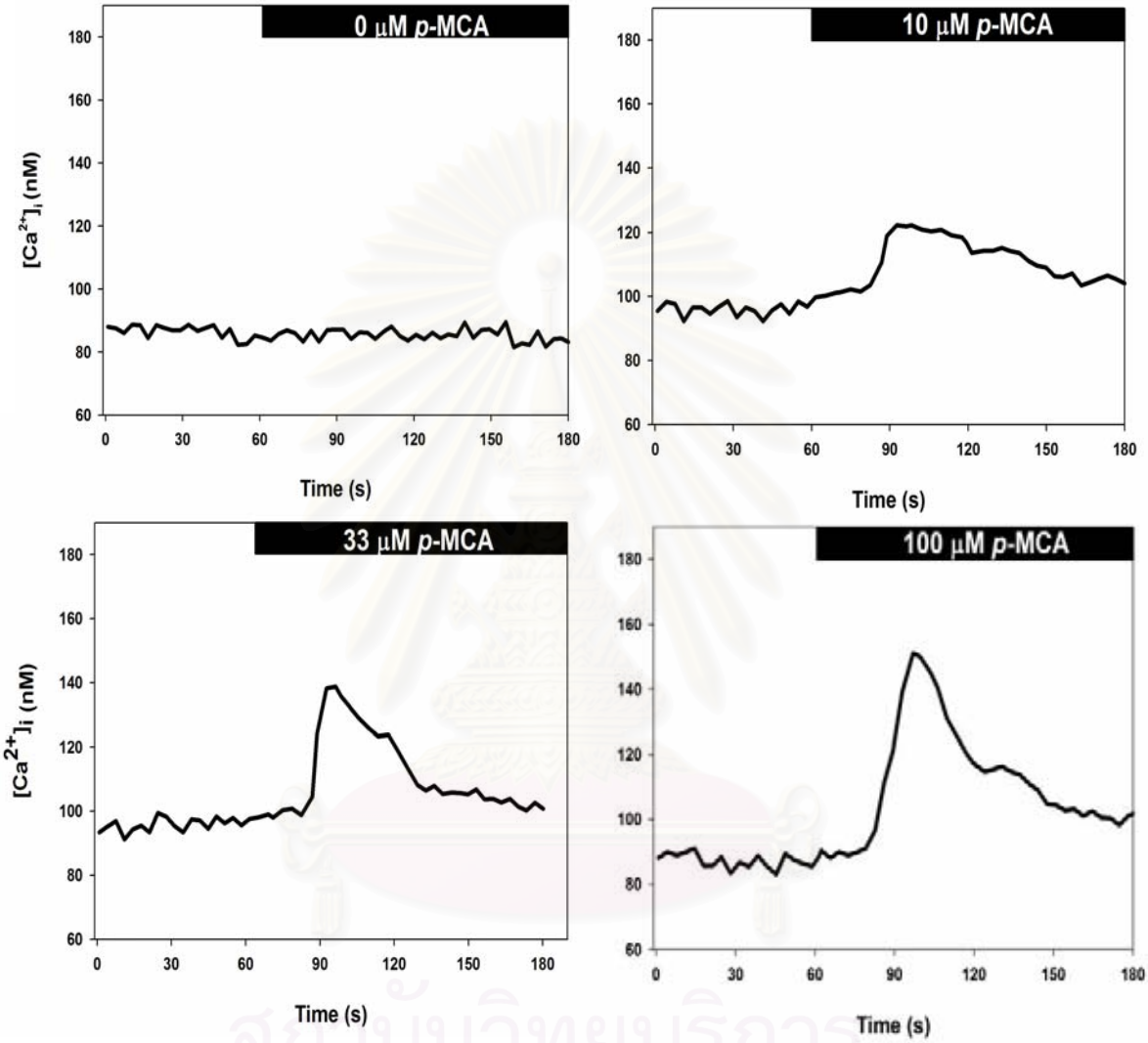

Figure 4.14 Concentration-dependent effect of *p*-MCA on $[Ca^{2+}]_i$ increase in INS-1 cells; (A) control group (B) 10 μM *p*-MCA, (C) 33 μM *p*-MCA, and (D) 100 μM *p*-MCA. Traces are representative of 4 independent experiments with 20 cells/experiment.

4.9 Effect of *p*-MCA-induced insulin secretions and $[Ca^{2+}]_i$ responses under a Ca^{2+}-free condition or in the presence of an L-type Ca^{2+} channel antagonist.

The roles of extracellular Ca^{2+} and VDCC in *p*-MCA-stimulated insulin secretion were examined using extracellular Ca^{2+}-free solution containing 0.1 mM EGTA, or an L-type Ca^{2+} channel blocker (nimodipine) in the presence of extracellular Ca^{2+} (Fig 4.15). In the Ca^{2+} containing KRB, *p*-MCA (100 μM) significantly increased insulin secretion by 60% in INS-1 cells over the basal control. The extracellular Ca^{2+}-free condition decreased basal insulin secretion when compared with Ca^{2+}-containing KRB. The results showed that *p*-MCA failed to increase insulin secretion in the absence of extracellular Ca^{2+}, and 1 μM nimodipine significantly blocked the secretory response to *p*-MCA. In the β-cells that were under the Ca^{2+}-free condition (Fig 4.16a), basal $[Ca^{2+}]_i$ were lower than those in Ca^{2+}-containing KRB. Under this circumstances, *p*-MCA failed to increase $[Ca^{2+}]_i$, whereas 1 μM thapsigargin, an endoplasmic reticulum Ca^{2+}-ATPase inhibitor, caused the rise in $[Ca^{2+}]_i$. Figure 4.16 b shows that $[Ca^{2+}]_i$ response to *p*-MCA was abolished by 1 μM nimodipine, which also blocked Bay K 8644-stimulated $[Ca^{2+}]_i$ elevation. In addition, 1 μM nimodipine alone did not significantly change the basal $[Ca^{2+}]_i$ or insulin secretion. These findings are consistent with those of insulin secretion studies.

4.10 Effects of *p*-MCA on insulin secretion and $[Ca^{2+}]_i$ response in the presence of a K_{ATP} channel opener

To determine whether *p*-MCA increases insulin secretion by closing K_{ATP} channels, *p*-MCA was incubated with diazoxide, a K_{ATP} channel opener. As shown in Fig. 4.17, diazoxide (400 μM) did not affect the basal insulin concentration in the presence of 4 mM glucose. Glyburide (10 μM), a K_{ATP} channel antagonist, significantly increased insulin secretion by ~2.0-fold, whereas its stimulatory effect was virtually abolished in the presence of diazoxide. In contrast, diazoxide did not block the effect of *p*-MCA-induced insulin secretion. The *p*-MCA-induced increase in $[Ca^{2+}]_i$ in the presence of diazoxide is shown in Fig. 4.18. It was found that diazoxide did not change the basal $[Ca^{2+}]_i$ in INS-1 cells. Meanwhile, diazoxide failed to inhibit *p*-MCA-induced

$[Ca^{2+}]_i$ increase. These findings are consistent with the effect of *p*-MCA on insulin secretion in the presence of diazoxide in INS-1 cells.

4.11 Enhancement of glucose-stimulated insulin release and $[Ca^{2+}]_i$ increase by *p*-MCA

The experiments were further determined the interaction between *p*-MCA and glucose on insulin secretion and $[Ca^{2+}]_i$ in INS-1 cells. Increasing glucose concentration from 5.5 mM to 10 mM caused a rapid and marked increase in insulin secretion from perfused rat pancreata (Fig 4.19). The first transient phase secretion peak was about 5-fold of the baseline level, which was followed a second phase that was observed after 10 min administration *p*-MCA (10 μM) alone caused a small increase in insulin secretion, and potentiated glucose-induced insulin secretion, when added to perfusion medium 20 min after the start of glucose administration. By expressing the data as percentage of control in AUC during 20-min treatments, there was a significant difference between glucose + *p*-MCA group and glucose alone group (glucose alone = 559.1 ± 18.0%; glucose + *p*-MCA = 750.3 ± 49.3%). When comparing those treatments with *p*-MCA alone and control groups (control = 100.0%; *p*-MCA 10 μM = 129.4 ± 8.8%), *p*-MCA markedly enhanced glucose-induced insulin secretion.

The effect of of *p*-MCA on glucose-induced insulin secretion was next performed in INS-1 cells using static incubation (Fig 4.20a and 4.20b). In these cells,10 mM glucose increased insulin concentration by 65% over the control group that had 4 mM glucose. Both 10 and 100 μM of *p*-MCA enhanced glucose-stimulated insulin secretions from INS-1 cells, which were consistent with the results in the pancreatic perfusion experiments.

$[Ca^{2+}]_i$ responses to glucose were further investigated in INS-1 cells. A rise in glucose concentrations (Fig 4.21) from 4 to 10 mM increased $[Ca^{2+}]_i$ in a small transient peak (120 ± 4 nM). Addition of *p*-MCA in the continued presence of glucose further potentiated the increase in $[Ca^{2+}]_i$, (10 μM *p*-MCA = 147± 4 nM; 100 μM *p*-MCA, 174±5 nM).

4.12 Interaction between *p*-MCA and others secretagogues on insulin secretion and $[Ca^{2+}]_i$ response

The experiments were examined the effect of *p*-MCA on insulin secretion stimulated by various secretagogues, which were through different mechanisms to cause ultimate opening of the L-type Ca^{2+} channels, e.g., glyburide, which blocks K_{ATP} channels; KCl, which is a membrane depolarizing agent; Bay K 8644, which directly activates the L-type Ca^{2+} channels. Figure 4.23 shows the effect of *p*-MCA on insulin secretion in INS-1 cells stimulated by glyburide. Glyburide (10 μM) significantly increased insulin secretion by 80% over the control group. The results revealed that *p*-MCA at 100 μM, but not 10 μM, markedly enhanced the glyburide-induced insulin secretion. The effect of glyburide on $[Ca^{2+}]_i$ response is shown in Fig. 4.24. When the cells was first stimulated with glyburide, the $[Ca^{2+}]_i$ response was 178±8 nM (an initial peak) and being followed by a more sustained phase (133 ± 12 nM), the subsequent addition of *p*-MCA further increased $[Ca^{2+}]_i$ (10 μM *p*-MCA= 170 ± 10 nM;100 μM *p*-MCA=245 ± 18 nM).

The next experiments were investigated the effect of *p*-MCA on insulin secretion and $[Ca^{2+}]_i$ response in the presence of either of 2 secretagougues, KCl and Bay K 8644. As shown in Fig 6B, KCl (15 mM) caused 3.6-fold increase in insulin secretion over the basal levels, whereas *p*-MCA (10 and 100 μM *p*-MCA) significantly potentiated insulin secretion by 4.8- and 5.6-fold in presence the of KCl, respectively. In $[Ca^{2+}]_i$ experiments, KCl (15 mM) evoked a transient Ca^{2+} increase, which reached the peak (250±10 nM) within 10 s, and followed by the sustained phase (148±12 nM). Addition of *p*-MCA potentiated KCl-induced increase in $[Ca^{2+}]_i$ (Fig 4.25). The mean amplitude of $[Ca^{2+}]_i$ response to 10 and 100 μM *p*-MCA were 212±5 nM and 228±9 nM, respectively.

The effect of *p*-MCA on Bay K 8644-stimulated insulin secretion was determined using static incubation in INS-1 cells and the pancreatic perfusion. Bay K 8644 (1 μM) increased insulin secretion in INS-1 cells by 4-fold over the basal level (Fig 4.26). 10 μM *p*-MCA and 100 μM *p*-MCA in the presence of Bay K 8644 potentiated insulin secretion by causing 5.4- and 8.0-fold increase, respectively. This potentiation

was confirmed by experiments in the perfused rat pancreata (Fig 4.27). Bay K 8644 (1 μM) increased insulin secretion from the perfused rat pancreata to 2.5 times of the basal control group. The potentiation by *p*-MCA of Bay K 8644-induced insulin secretion was also observed during 30-min administration. By expressing the data as the percentage of control in AUC for Bay K 8644 and *p*-MCA as well as comparing them with those of Bay K 8644 alone, there was a significant increase in insulin secretion (control = 100 %;10 μM *p*-MCA = 142.4 ± 22.1%; Bay K 8644 = 251.2 ± 16.6%; Bay K 8644 + *p*-MCA = 628.5 ± 23.7%). The effects of Bay K 8644 on $[Ca^{2+}]_i$ response were also examined in INS-1 cells (Fig. 4.28). When Bay K 8644 (1 μM) was applied to INS-1 cells, it caused rapid and persistent increase in $[Ca^{2+}]_i$ from 89 ± 4 nM to 129 ± 6 nM. *p*-MCA potentiated Bay K 8644-induced increase in $[Ca^{2+}]_i$ (10 μM *p*-MCA= 189 ± 12 nM;100 μM *p*-MCA=225 ± 9 nM).

4.13 Effects of *p*-MCA insulin secretion and cAMP contents in the presence of forskolin and IBMX in INS-1 cells

Since an increase in cyclic AMP content may mediate the effect of some of the insulin secretagogues, the experiments were determined if *p*-MCA increases the level of this signal in INS-1 cells. As shown in Table 1, 100 μM *p*-MCA , but not 10 μM *p*-MCA, increased cyclic AMP content by 46% in INS-1 cells. The interactions of *p*-MCA with an adenylyl cyclase activator forskolin and a phosphodiesterase inhibitor IBMX were studied as well. Forskolin (1 μM) and IBMX (100 μM) also increased cyclic AMP content. *p*-MCA (100 μM) enhanced forskolin-induced, but not IBMX-induced, increase in cyclic AMP contents. The further experiments were investigated the effects of forskolin and IBMX on *p*-MCA-induced increase in insulin secretion. The results of these experiments are shown in Fig 4.28a and 4.28b. Forskolin and IBMX increased insulin secretion by 70% and 50%, respectively. *p*-MCA enhanced forskolin-induced insulin secretion (Fig. 4.28). In contrast, *p*-MCA failed to enhance IBMX-induced insulin secretion.

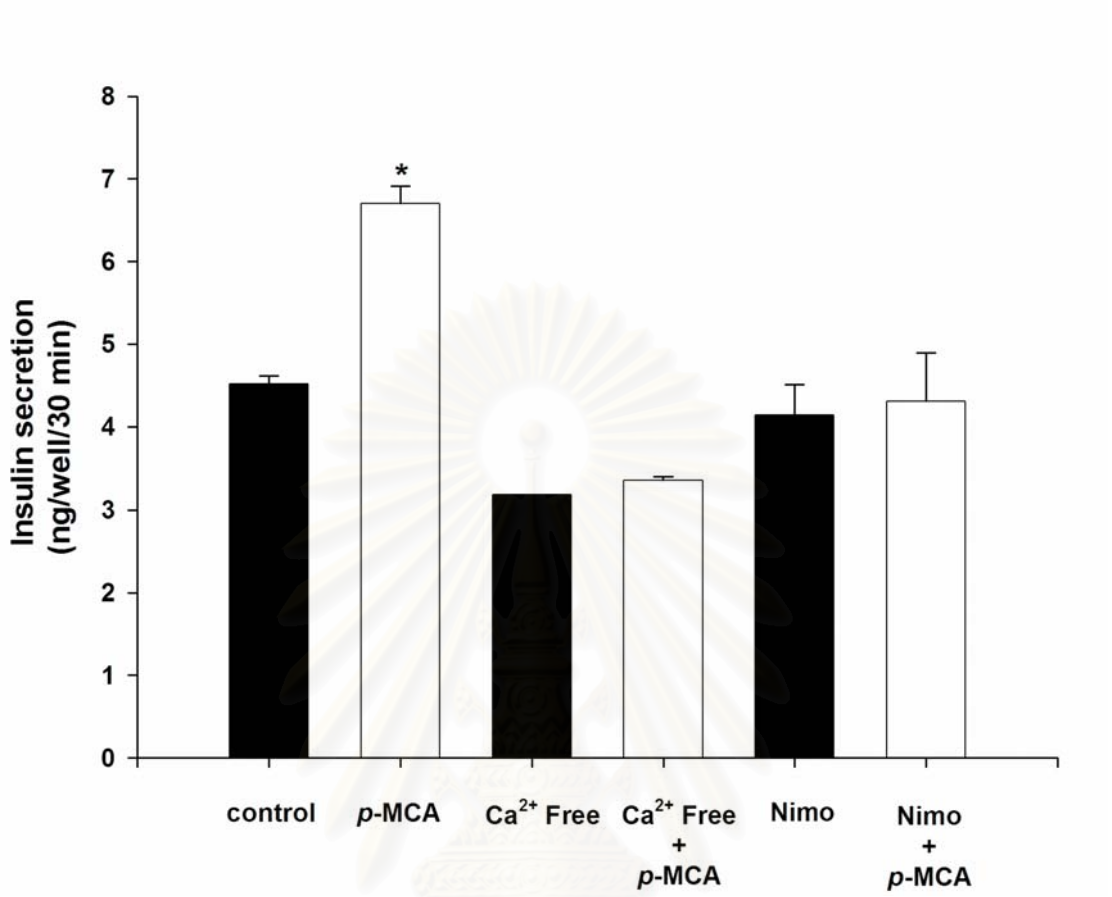

Figure 4.15 Effect of 100 μM *p*-MCA on insulin secretion in INS-1 cells in the presence of Ca^{2+} free KRB or 1 μM nimodipine(Nimo). Values are mean ± SE; *n* = 3 independent experiments with quadruplicates in each experiment. **P*<0.05 compared with control.

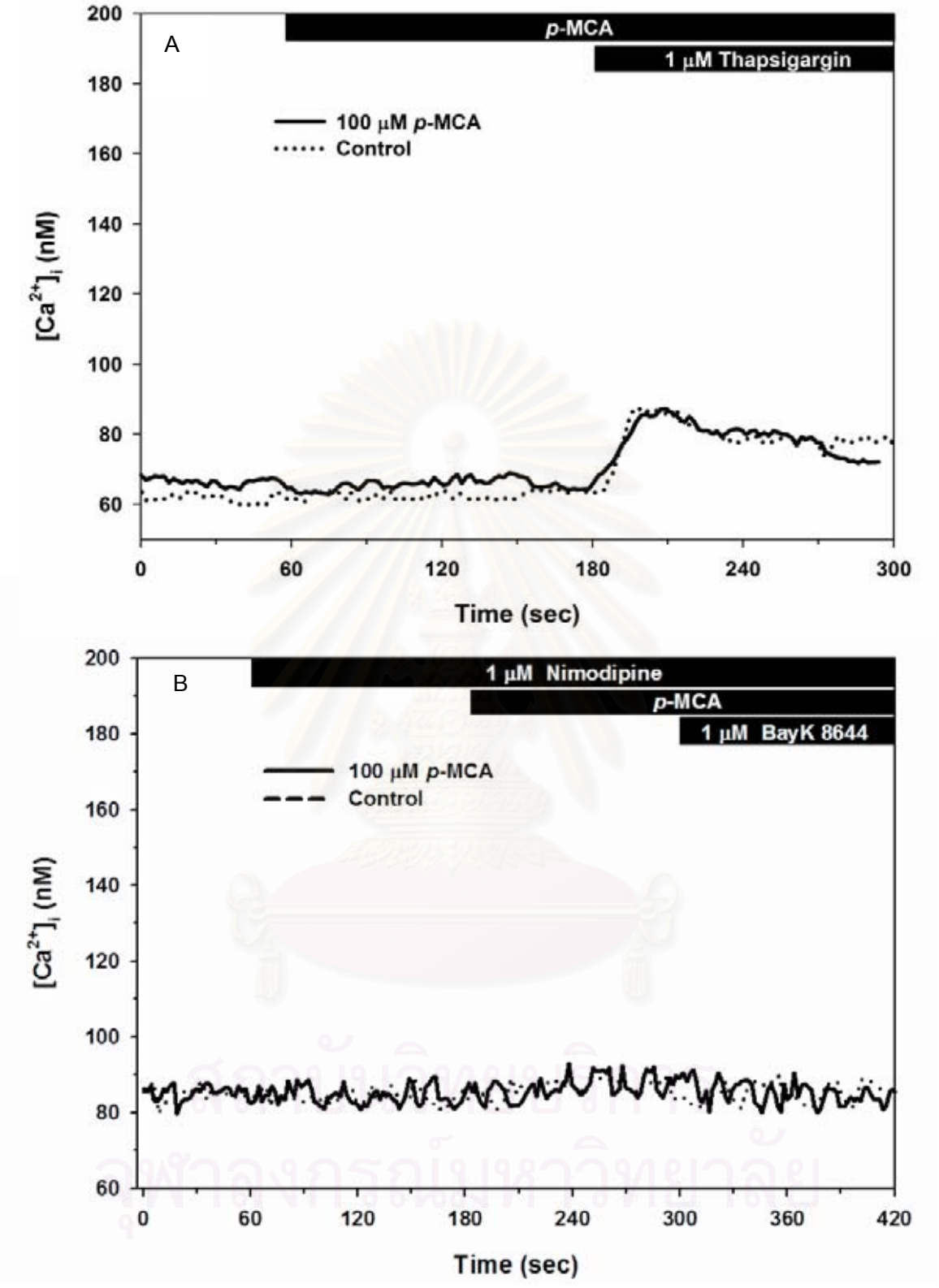

Figure 4.16 (A) Effect of 100 μM *p*-MCA on $[Ca^{2+}]_i$ in the presence of Ca^{2+} free KRB. (B) Effect of 1μM nimodipine on100μM *p*-MCA-induced increase in $[Ca^{2+}]_i$. Traces shown are representative of 4 independent experiments with 20 cells/experiment.

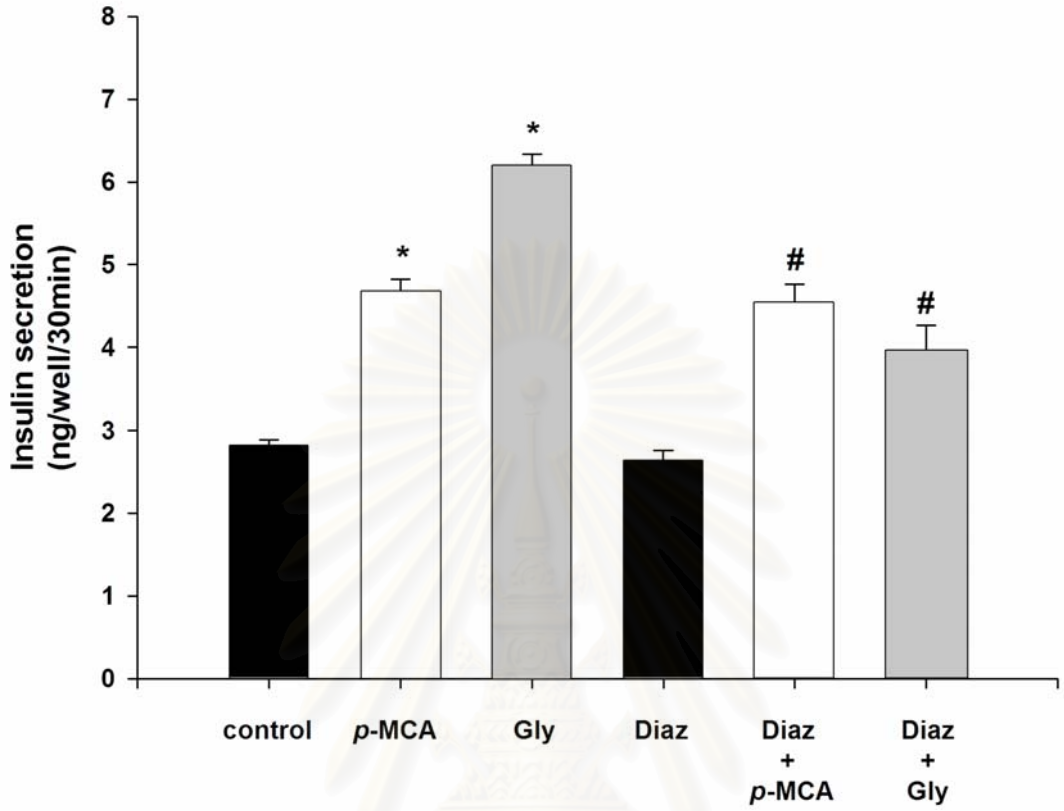

Figure 4.17 Effects of 400 μM diazoxide (Diaz) on *p*-MCA (100 μM)- and 10 μM glyburide (Gly)-stimulated insulin secretion in INS-1 cells. Values are means ± S.E.M.; $n = 3$ independent experiments with quadruplicates in each experiment. $^{*}P<0.05$ compared with control, $^{\#}P<0.05$ compared with diazoxide alone.

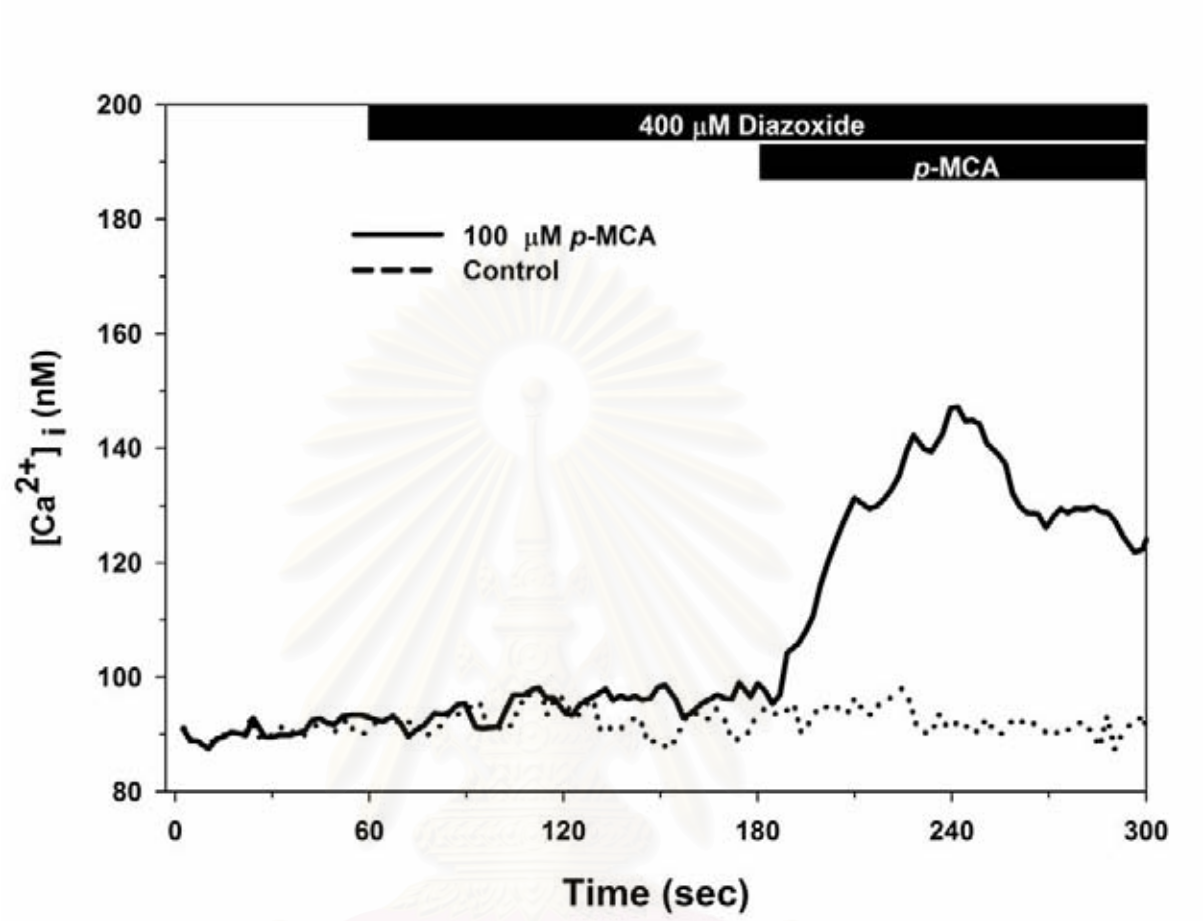

Figure 4.18 Effect of diazoxide on *p*-MCA-induced increase in $[Ca^{2+}]_i$. Data shown are representative of 4 independent experiments with 20 cells/experiment.

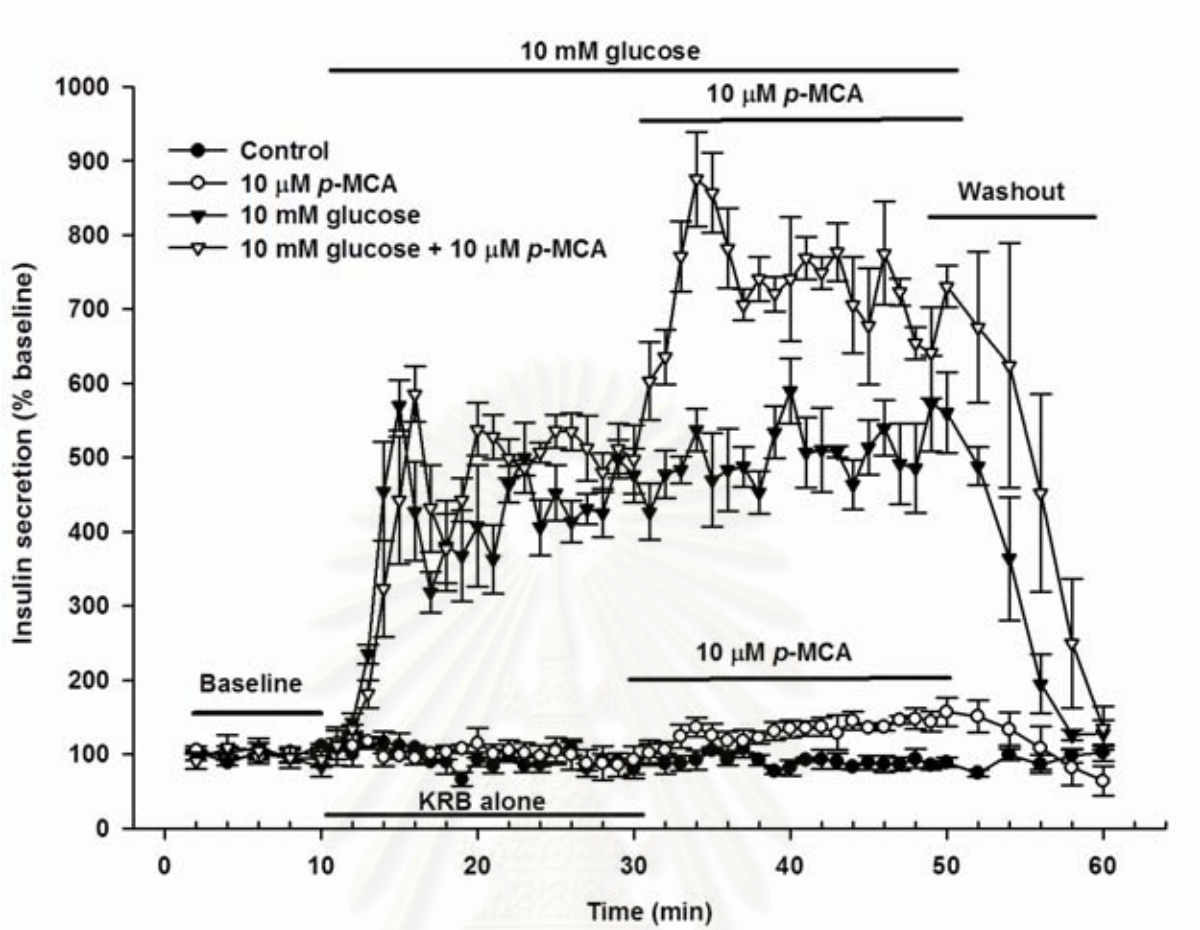

Figure 4.19 Effect of *p*-MCA (10 μM) on glucose-induced insulin secretion in perfused rat pancreata. In these experiments, a 20-min equilibration period preceded *time 0*. The pancreata were perfused with KRB for a 10-min baseline period and then followed by 10 mM glucose for 20min. *p*-MCA was administered for 20 min in the presence of 10 mM glucose. Range of baseline insulin concentrations of effluents was 1.5 – 3.2 ng/ml. Values are means ± S.E.M.; *n* = 3 pancreata.

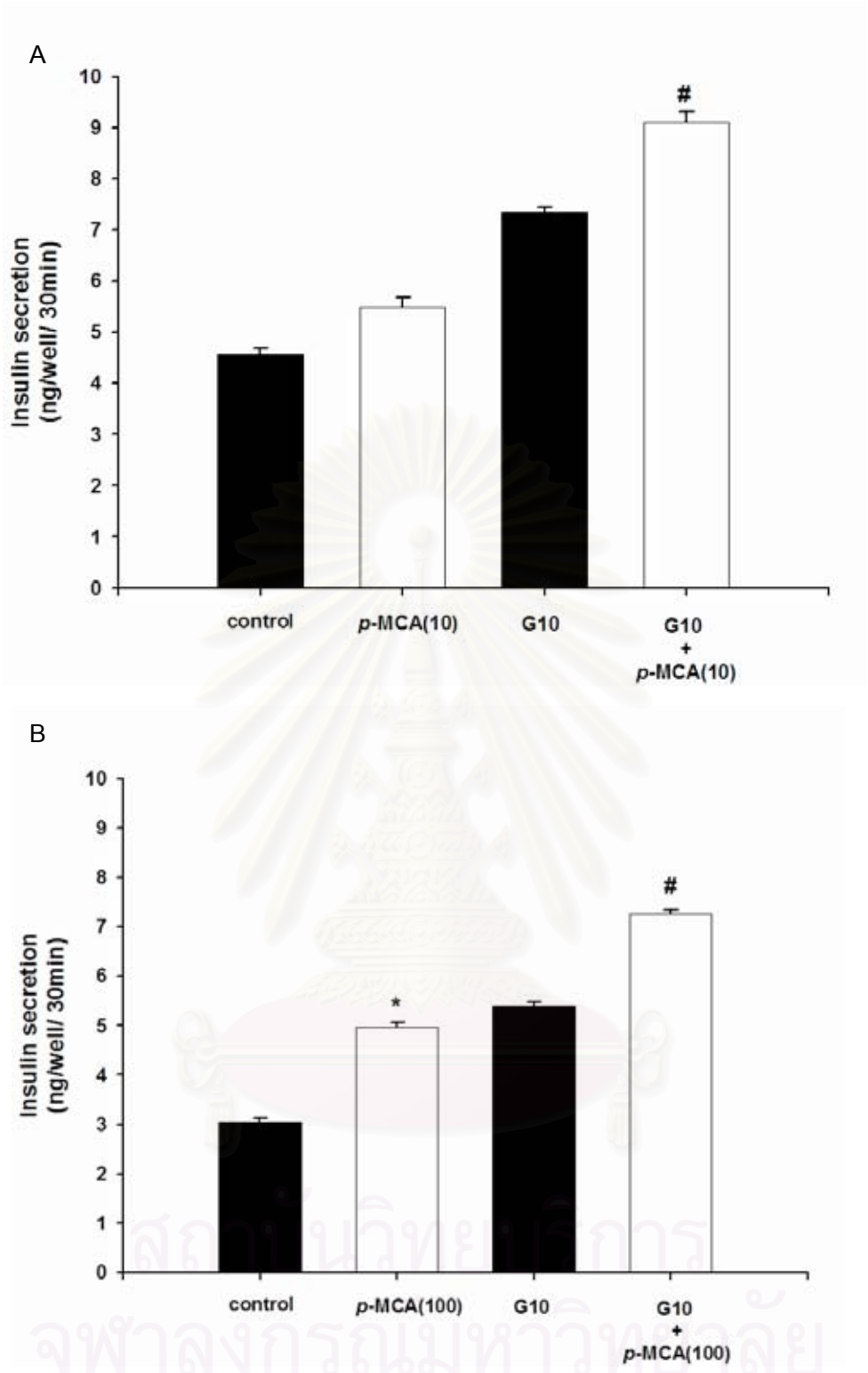

Figure 4.20 (A) Effect of 10 μM *p*-MCA on glucose-induced insulin secretion in INS-1 cells. (B) Effect of 100 μM *p*-MCA on glucose-induced insulin secretion in INS-1 cells. Values are means ± S.E.M.; $n = 3$ independent experiments with quadruplicates in each experiment. *$P<0.05$ compared with control (4 mM glucose alone), $^{\#}P<0.05$ compared with 10 mM glucose alone.

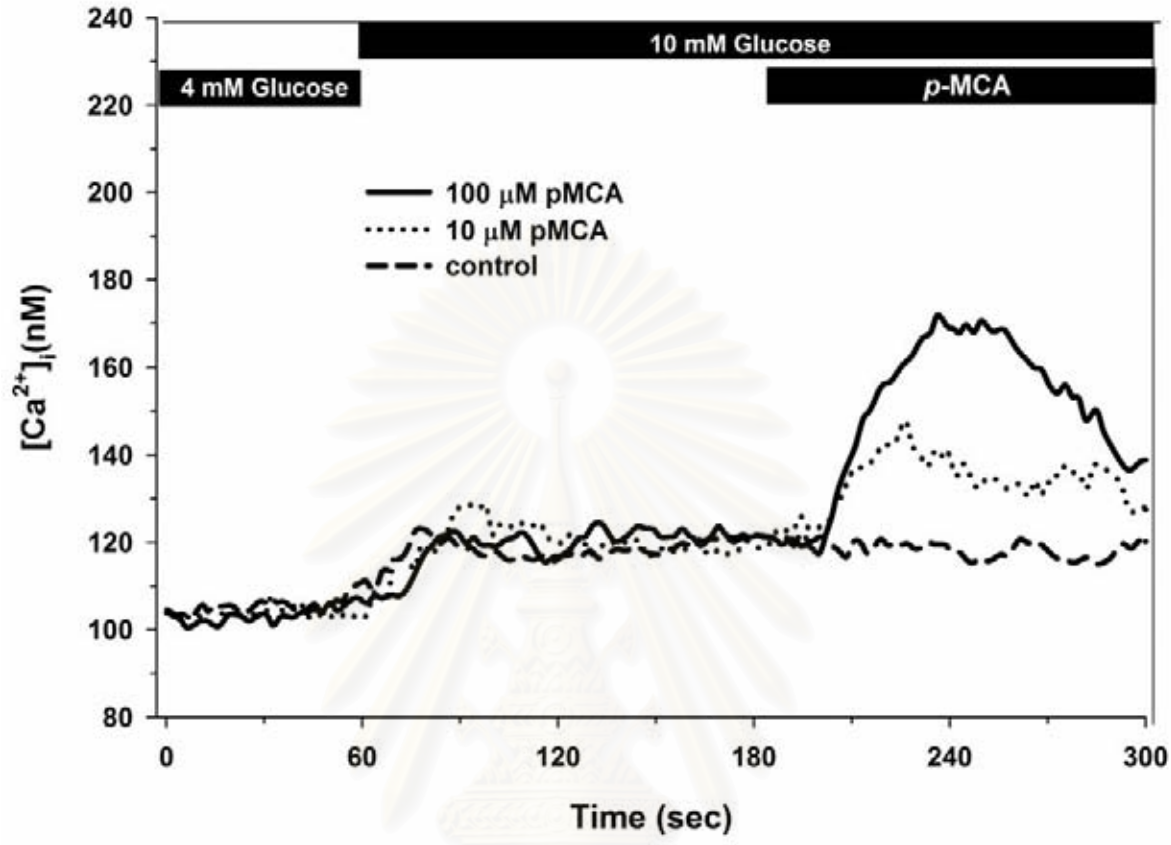

Figure 4.21 Effect of *p*-MCA on glucose-induced increase in $[Ca^{2+}]_i$. Data shown are representative of 4 independent experiments with 20 cells/experiment.

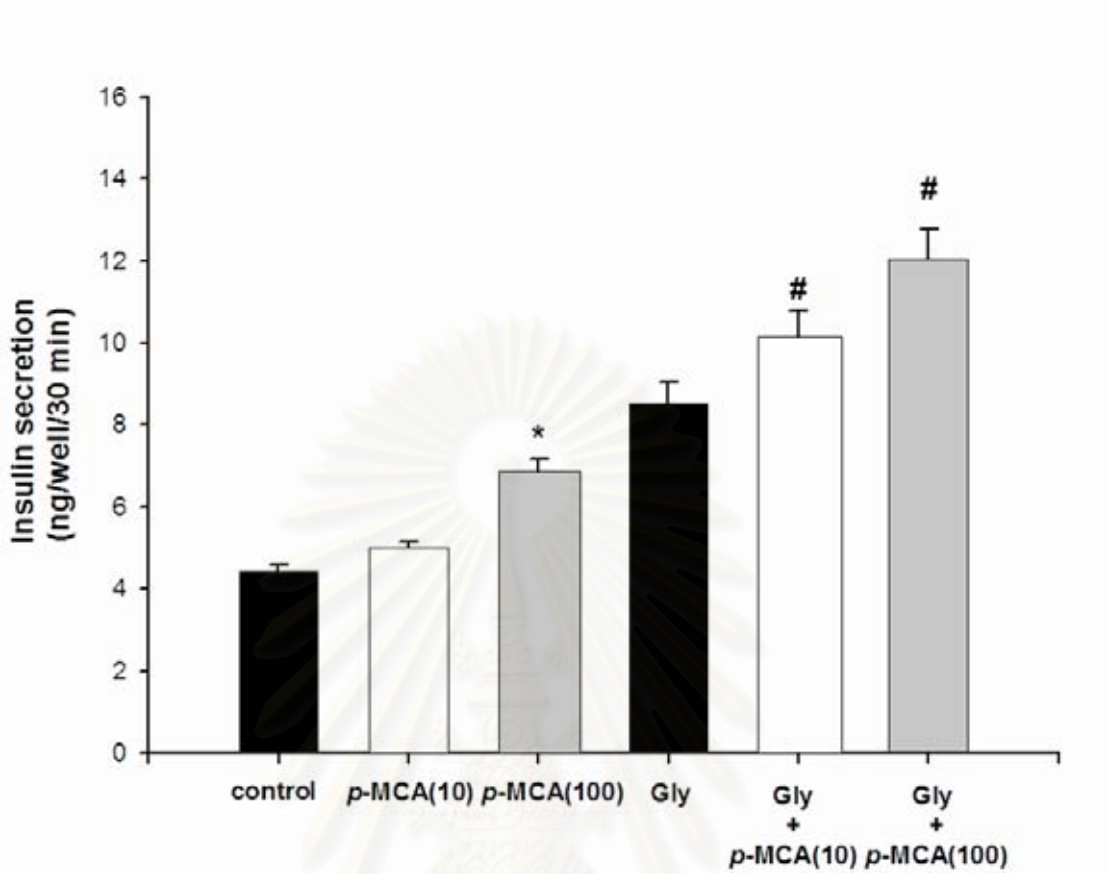

Figure 4.22 Effect of *p*-MCA on insulin secretion in INS-1 cells in presence of 100 μM glyburide. Values are means ± S.E.M.; $n = 3$ (quadruplicate) independent experiments with quadruplicates in each experiment. $^{*}P<0.05$ compared with control, $^{\#}P<0.05$ compared with glyburide alone.

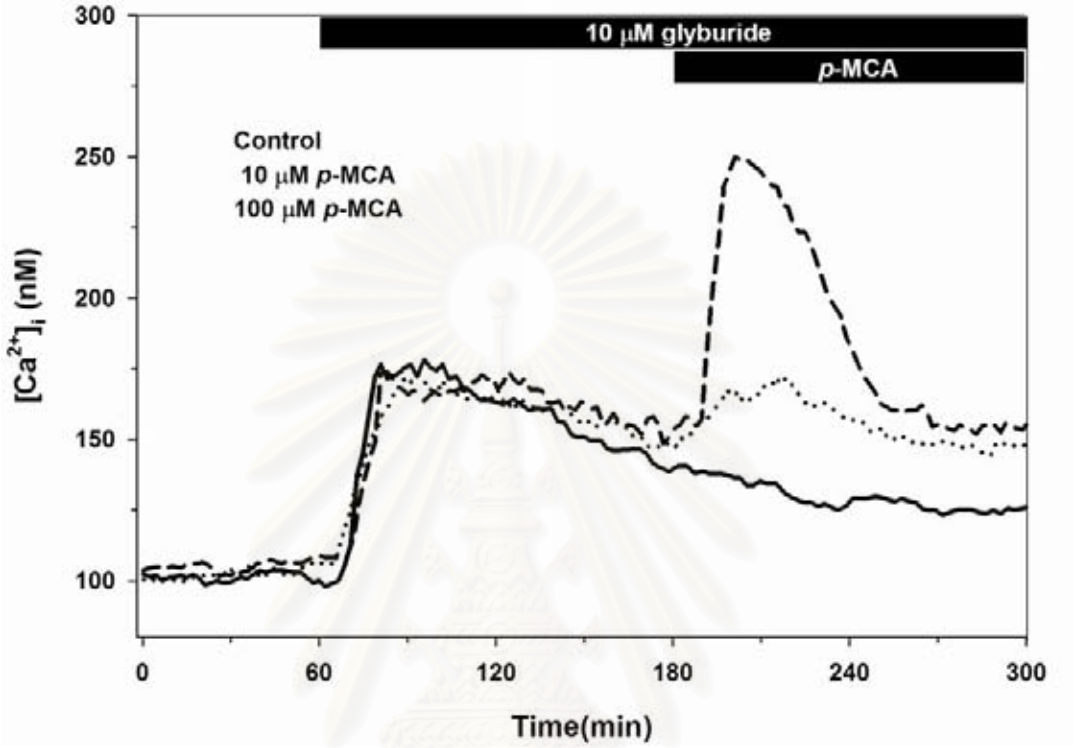

Figure 4.23 Effect of *p*-MCA on glyburide-induced $[Ca^{2+}]_i$ increase. Data shown are representative of 4 independent experiments with 20 cells/experiment.

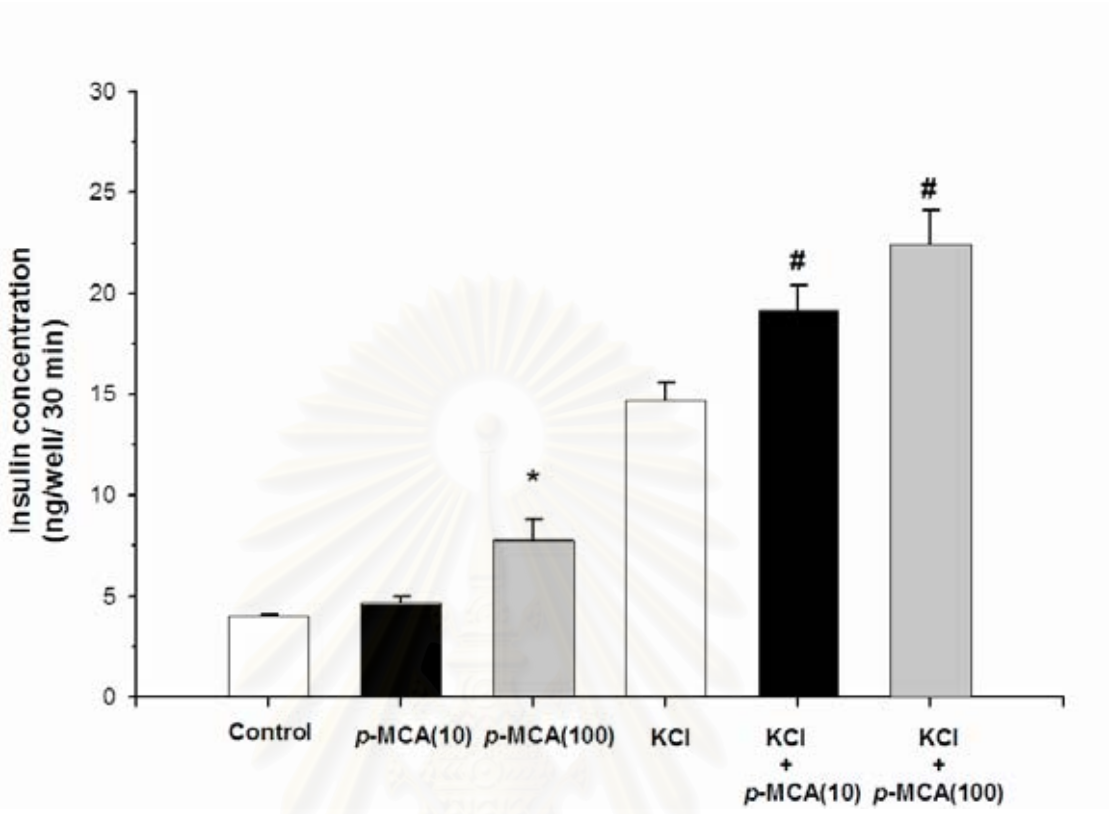

Figure 4.24 Effect of *p*-MCA on insulin secretion in INS-1 cells in presence of 15 mM KCl. Values are means ± S.E.M.; $n = 3$ (quadruplicate) independent experiments with quadruplicates in each experiment. $^{*}P<0.05$ compared with control, $^{\#}P<0.05$ compared with KCl alone.

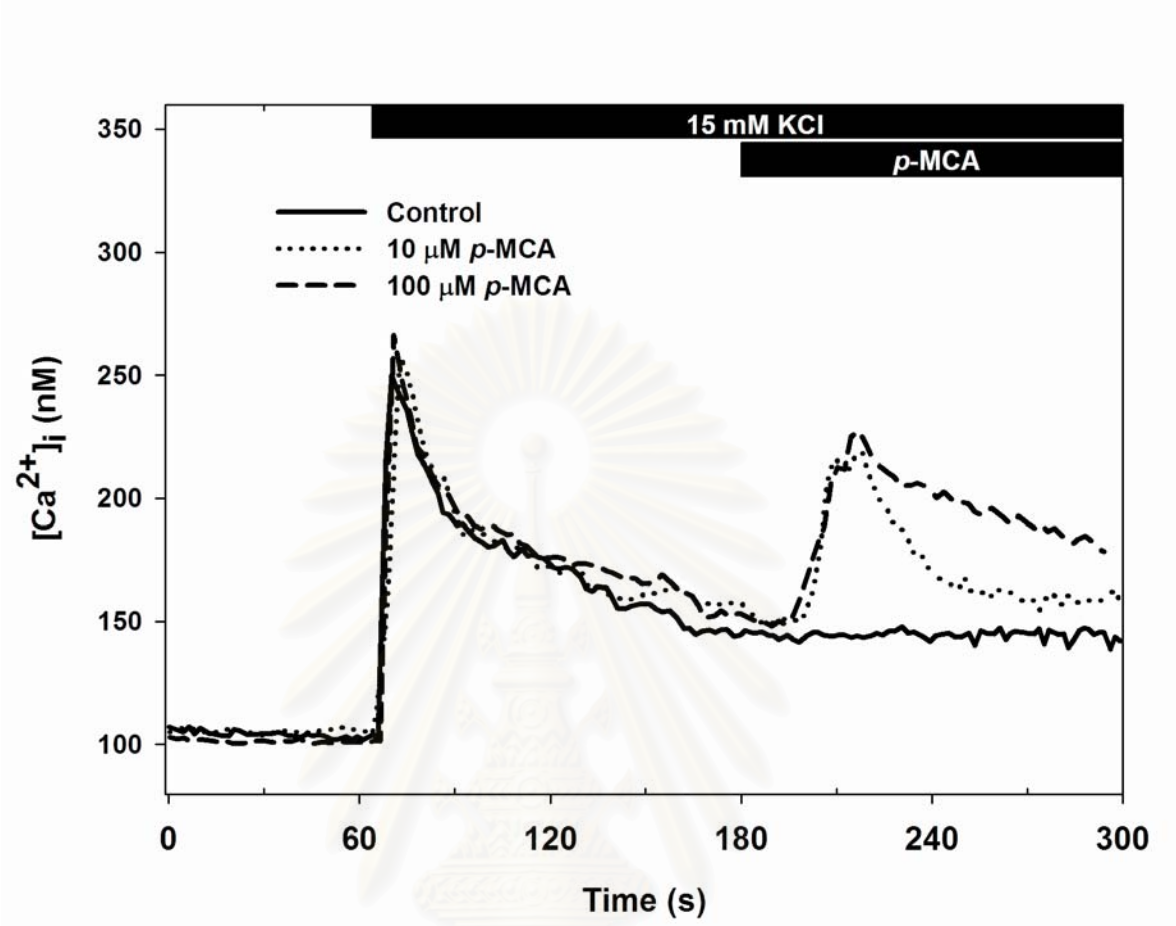

Figure 4.25 Effect of *p*-MCA on KCl-induced $[Ca^{2+}]_i$ increase. Data shown are representative of 4 independent experiments with 20 cells/experiment.

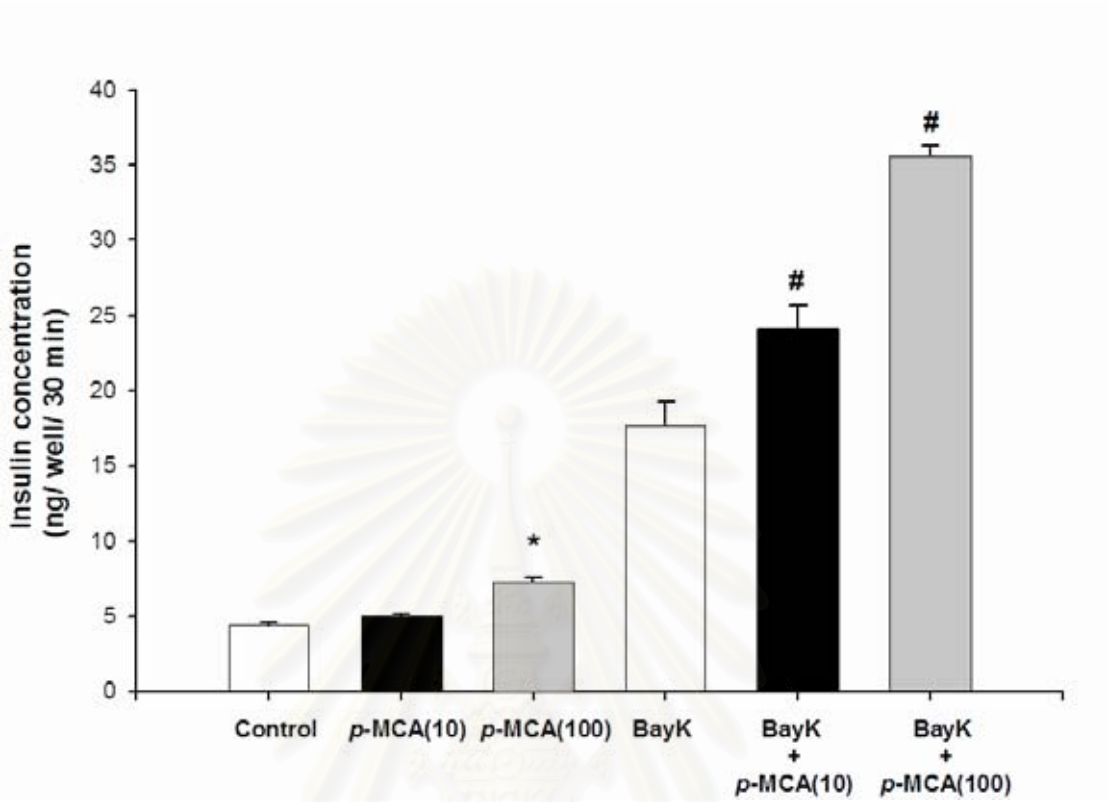

Figure 4.26 Effect of *p*-MCA on insulin secretion in INS-1 cells in the presence of 1 μM Bay K 8644. Values are means ± S.E.M.; $n = 3$ independent experiments with quadruplicates in each experiment. *$P<0.05$ compared with control, $^{\#}P<0.05$ compared with Bay K 8644 alone.

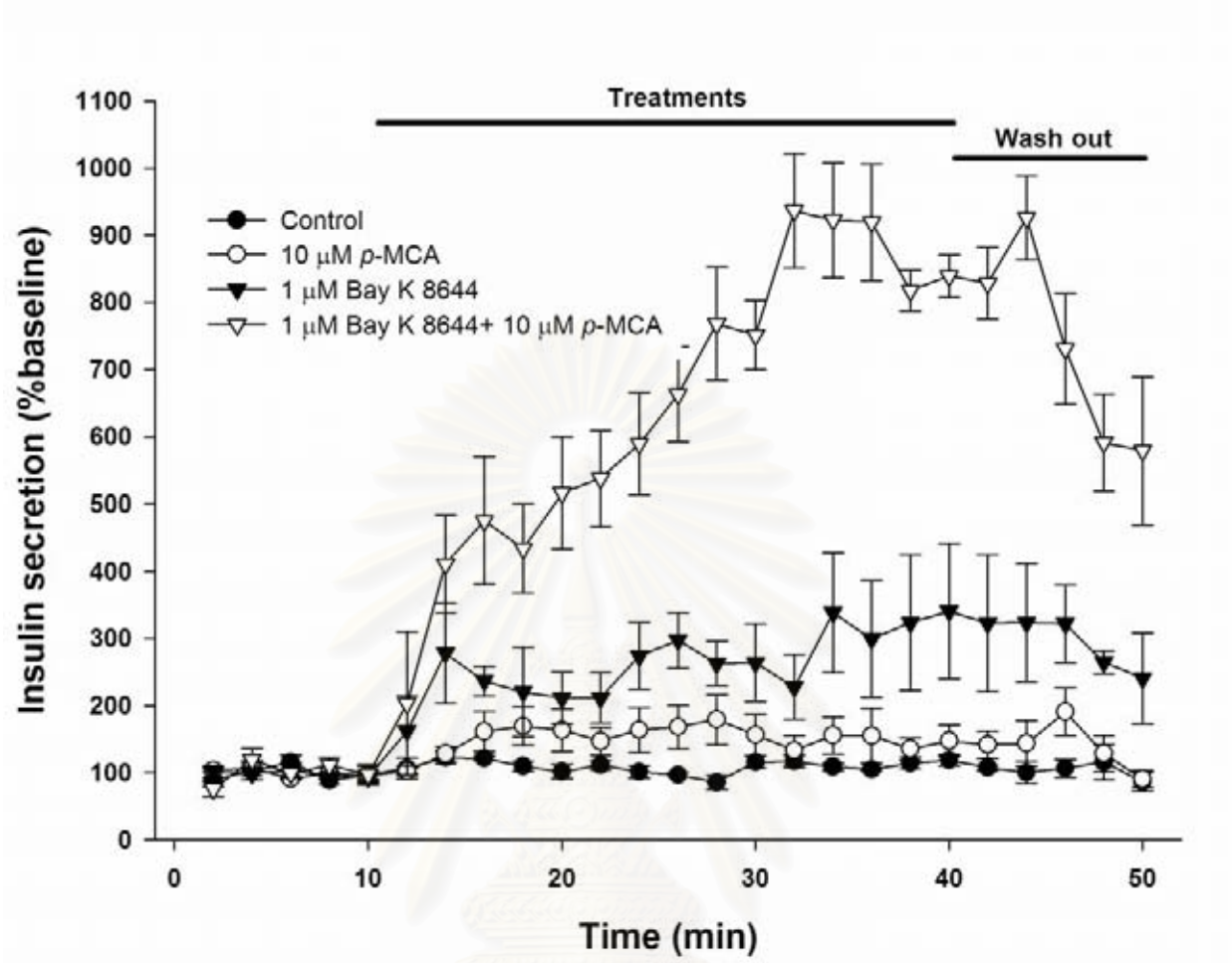

Figure 4.27 Effect of 10 μM *p*-MCA on insulin release from perfused rat pancreas. In these experiments, a 20-min equilibration period preceded *time 0*. Bay K 8644 (1 μM) was administered for 30 min with or without 10 μM *p*-MCA. Values are means ± S.E.M.; *n* = 3. Range of baseline insulin concentrations of effluents was 2.2 – 3.7 ng/ml.

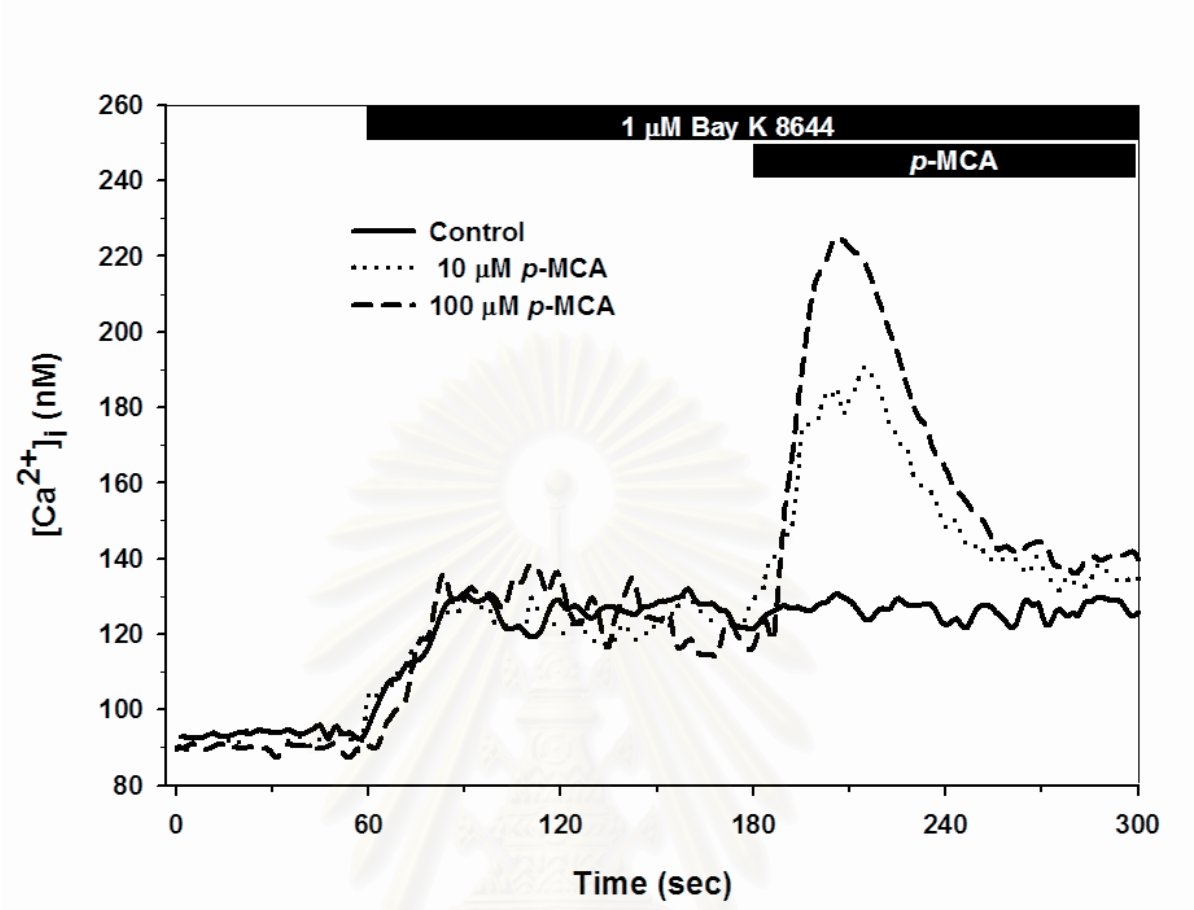

Figure 4.28 Effect of *p*-MCA on Bay K 8644- induced $[Ca^{2+}]_i$ response. Data shown are representative of 4 independent experiments with 20 cells/experiment.

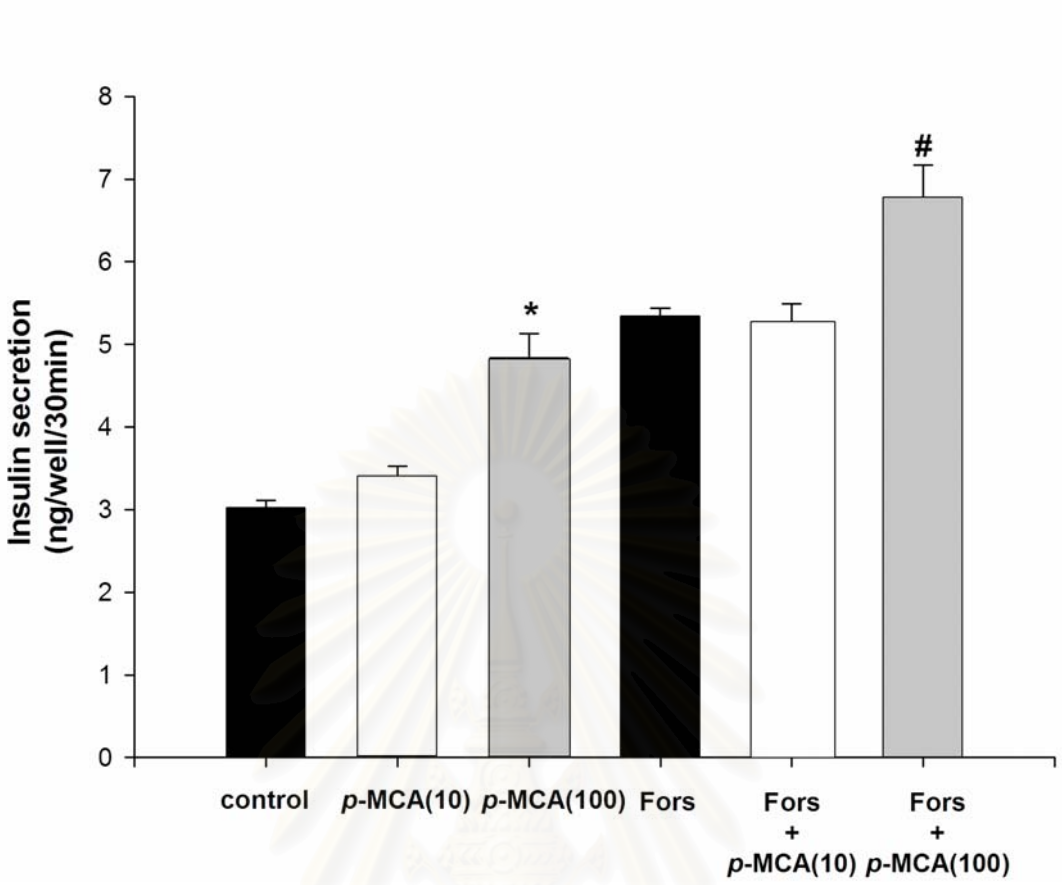

Figure 4.29 Effect of *p*-MCA on insulin secretion in INS-1 cells in the presence of 1 μM forskolin(fors). Values are means ± S.E.M.; $n = 3$ independent experiments with quadruplicates. *$P<0.05$ compared with control, $^{\#}P<0.05$ compared with forskolin alone.

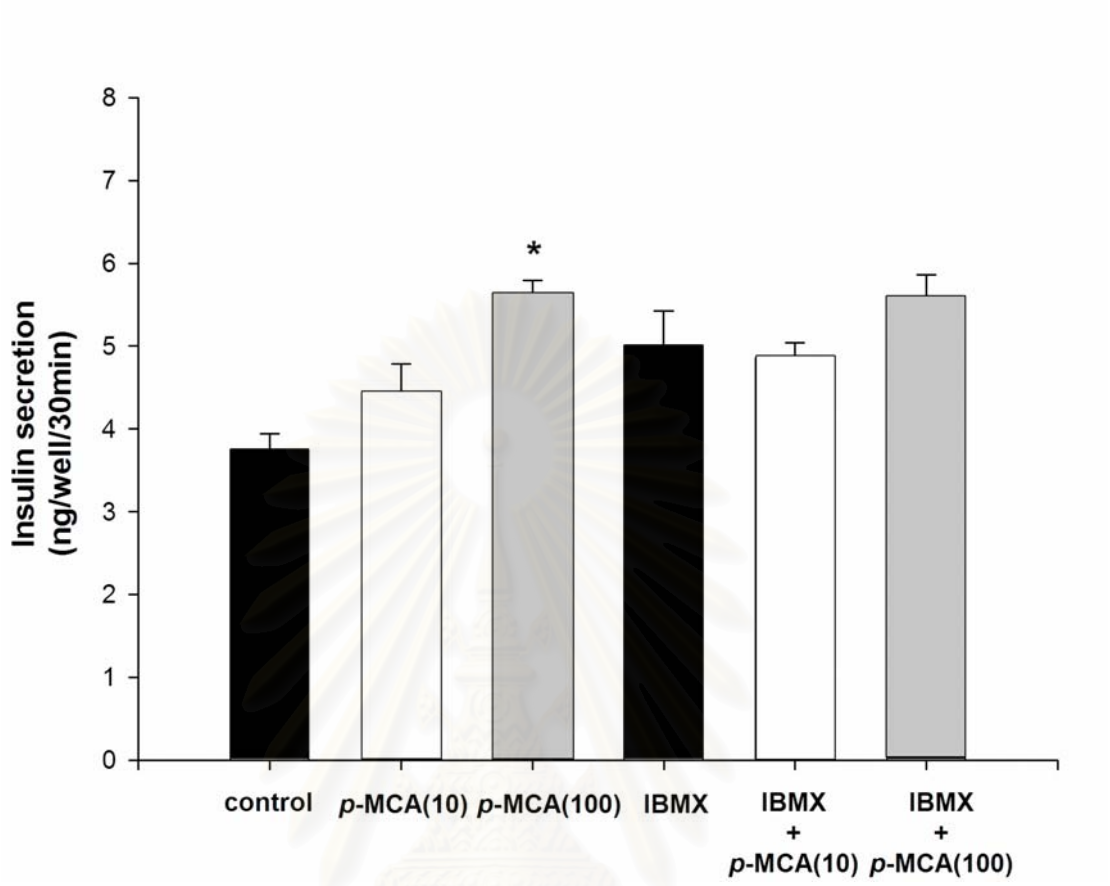

Figure 4.30 Effect of *p*-MCA on insulin secretion in INS-1 cells in the presence of 100 μM IBMX. Values are means ± S.E.M.; $n = 3$ independent experiments with quadruplicates. *$P<0.05$ compared with control.

Table 4.3 Effects of *p*-MCA on cAMP concentrations in INS-1 cells in the presence of 1 μM forskolin and 100 μM IBMX

cAMP level (pmol/well/ 30min)	Control	*p*-MCA(10)	*p*-MCA(100)	Forskolin	Forskolin + *p*-MCA(10)	Forskolin + *p*-MCA(10)
	1.27 ± 0.11	1.37 ± 0.19	1.87 ± 0.14*	26.00 ± 0.28	29.13 ± 1.96	30.27 ± 0.28#

cAMP level (pmol/well/ 30min)	Control	*p*-MCA(10)	*p*-MCA(100)	IBMX	IBMX + *p*-MCA(10)	IBMX + *p*-MCA(100)
	1.08 ± 0.32	1.21 ± 0.04	1.76 ± 0.14*	8.52 ± 1.53	7.13 ± 0.81	8.68 ± 1.25

Values are means ± S.E.M.; 3 independent experiments with quadruplicates in each experiment. *$P<0.05$ compared with control, #$P<0.05$ compared with forskolin alone.

4.14 Effect of *p*-MCA on α-glucosidases and α-amylase inhibition

Effect of *p*-MCA on α-glucosidases and α-amylase inhibition was shown in Table. *p*-MCA showed had more potent yeast α-glucosidase inhibiting activity (IC_{50} = 0.04 ± 0.01 mM) than that of 1-deoxynorjirimycin (IC_{50} = 5.60 ± 0.42 mM). However, *p*-MCA had no the inhibitory effect on mammalian α-glucosidase such as sucrase and maltase. Lineweaver-burk plot of α-glucosidase kinetics was shown in Figure 4.31. The kinetic result demonstrated that the mechanism of α-glucosidase inhibition of *p*-MCA was a non-competitive inhibition with K_i value of 0.060 ± 0.01 mM. Moreover, *p*-MCA had no inhibitory activity against pancreatic α-amylase.

Table 4.4 *In vitro* studies of inhibitory effect of *p*-MCA on α-glucosidase, and α -amylase inhibition

	Types of enzyme inhibition (IC_{50})			
	Yeast α-glucosidase	Mammalian α- glucosidases		Pancreatic α-amylase
	(mM)	Maltase (μM)	Sucrase (μM)	(μM)
p-MCA	0.04 ± 0.01	N.I.	N.I.	N.I.
1-Deoxynorjirimycin	5.60 ± 0.42	N.D.	N.D.	N.D.
Acarbose	N.D.	2.51± 0.37	21.82± 3.23	19.80± 0.15

The IC_{50} values was expressed as means ± S.E.M., (*n=3*). N.I = No inhibition, N.D. = No detection

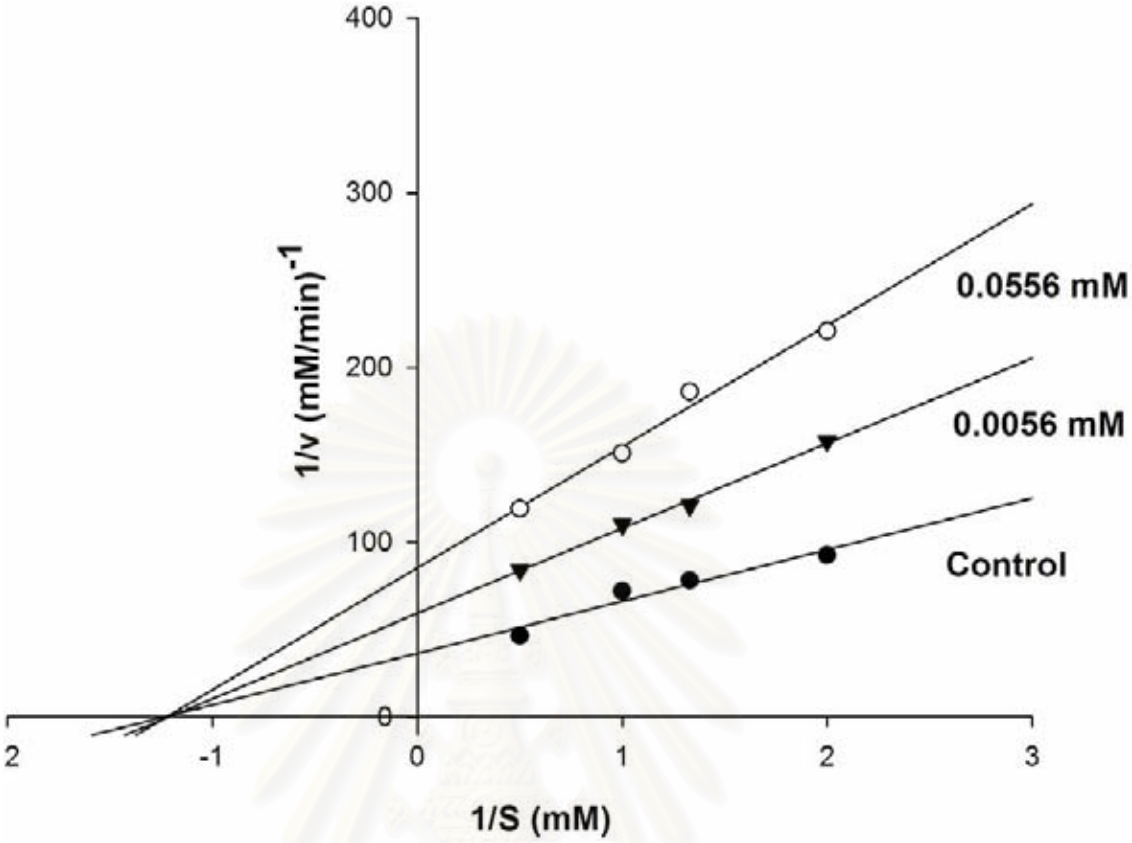

Figure 4.31 Lineweaver-burk plot analysis of the inhibition kinetics of α-glucosidase inhibitory effects by *p*-MCA

CHAPTER V

DISCUSSION

This was a study to evaluate the antihyperglycemic effect of *p*-MCA in normal and STZ-induced diabetic rats. The study was also to investigate the effect of *p*-MCA on the activity of hepatic enzymes such as hexokinase, glucokinase, phosphofructokinase, and glucose-6-phosphatase. In addition, the study was undertaken to elucidate the mechanisms underlying *p*-MCA-induced insulin secretion.

The liver is an important organ that plays a pivotal role in glycolysis and gluconeogenesis. A partial or total deficiency of insulin causes derangement in carbohydrate metabolism that decreases activity of hexokinase, glucokinase and phosphofructokinase (Hikino et al., 1989), causing impaired peripheral glucose utilization and augmented hepatic glucose production. Administration of insulin causes normalization of glycolytic enzymatic activity (Shanmugasundaram et al., 1983). The results showed that the activities of hexokinase, glucokinase and phosphofructokinase decreased in STZ-induced diabetic rats, which are consistent with other studies on hexokinase (Latha and Pari, 2003), glucokinase (Barbera et al., 1994), and phosphofructokinase (Grover et al., 2000). The chronic administration of *p*-MCA to diabetic rats markedly raised the activity of all 3 glycolytic enzymes but it did not increase the enzyme activities in normal rats, suggesting that antihyglycemic action of *p*-MCA is the result of increased glucose utilization by the liver. Interestingly, single administration of *p*-MCA to normal and diabetic rats reduced plasma glucose concentration within 30 min. The regulation of glycolytic enzymes gene expression, which leads to an increase the enzymatic activity, would not appear in short-term treatment. These findings indicated that *p*-MCA may play other roles in the control of hyperglycemia in normal and diabetic rats such as the stimulation of insulin secretion and/or glucose uptake activity. Other cinnamic acid derivatives have been reported to increase in insulin secretion and glucose uptake in myocytes. For examples, ferulic

acid increases insulin release in clonal β-cells RIN-5F (Nomura et.al, 2003). Caffeic acid enhances glucose uptake into adipocytes and C_2C_{12} myocytes by activating α_{1A}-adrenoceptors via phospholipase C-protein kinase C pathway (Cheng and Liu, 2000). Further studies are needed to evaluate the insulinotropic and glucose uptake of *p*-MCA.

Glucose-6-phosphatase (G6Pase) is a crucial enzyme for the final step of gluconeogenesis or glycogenolysis in which it catalyzes the hydrolysis of glucose-6-phosphate (G6P) to glucose and phosphate. Glucose is transported out of the liver to increase blood glucose concentration. STZ increases the expression of G6Pase (Massillon et al., 1996; Liu et. al, 1994). In contrast, insulin and metformin inhibit the hepatic glucose production by suppressing G6Pase activity (Chen et. al, 2000; Wiernsperger et. al, 1999). In the present study, administration of *p*-MCA enhanced the reversal of high G6Pase activity in diabetic rats. The reduction in G6Pase can lead to a decrease in gluconeogenesis and blood glucose concentration. Moreover, the inhibition of expression of phosphoenolpyruvate carboxykinase (PEPCK) can reduce hepatic glucose production (Lochhead et al., 2001). Isoferulic acid lowers plasma glucose concentrations in STZ-induced diabetic rats through suppressing the expression of PEPCK (Liu et al., 1999). Additional studies are needed to investigate the effect of *p*-MCA on PEPCK activity.

The liver and skeletal muscle are the major organs for glucose disposal. The repeat study regarding STZ-induced diabetic rats diminished glycogen storage in the liver are consistent with those of others (Ramachandran et. al, 2003, Singh et. al, 2003). One of the keys for controlling glycogen deposition in peripheral tissue is G6P. When blood glucose concentration increases over the threshold level, glucokinase begins to phosphorylate glucose to G6P for glycogen synthesis (Ferrer et. al, 2003). In the present study, *p*-MCA administration increased glycogen storage in diabetic rats by ~ 80%. *p*-MCA also increased hepatic G6P concentrations in diabetic rats. The results demonstrated that *p*-MCA markedly increased the glucokinase activity in diabetic rats.

The insulinotropic activity of *p*-MCA was determined by using the perfused rat pancreas. In agreement with the results obtained from the perfused rat

pancreas, this stimulatory effect of *p*-MCA was also found in clonal β-cells INS-1, suggesting a direct effects on β-cells. The insulinoma cell line INS-1 has become a useful model for studying the molecular mechanism of Ca^{2+}-dependent and Ca^{2+}-independent insulin secretion (Wollheim, 2000). It has been shown to respond to glucose at physiological concentrations (Asfari et al., 1992). Thus, this cell line was used to study the mechanisms underlying *p*-MCA-induced insulin secretion. Moreover, the results indicated that *p*-MCA-induced $[Ca^{2+}]_i$ increase is linked to insulin secretion in INS-1 cells.

We hypothesized that *p*-MCA stimulates insulin secretion by increasing Ca^{2+} influx through L-type Ca^{2+} channels. These findings supported this hypothesis by demonstrating that the effects of *p*-MCA-induced insulin secretion were abolished under Ca^{2+} free condition and in the presence of a L-Ca2+ channel blocker. Such a good correlation between data obtained from insulin secretion and $[Ca^{2+}]_i$ response strongly suggests that the effects of *p*-MCA on insulin secretion from β-cells is mediated by Ca^{2+} influx through the L-type Ca^{2+} channels. The question arises as to whether the insulinotropic effect of *p*-MCA is mediated via the same mechanism as sulfonylureas. The main mechanism responsible for the insulin releasing capacity of hypoglycemic sulfonylureas implicates the closure of K_{ATP} channels, heteromultimers composed of sulfonylurea receptor (SUR) and Kir 6.2 units, leading to cell depolarization, Ca^{2+} entry and exocytosis of secretory granules (Ämmälä et al., 1996). In contrast, diazoxide behaves in the opposite manner by opening K_{ATP} channels, which leads to hyperpolarization of β-cells, thereby inhibiting insulin secretion. It is known that binding of diazoxide to its receptor partially suppresses the binding of a sulfonylurea to SUR1, and disturbs the effects of the sulfonylurea on both electrical activity and ion fluxes (Ashcroft and Ashcroft, 1992). This study showed that glyburide stimulated insulin secretion from INS-1 cells, which was partially inhibited by diazoxide. These results are consistent with previous findings in pancreatic islets and β-cell lines (Ämmälä et al., 1996; Park et al., 2002). In contrast, diazoxide did not antagonize the stimulatory effect of *p*-MCA on insulin secretion and rise of $[Ca^{2+}]_i$, suggesting that *p*-MCA does not evoke membrane depolarization by closing of K_{ATP} channels.

Recently, cinnamic acid derivatives have been reported to exert their activities on cation channels. For examples, the transient receptor potential (TRP) family of ion channels now comprises more than 30 cation channels, most of which are permeable to Ca^{2+} (Pedersen et al., 2005). Cinnamaldehyde and cinnamic alcohol activate TRPA1 to increase Ca^{2+} influx (Bandell et al., 2004). It is well known that VDCC plays a very important role in the regulation of $[Ca^{2+}]_i$ in pancreatic β-cells. From the studies of cinnamic acid derivatives, we speculate that *p*-MCA may directly bind to L-type Ca^{2+} channels and activate them. Further study is needed to characterize the binding affinity of *p*-MCA on L-type Ca^{2+} channels and to determine the effect of *p*-MCA on these channels.

Our results showed that the direct exposure of pancreatic β-cells to *p*-MCA in the presence of glucose amplified the insulin secretion. In STZ-induced diabetic rats, *p*-MCA (40 mg/kg) decreased plasma glucose concentration and increased insulin concentration after glucose loading. Therefore, *p*-MCA improves glucose intolerance in diabetic rats. Our findings suggested that *p*-MCA may be beneficial to patients with diabetes mellitus who have defects in the response of insulin secretion to glucose stimulation.

The experiments were further investigated whether *p*-MCA potentiates the effects of other secretagogues than glucose. Glyburide is an antidiabetic agent, which has been used in those patients with maturity onset or type 2 diabetes. In this study, glyburide (10 μM) produced the maximum effective concentration on insulin secretion in INS-1 cells (data not shown). *p*-MCA at 100 μM exerted the additive effect of glyburide on insulin secretion. These findings suggested that *p*-MCA may benefit the use of glyburide in the control of type 2 diabetes.

The depolarization of membrane by a rise of extracellular KCl and the opening of L-type Ca^{2+} channel by Bay K 8644 could potentiate the effect of *p*-MCA-induced insulin secretion. Bay K 8644 is a dihydropyridine (DHP) compound, which increases the mean open time and opens probability of the L-type Ca^{2+} channels in a

variety of cells (Striessnig et al., 1991), including cardiac cells (Skasa et al., 2001) and β-cells (Larsson-Nyren and Sehlin, 1996). L-type Ca^{2+} channels are complex proteins that consist of a pore-forming α_1 subunit, disulfide-linked transmembrane complex of α_2 and δ subunits (α_2/δ), intracellular β subunit, and γ subunit. α_1 Subunits are further divided into five major subtypes based on biophysical and pharmacological characteristics (Hofmann et al., 1999). DHP compounds bind to L-type Ca^{2+} channel α_1 subunits with high affinity. Interestingly, DHP at high concentrations or administered at depolarized membrane potentials can close these channels(Usowicz et al., 1995). Similarly, a benzoylpyrrole derivative, FPL-64176,a classical Ca^{2+} channel agonist, increase in $[Ca^{2+}]_i$ and subsequent insulin release from βTC3-cells (Springborg et al.,1997). These compounds act at the same region but bind to the different amino acid residue within IIIS5 and IIIS6 transmembrane segments of L-type Ca^{2+} channel α_{1C} subunit (Rampe and Lacerda, 1991; Zheng et al.,1991). Thus, we speculate that *p*-MCA potentiates Bay K 8644-induced insulin secretion by activating of the different binding site or subunit of the L-type Ca^{2+} channel. Further work is needed to prove this speculation.

Since, *p*-MCA (100 μM) enhanced forskolin-induced insulin secretion and cAMP content but it failed to increase IBMX-induced insulin secretion and cAMP content. These results suggested that the agent may increase insulin secretion and cAMP content by inhibiting PDE. Several studies have reported the presence of both PDE3 and PDE4 in pancreatic islets (Beavo, 1995), but only the inhibitors specific for PDE3 actually potentiate insulin secretion (Shafiee-Nick et al., 1995;Parker et al., 1995). It is likely *p*-MCA inhibits PDE3 to increase cAMP content in β-cells. Further studies are needed to determine which PDE isoform is inhibited by *p*-MCA in β-cells. On the other hand, the *p*-MCA (100 μM)-induced increase in cAMP level was much less than those induced IBMX (100 μM) or forskolin (1 μM). Interestingly, forskolin increased cAMP levels by ~20 fold, but the increase in insulin secretion was only 1.6 fold of the basal control group. Thus, *p*-MCA-induced increase in cAMP probably plays a minor role in its insulinotropic effect.

As the results of α-glucosidase inhibition, *p*-MCA was the potent yeast α-glucosidase inhibitor which is the competitive inhibition. Acarbose showed a potent mammalian α-glucosidase and α-amylase inhibitor, whereas *p*-MCA had no any inhibitory activity on these enzymes activity. These findings suggested that *p*-MCA has more specific inhibition on yeast than mammalian α-glucosidase.

Recent years have apparent evidence of the inhibitory α-glucosidase activities through interference with biosynthesis of glycoprotein processing on the surface of the viral cell wall, which have exhibited promising activities as anti-viral agents. *N*-linked oligosaccharides play roles in the fate and functions of glycoproteins. One function is to assist in the folding of proteins by mediating interactions of the lectin-like chaperone proteins calnexin and calreticulin with nascent of the α-glucosidases. This causes some proteins to be misfolded and retained within the endoplasmic reticulum. HIV-1, the causative agent of acquired immunodeficiency syndrome (AIDS), encodes two essential envelope glycoprotiens (gp120 and gp41) through the endoprolytic cleavage of the precursor protein within *cis*-golgi apparatus by α-glucosidases activities (Robina et al., 2004). Treatment of HIV-1 infected cells with N-butyldeoxynojirimycin (NB-DNJ), an inhibitor of the α-glucosidases, inhibits syncytium formation and the formation of infectious virus (Fischer et al.,1995). Thus, *p*-MCA may lead to be a new anti-HIV agent in the future.

The regulation of carbohydrate absorption via inhibition of these luminal α-glucosidases effectively reduces postprandial hyperglycemia, and thus, improves glycemic control in patients with type 2 diabetes mellitus. The main digestible carbohydrates in human diet are starch and sucrose. Starch granules constitute a mixture of two different plant polysaccharides, amylose, a linear [4-*O*-α-D-glucopyranosyl-D-glucose]$_n$ polymer, and amylopectin, with additional 6-*O*-α-D-glucopyranosyl-D-glucose links in the branched structure. In view of nutritional information, dietary starches are a mixture of 25% amylose with 75% amylopectin (Nichols et al., 2003). The processing of starch digestion begins in the intestinal lumen by α-amylase, which is found in salivary and pancreatic secretions, producing linear malto-oligosaccharides and α-limit dextrins containing both α-(1→4) linkages and one

or more α-(1→6) branching links. Both families of malto-oligosaccharides are not absorbable without further processing to glucose by hydrolysis at the nonreducing ends of 1-4 and 1-6 oligomers by α-glucosidase enzymes (Nichols et ., 1998). α-Glucosidase enzymes (sucrase, isomaltase, maltase, glycoamylase and trehalase) break down non-absorbable complex carbohydrate into absorbable monosaccharides at the brush border membrane of enterocyte in small intestine before transportation of glucose across intestinal microvilli to circulation (Bischoff, 1995). The antidiabetic drugs of the family of α-glucosidase inhibitors comprise three compounds: acarbose, which is the best studied, and most widely used agent.

Additional structure-activity relationship studies on yeast α-glucosidase inhibition, *p*-MCA showed the highest potent inhibitory activity among those of seventeen cinnamic acid derivatives. Additional studies on structure-activity relationship, the presence of substituents at *para*-position in cinnamic acid altered the α-glucosidase inhibitory activity. The increase of bulkiness and the chain length of *para* -alkoxy substituents as well as the increasing of the electron withdrawing group have been shown to decrease the inhibitory activity.

CONCLUSION

p-MCA markedly decreased fasting plasma glucose concentrations and reduced hyperglycemia in normal and diabetic rats. In addition, *p*-MCA increased plasma insulin concentrations in normal and diabetic rats. During the 4-week study, *p*-MCA reduced plasma glucose concentration in diabetic rats and it exert the antihyperglycemic effect by increasing glycolysis, and by decreasing gluconeogenesis. *p*-MCA stimulated insulin secretion from pancreatic β-cells by increasing Ca^{2+} influx via the L-type Ca^{2+} channels, but not through the closure of ATP-sensitive K^{+} channels. Moreover, *p*-MCA showed the potent inhibitory activity against yeast α-glucosidase in a competitive manner. However, it had no inhibitory activities on mammalian α-glucosidases, and α-amylase. *p*-MCA should be further studied for its role in the regulation of insulin secretion and the control of type 2 diabetes.

REFERENCES

Aldhahi W, Hamdy O. Adipokines, inflammation and the endothelium in diabetes. Curr Diab Rep 2003;3:293-298.

Altan VM. The pharmacology of diabetic complications. Curr Med Chem 2003;10:1317-1327.

Ämmälä C, Ashcroft FM and Rorsman P. Calcium-independent potentiation of insulin release by cyclic AMP in single beta-cells Nature 1993;363:356-8.

Ämmälä C, Moorhouse A, Ashcroft FM. The sulphonylurea receptor confers diazoxide sensitivity on the inwardly rectifying K^+ channel Kir6.1 expressed in human embryonic kidney cells. J. Physiol 1996;494:709-714.

American Association Diabetes; Report of the Expert Committee on the Diagnosis and Classification of Diabetes Mellitus. Diabetes Care 1997;20:1183-1197.

Ashcroft FM. ATP-sensitive potassium channelopathies: focus on insulin secretion. J Clin Invest 2005;115:2047-2058.

Ashcroft SJH, Ashcroft F.M. The sulfonylurea receptor. Biochim Biophys Acta 1992;1175:45-59.

Bailey CJ, Turner RC. Metformin. N Engl J Med 1996;334:574-579.

Bandell M, Story GM, Hwang SW, Viswanath V, Eid SR, Petrus MJ, Earley TJ, Patapoutian A. Noxious cold ion channel TRPA1 is activated by pungent compounds and bradykinin. Neuron. 2004;41:849-857.

Barbera A, Rodriguez-Gil JE, Guinovart JJ. Insulin-like actions of tungstate in diabetic rats. Normalization of hepatic glucose metabolism. J Biol Chem 1994; 269:20047-20053.

Beckers CJM, Balch WE. Ca^{2+} &GTP: Essential components in vesicular trafficking between the ER and Golgi apparatus. J Cell Biol 1989;108:1245-1256.

Bischoff H. The mechanism of alpha-glucosidase inhibition in the management of diabetes. Clin Invest Med 1995;18:303-311.

Bollen M, Keppens S, Stalmans W. Specific features of glycogen metabolism in the liver. Biochem J 1998;336:19–31.

Bolzan AD, Bianchi MS. Genotoxicity of streptozotocin. Mutat Res 2003;512:121-134.

Bradford MM. A rapid and sensitive method for the quantitation of microgram quantities of protein utilizing the principle of protein-dye binding. Anal Biochem 1976;72:248-254.

Buchanan TA. Pancreatic beta-cell loss and preservation in type 2 diabetes. Clin Ther 2003;25(Suppl B):B32-B46.

Bylka W. *E*- and *Z*-*p*-methoxycinnamic acid from Aquilegia vulgaris. Acta Pol Pharm 2004;61:307-308.

Cawthorn EG, Chan CB. Effect of pertussis toxin on islet insulin secretion in obese (fa/fa) Zucker rats. Mol Cell Endocrinol 1991;75:197-204.

Chang HK, Hsu FL, Liu IM, Cheng JT. Stimulatory effect of cinnamic acid analogues on alpha1A-adrenoceptors in-vitro. J Pharm Pharmacol 2003; 55: 833-837.

Charpentier G. Oral combination therapy for type 2 diabetes. Diabetes Metab Res Rev 2002;18 (Suppl 3):S70-S76.

Cheng AY, Fantus IG. Oral antihyperglycemic therapy for type 2 diabetes mellitus. CMAJ. 2005;172:213-226.

Chen R, Meseck M, McEvoy RC, Woo SL. Glucose-stimulated and self-limiting insulin production by glucose 6-phosphatase promoter driven insulin expression in hepatoma cells. Gene Ther 2000;7:1802-1809.

Cheng H, Grodnitzky JA, Yibchok-anun S, Ding J, Hsu WH. Somatostatin increases phospholipase D activity and phosphatidylinositol 4,5-bisphosphate synthesis in clonal beta cells HIT-T15. Mol Pharmacol 2005;67:2162-2172.

Cheng JT, Liu IM. Stimulatory effect of caffeic acid on alpha1A-adrenoceptors to increase glucose uptake into cultured C_2C_{12} cells. Naunyn Schmiedebergs Arch Pharmacol 2000;362:122-127.

Cherksey B, Mendelsohn S, Zadunaisky J, Altszuler N. Displacement of alpha- and beta-radioligands by specific adrenergic agonists in rat pancreatic islets. Pharmacology 1983;27:95-102.

Conti M. Phosphodiesterases and cyclic nucleotide signalling in endocrine cells. Mol Endocrinol 2000;14:1317-1727.

Di Guglielmo GM, Drake PG, Baass PC, Authier F, Posner BI, Bergeron JJ. Insulin receptor internalization and signalling. Mol Cell Biochem 1998;182:59-63.

Doyle ME and Egan JM. Pharmacological agents that directly modulate insulin secretion. Pharmacol Rev. 2003; 55:105-131.

Eliasson L, Renstrom E, Ding WG, Proks P, Rorsman P. Rapid ATP-dependent priming of secretory granules precedes Ca^{2+}-induced exocytosis in mouse pancreatic β-cells. J Physiol (Lond) 1997;503:399-412.

Ferner RE, Neil HAW. Sulphonylureas and hypoglycaemia. Br Med J 1988;296:949-950.

Ferrer JC, Favre C, Gomis RR, Fernandez-Novell JM, Garcia-Rocha M, de la Iglesia N, Cid E, Guinovart JJ. Control of glycogen deposition FEBS Letters 2003;546:127-132.

Firth R, Bell P, Pizza R. Insulin action in non-insulin-dependent-diabetes mellitus: the relationship between hepatic and extrahepatic insulin resistance and obesity. Metabolism 1987;36:1091-1095.

Fischer PB, Collin M, Karlsson GB, James W, Butters TD, Davis SJ, Gordon S, Dwek RA, Platt FM. The alpha-glucosidase inhibitor N-butyldeoxynojirimycin inhibits human immunodeficiency virus entry at the level of post-CD4 binding. J Virol 1995;69:5791-5797.

Fiske CH, Subbarow Y. The colorimetric determination of phosphorus. J Biol Chem 1925;66:375-400.

Fonseca VA. Management of diabetes mellitus and insulin resistance in patients with cardiovascular disease. Am J Cardiol 2003;92(suppl):50J-60J.

Fyles JM, Cawthorne MA, Howell SL. The characteristics of beta-adrenergic binding sites on pancreatic islets of Langerhans. J Endocrinol 1986;111:263-270.

Gabir MM, Hanson RL, Dabelea D, Imperatore G, Roumain J, Bennett PH, Knowler WC. The 1997 American Diabetes Association and 1999 World Health Organization criteria for hyperglycemia in the diagnosis and prediction of diabetes. Diabetes Care 2000;23:1108-1112.

Gerich JE. Oral hypoglycemic agents. N Engl J Med 1989;321:1231-1245.

Gilon P, Henquin JC. Mechanisms and physiological significance of the cholinergic control of pancreatic beta-cell function. Endocr Rev 2001;22:565-604.

Gonoi T, Mizuno N, Inagaki N, Kuromi H, Seino Y, Miyazaki J, Seino S. Functional neuronal ionotropic glutamate receptors are expressed in the non-neuronal cell line MIN6. J Biol Chem 1994;269:16989-16992.

Gerritsen VB. Insulin: Protein of the 20th century. 2001. Available from http://www.expasy.org/spotlight/back_issues/sptlt009.shtml.

Grover JK, Vats V, Rathi SS. Anti-hyperglycemic effect of *Eugenia jambolana* and *Tinospora cordifolia* in experimental diabetes and their effects on key metabolic enzymes involved in carbohydrate metabolism. J Ethnopharmacol 2000;73:461-470.

Harndahl L, Jing XJ, Ivarsson R, Degerman E, Ahren B, Manganiello VC, Renstrom E, Holst LS. Important role of phosphodiesterase 3B for the stimulatory action of cAMP on pancreatic beta-cell exocytosis and release of insulin. J Biol Chem. 2002 ;277:37446-37455.

Hauner H. Managing type 2 diabetes mellitus in patients with obesity. Treat Endocrinol. 2004;3:223-232.

Hikino H, Kobayashi M, Suzuki Y, Konno C. Mechanisms of hypoglycemic activity of aconitan A, a glycan from *Aconitum carmichaeli* roots. J Ethnopharmacol 1989;25: 295-304.

Hofmann F, Lacinova L, Klugbauer N. Voltage-dependent calcium channels: from structure to function. Rev Physiol Biochem Pharmacol 1999;39:33-87.

Holmes BF, Kurth-Kraczek EJ, Winder WW. Chronic activation of 5'-AMP-activated protein kinase increases GLUT-4, hexokinase, and glycogen in muscle. J Appl Physiol 1999;87:1990-1995.

Holz GG and Habener JF. Signal transduction crosstalk in the endocrine system: pancreatic beta-cells and the glucose competence concept. Trends Biochem Sci. 1992;17:388-393.

Islam MS, Leibiger I, Leibiger B, Rossi D, Sorrentino V, Ekstrom TJ, Westerblad H, Andrade FH, Berggren PO. In situ activation of the type 2 ryanodine receptor in pancreatic beta cells requires cAMP-dependent phosphorylation. Proc Natl Acad Sci USA 1998;95:6145-6150.

Jackson JE, Bressler R. Clinical pharmacology of sulphonylurea hypoglycaemic agents: part 1. Drugs 1981;22: 211-245.

Jarvill-Taylor KJ, Anderson RA, Graves DJ. A hydroxychalcone derived from cinnamon functions as a mimetic for insulin in 3T3-L1 adipocytes. J Am Coll Nutr 2001;20: 327-336.

Jennings A, Wilson R, Ward J. Symptomatic hypoglycemia in NIDDM patients treated with oral hypoglycemic agents. Diabetes Care 1989;12:203-208.

Jiang G, Zhang BB. Modulation of insulin signalling by insulin sensitizers. Biochem Soc Trans 2005;33:358-361.

Kandra L, Zajacz A, Remenyik J, Gyemant G. Kinetic investigation of a new inhibitor for human salivary alpha-amylase. Biochem Biophys Res Commun 2005;334:824-8.

Kang G, Chepurny OG, Holz GG. cAMP-regulatedguanine nucleotide exchange factor II (Epac2) mediates Ca2+-induced Ca2+ release in INS-1 pancreatic beta-cells. J Physiol 2001;536:375-385.

Kanno T, Suga S, Wu J, Kimura M, Wakui M. Intracellular cAMP potentiates voltage-dependent activation of L-type Ca^{2+} channels in rat islet beta-cells. Pflugers Arch. 1998;435:578-580.

Kashyap S, Belfort R, Gastaldelli A, Pratipanawatr T, Berria R, Pratipanawatr W, et al. A sustained increase in plasma free fatty acids impairs insulin secretion in nondiabetic subjects genetically predisposed to develop type 2 diabetes. Diabetes 2003;25:2461-2474.

Keppler D, Decker K, Glycogen. In: Bergmeyer, H.U. editor, Methods of Enzymatic Analysis, Vol. 6, Academic Press., New York, 1974:11-17.

Khan A, Safdar M, Ali Khan MM, Khattak KN, Anderson RA.. Cinnamon improves glucose and lipids of people with type 2 diabetes. Diabetes Care 2003;26:3215-3218.

Kim SR, Kang SY, Lee KY, Kim SH, Markelonis GJ, Oh TH, Kim YC. Anti-amnestic activity of *E-p*-methoxycinnamic acid from *Scrophularia buergeriana*. Brain Res Cogn 2003;17:454-461.

Kim SR, Sung SH, Jang YP, Markelonis GJ, Oh TH, Kim YC (2002) *E-p*-methoxycinnamic acid protects cultured neuronal cells against neurotoxicity induced by glutamate. Br J Pharmacol 2002;135:1281-1291.

Kirpichnikov D, McFarlane SI, Sowers JR. Metformin: an update. Ann Intern Med 2002; 137:25-33.

Koida H, Oda, T. Pathological occurrence of glucose-6-phosphatase in liver disease. Clin Chim Acta 1959;74:554-561.

Landau BR. Methods for measuring glycogen cycling. Am J Physiol Endocrinol Metab. 2001;281:E413-419.

Lang G, Michal G. D-Glucose-6-phosphate and D-Fructose-6-phosphate, In: Bergmeyer, H.U., editor, Methods of Enzymatic Analysis, Vol. 3, Academic Press. Inc., New York, 1974:1238-1242.

Larsson-Nyren G, Sehlin J. Comparison of the effects of perchlorate and Bay K 8644 on the dynamics of cytoplasmic Ca2+ concentration and insulin secretion in mouse beta-cells. Biochem J 1996;314:167-173.

Latha M, Pari L. Antihyperglycaemic effect of *Cassia auriculata* in experimental diabetes and its effects on key metabolic enzymes involved in carbohydrate metabolism. Clin Exp Pharmacol Physiol 2003;30:38-43.

Lebovitz HE. Alpha-glucosidase inhibitors. Endocrinol Metab Clin North Am 1997;26: 539-51

Lee EJ, Kim SR, Kim J,Kim YC. Hepatoprotective phenylpropanoids from *Scrophularia buergeriana* roots against CCl_4-induced toxicity: action mechanism and structure-activity relationship. Planta Med 2002;68:407-411.

Lee HS. Tyrosinase inhibitors of Pulsatilla cernua root-derived materials. J Agric Food Chem 2002;50:1400-1403.

Liu IM, Chi TC, Hsu FL, Chen CF, Cheng JT. Isoferulic acid as active principle from the rhizoma of *Cimicifuga dahurica* to lower plasma glucose in diabetic rats. Planta Med 1999;65:712-714.

Liu IM, Hsu FL, Chen CF, Cheng JT. Antihyperglycemic action of isoferulic acid in streptozotocin-induced diabetic rats. Br J Pharmacol 2000;129:631-636.

Liu Z, Barrett EJ, Dalkin AC, Zwart AD, Chou JY.. Effect of acute diabetes on rat hepatic glucose-6-phosphatase activity and its messenger RNA level. Biochem Biophys Res Commun 1994;205:680-686.

Lochhead PA, Coghlan M, Rice SQ, Sutherland C. Inhibition of GSK-3 selectively reduces glucose-6-phosphatase and phosphatase and phosphoenolypyruvate carboxykinase gene expression. Diabetes 2001;50:937-946.

Lohray BB, Bhushan V. Advances in insulin sensitizers. Curr Med Chem 2004;11:2467-503.

Massillon D, Barzilai N, Chen W, Hu M, Rossetti L. Glucose regulates in vivo glucose-6-phosphatase gene expression in the liver of diabetic rats. J Biol Chem 1996;271:9871-9874.

Matsui T, Yoshimoto C, Osajima K, Oki T, Osajima Y. In vitro survey of alpha-glucosidase inhibitory food components. Biosci Biotechnol Biochem 1996;60:2019-2022.

Mayer ML, Armstrong N. Structure and function of glutamate receptor ion channels. Annu Rev Physio. 2004;66:161-181.

Morozumi S. Isolation, purification, and antibiotic activity of o-methoxycinnamaldehyde from cinnamon. Appl Environ Microbiol 1978;36:577-583.

Natella F, Nardini M, Di Felice M, Scaccini C. Benzoic and cinnamic acid derivatives as antioxidants: structure-activity relation. J Agric Food Chem 1999;47:1453-1459.

Nichols BL, Avery S, Sen P, Swallow DM, Hahn D, Sterchi E. The maltase-glucoamylase gene: common ancestry to sucrase-isomaltase with complementary starch digestion activities. Proc Natl Acad Sci U S A 2003;100:1432-1437.

Nichols BL, Eldering J, Avery S, Hahn D, Quaroni A, Sterchi E. Human small intestinal maltase-glucoamylase cDNA cloning. Homology to sucrase-isomaltase. J Biol Chem 1998;273:3076-3081.

Nomura E, Kashiwada A, Hosoda A, Nakamura K, Morishita H, Tsuno T, Taniguchi H. Synthesis of amide compounds of ferulic acid, and their stimulatory effects on insulin secretion in vitro. Bioorg Med Chem 2003;11:3807-3813.

Nordlie RC, Foster JD, Lange AJ. Regulation of glucose production by the liver. Annu Rev Nutr 1999;19:379-406.

Park KH, Song SC, Akaike T. Determination of the specific interaction between sulfonylurea-incorporated polymer and rat islets. J Biochem (Tokyo) 2002 131: 359-364.

Perez-Alvarez V, Bobadilla RA, Muriel P. Structure-hepatoprotective activity relationship of 3,4-dihydroxycinnamic acid (caffeic acid) derivatives. J Appl Toxicol 2001;21, 527-531.

Pilkis SJ. Carbohydrate Metabolism, In: SP Colowick, NO Kaplan, editor, Methods of Enzymology, Vol. 42, Academic Press., New York, 1975:31-32.

Phillips LS, Dunning BE. Nateglinide (Starlix): update on a new antidiabetic agent. Int J Clin Pract 2003;57:535-541.

Prapong T, Uemura E, Hsu WH. G protein and cAMP-dependent protein kinase mediate amyloid beta-peptide inhibition of neuronal glucose uptake. Exp Neurol 2001;167: 59-64.

Proks P, Reimann F, Green N, Gribble F, Ashcroft F. Sulfonylurea stimulation of insulin secretion. Diabetes 2002;51 Suppl 3:S368-S376.

Qin B, Nagasaki M, Ren M, Bajotto G, Oshida Y, Sato Y. Cinnamon extract (traditional herb) potentiates in vivo insulin-regulated glucose utilization via enhancing insulin signaling in rats. Diabetes Res Clin Pract 2003;62:139-148.

Rajan AS, Aguilar-Bryan L, Nelson DA, Yaney GC, Hsu WH, Kunze DL, Boyd AE. Ion channels and insulin secretion. Diabetes Care 1990;13:340-363.

Ramachandran B, Kandaswamy M. Narayanan V. Subramanian S. Insulin mimetic effects of macrocyclic binuclear oxovanadium complexes on streptozotocin-induced experimental diabetes in rats. Diabetes Obes Metab 2003;5:455-461.

Rampe D, Lacerda AE. A new site for the activation of cardiac calcium channels defined by the nondihydropyridine FPL 64176. J Pharmacol Exp Ther 1991;259:982-987.

Robina I, Moreno-Vargas AJ, Carmona AT, Vogel P. Glycosidase inhibitors as potential HIV entry inhibitors? Curr Drug Metab 2004;5:329-361.

Rorsman P, Bokvist K, Ammala C, Arkhammar P, Berggren PO, Larsson O, Wahlander K Activation by adrenaline of a low-conductance G protein-dependent K+ channel in mouse pancreatic B cells. Nature (Lond) 1991;349:77-79.

Saltiel AR, Kahn CR. Insulin signaling and the regulation of glucose and lipid metabolism. Nature 2001;414:799-806.

Scott LJ, Spencer CM. Miglitol: a review of its therapeutic potential in type 2 diabetes mellitus. Drugs. 2000;59:521-549.

Shanmugasundaram KR, Panneerselvam C, Samudram P, Shanmugasundaram ERB. Enzyme changes and glucose utilisation in diabetic rabbits: The effect of *Gymnema sylvestre, R.Br.* J Ethnopharmacol 1983;7:205–234.

Shepherd PR, Withers DJ, Siddle K. Phosphoinositide 3-kinase: the key switch mechanism in insulin signalling. Biochem J 1998;333:471-490.

Singh SN, Vats P, Suri S, Shyam R, Kumria MM, Ranganathan S, Sridharan K. Effect of an antidiabetic extract of *Catharanthus roseus* on enzymic activities in streptozotocin induced diabetic rats J Ethnopharmacol 2001;76:269-277.

Springborg J, Gromada J, Madsen P, Varming AR, Fuhlendorff J. Increase in [Ca2+]i and subsequent insulin release from beta TC3-cells with the L-type Ca(2+)-channel activator, FPL 64176. Adv Exp Med Biol 1997;426:149-157.

Sodoyez JC, Sodoyez-Goffaux F, Guillaume M, Merchie G. [^{123}I] Insulin metabolism in normal rats and humans: external detection by scintillation camera. Science 1983; 219:865-867.

Skasa M, Jungling E, Picht E, Schondube F, Luckhoff A. L-type calcium currents in atrial myocytes from patients with persistent and non-persistent atrial fibrillation. Basic Res Cardiol 2001;96: 151-159.

Strojek K. Features of macrovascular complications in type 2 diabetic patients. Acta Diabetol 2003;40 (Suppl 2): S334-S337.

Szkudelski T. The mechanism of alloxan and streptozotocin action in B cells of the rat pancreas. Physiol Res 2001;50:537-546.

Thomas H, Massey C, William C, Deal Jr. Unusual, Metabolite-dependent Solubility Properties of Phosphofructokinase. The basis for a new and rapid purification from liver, kidney, and other tissues. J Biol Chem 1973;248:56-62.

Toda M, Kawabata J, Kasai T. Alpha-glucosidase inhibitors from clove (Syzgium aromaticum). Biosci Biotechnol Biochem. 2000;64:294-298.

Usowicz MM, Gigg M, Jones LM, Cheung CW, and Hartley SA. Allosteric interactions at L-type calcium channels between FPL 64176 and the enantiomers of the dihydropyridine Bay K 8644. J Pharmacol Exp Ther 1995; 275:638-645.

Villar-Palasi C, Guinovart JJ, The role of glucose 6-phosphate in the control of glycogen synthase. FASEB J 1997;11:544–558.

Virkamaki A, Ueki K, Kahn CR. Protein–protein interaction in insulin signaling and the molecular mechanisms of insulin resistance. J Clin Invest 1999;103;931-43.

von Herrath M, Homann D. Introducing baselines for therapeutic use of regulatory T cells and cytokines in autoimmunity. Trends Immunol 2003;24:540-545.

Wiesner J, Mitsch A, Wissner P, Jomaa H, Schlitzer M. Structure-activity relationships of novel anti-malarial agents. Part 2: cinnamic acid derivatives. Bioorg Med Chem Lett 2001;11: 423-424.

Wiernsperger NF, Bailey CJ,. The antihyperglycaemic effect of metformin: therapeutic and cellular mechanisms. Drugs 1999;58 (Suppl 1):31-39.

Yaney GC, Corkey BE. Fatty acid metabolism and insulin secretion in pancreatic beta cells. Diabetologia 2003;46:1297-312.

Yibchok-anun S, Cheng H, Abu-Basha EA, Ding J, Ioudina M, Hsu WH. Mechanisms of bradykinin-induced glucagon release in clonal alpha-cells In-R1-G9: involvement of Ca(2+)-dependent and-independent pathways. Mol Cell Endocrinol 2002;192: 27-36.

Yibchok-Anun S, Cheng H, Heine PA, Hsu WH. Characterization of receptors mediating AVP-and OT-induced glucagon release from the rat pancreas. Am J Physiol 1999;277: E56-E62.

Zheng W, Rampe D, Triggle DJ. Pharmacological, radioligand binding, and electrophysiological characteristics of FPL 64176, a novel nondihydropyridine Ca2+ channel activator, in cardiac and vascular preparations. Mol Pharmacol 1991;40:734-741.

Zhou G, Myers R, Li Y, Chen Y, Shen X, Fenyk-Melody J, et al. Role of AMP-acitvated protein kinase in mechanism of metformin action. J Clin Invest 2001;108:1167-1174.

VITA

Name Sirichai Adisakwattana

Date of birth 8 December 1978

Place of birth Samutprakarn, Thailand

Institution attended

1992-1996 Watrajabopit School

1997-2000 Department of Chemistry, Faculty of Science
Chulalongkorn Univerisity

2001-2005 Inter-department graduate school (Pharmacology)
Chulalongkorn University

Scholarships

Local Graduate Scholarship by National Science and Technology Developmeny Agent (NSTDA), Thailand

The Royal Golden Jubilee Ph.D scholarship by Thailand Research Fund, Thailand